Assessment of Potential for Solar Pond Development at Chott el Djerid, Tunisia through Multi-criteria Analysis

MOHAMMAD OMER FARUK KHAN

August, 2021

SUPERVISORS:

dr. ir. Christiaan van der Tol
dr. B.H.P. Maathuis

Assessment of Potential for Solar Pond Development at Chott el Djerid, Tunisia through Multi-criteria Analysis

MOHAMMAD OMER FARUK KHAN
Enschede, The Netherlands, August, 2021

Thesis submitted to the Faculty of Geo-Information Science and Earth Observation of the University of Twente in partial fulfilment of the requirements for the degree of Master of Science in Geo-information Science and Earth Observation.
Specialization: Water Resources and Environmental Management

SUPERVISORS:
Dr. ir. Christiaan van der Tol
Dr. B.H.P. Maathuis

THESIS ASSESSMENT BOARD:

Dr. ir. Suhyb Salama (Chair)
Dr. Ir. L.G.J. Boerboom (External examiner)

ABSTRACT

The potential for developing artificial solar pond in Chott el Djerid, Tunisia has been investigated. Solar pond is a simple technology to harness the solar energy. The three layers in a the most common type of solar pond or Salinity Gradient Solar Pond (SGSP)- a relatively fresh water layer at the top, a gradient zone at the middle with increasing salinity and density, and a brine layer at the bottom consist a solar pond. The solar energy upon entering into the pond is absorbed in these three layers. Convection cells generate in the top and bottom layers called the Upper and Lower convective zones respectively, but is prevented by the gradient middle layer hence called the Non-Convective Zone. Thus, heat is prevented from transported to the top and made to be trapped in the bottom layer. The bottom layer is thus heated and the temperature may rise up to 100 °C, which may be used for different purposes along with generating electricity.

Natural occurrences of solar ponds are rare and may not be optimal for commercial use. Thus, artificial solar ponds may be developed in suitable locations where remote sensing and GIS come into play. Certain geo-environmental criteria may be favorable for the artificial development of solar pond such as solar irradiation, flat land and low wind speed. Suitable location should also be near settlement areas and water bodies. However, solar pond may not be developed in already developed areas such as settlements, roads, vegetated areas and natural water bodies and should be at a suitable distance. Thus, the problem of identifying a suitable location for solar pond is a multi-criteria geospatial decision problem and hence a multi-criteria analysis has been performed for identifying suitable locations for solar pond.

It has been found that three areas are most suitable for solar pond development in the chott- northwest, south and northeast. The best locations has been chosen with considerable areal extent where all the suitability criteria has been fulfilled.

Keywords: Solar pond, multi-criteria analysis, analytical hierarchy process (AHP), Salinity Gradient Solar Pond (SGSP), Chott el Djerid.

ACKNOWLEDGEMENTS

I would like to express my heartfelt gratitude to my first supervisor dr. ir. Christiaan van der Tol for allowing me to work on the research idea which has originally been his own. He has been very generous and accepting to all my efforts and experiments which has made this research work a pleasant experience.

I also express my sincere thanks to my second supervisor dr. B.H.P. Maathuis who has been very positive about the research form the very beginning and has given a lot of feedback from his personal experiences in the study area.

I am feeling very happy to express special thanks to the honourable chair dr. ir. Suhyb Salama who has been very insightful about the research and influenced the progress to a great deal.

I would be always grateful to my family members who have sacrificed a great deal for my own development. Also my friends who have encouraged me in the toughest of times played a very important role in the successful completion of the thesis.

Last but not the least all the teaching and supporting stuffs of ITC deserve special thanks for bearing with all my nuisances. Thank you very much.

TABLE OF CONTENTS

Contents

LIST OF FIGURES

LIST OF TABLES

1. INTRODUCTION

1.1. Background

A solar pond is a natural or artificial body of water that can collect and store solar energy as heat energy that can be used for different purposes. Natural solar ponds are rare and they may not be found where they are necessary and they may be constructed if all the necessary condition are met. Since a solar pond consists of components such as solar energy, fresh water, saline water or salt, and requires favorable geo-environmental conditions such as flat and barren land, low wind speed for their development, it may be feasible to construct artificial solar pond where these components are available. The research is about the assessment of the necessary conditions for development of artificial solar ponds in an area. For that reason an area in Southern Tunisia namely "Chott el Djerid" has been chosen for its known geo-environmental characteristics that may favor the development of solar ponds.

Solar pond can be regarded as a renewable energy source as it harnesses the solar energy. However, the solar pond technology is not very well known and widespread, but it has a high potential to be used as a good renewable energy source. The technology has been in use in only very limited cases but research need to be carried out to utilize its potential as an effective renewable energy source. Since, it is a well-known fact that the solar energy is abundant at some places of the earth, and only a fraction of it is used (Mahdi and Jebber, 2019). However, the existing technologies for solar energy are either very sophisticated or costly, where solar pond can be an easy and cheap alternative.

1.2. Description of a typical solar pond

Solar ponds are very shallow water bodies with overall thickness rarely exceeding 3 m which is a simple and economical device to capture and store solar energy as heat energy (Alcaraz et al., 2018; Elsarrag et al., 2016; Ganguly et al., 2017; Ines et al., 2019; Sogukpinar, 2019). A solar pond as the name implies is a pond with specific physico-chemical property that enables it to gain and store the Sun's electromagnetic energy as heat energy. The physico-chemical property of a typical solar pond (Salt/Salinity Gradient Solar Pond, SGSP) is such that there are three layers of water having varying salinity and density. The top layer of the pond has relatively fresh water (salinity 2-3 %) and the bottom layer has saline water (near sea/brine). The salinity and density of these layers are constant. They undergo convection when heated with solar radiation and hence termed as Upper and Lower Convective Zones (UCZ and LCZ) respectively. These layers are separated by a gradient layer in the middle with increasing salinity, density and temperature towards the bottom. This middle layer acts as a thermal insulator that prevents heat to transfer from bottom to top. Thus the heat captured from the incident solar radiation entering into the pond is trapped in the bottom layer and it is stored there. The hot brine of the lower layer will not rise to the top because the effect of temperature on density is not greater than the effect of salinity. Thus the only mechanism heat can transfer to the atmosphere from the bottom layer through the middle and upper layer is conduction. However, due to the relatively low thermal conductivity of brine that heat loss due to conduction is very low (Suarez et al., 2010). The temperature of the bottom layer is thus increased gradually and may reach up to 100 °C or more (Elsarrag et al., 2016). The stored heat energy can be extracted continuously (Amigo et al., 2017) and used to generate electricity and for different other purposes. Fig-1.1 shows the main components of a solar pond along with the electricity generating unit.

Solar ponds can be either Non-Convective or Convective. A Non-convective solar pond is characterized by a non-convective zone between an upper convective zone (UCZ) and a lower convective zone (LCZ). The third layer is also aptly referred to as the storage zone. This simplest type of Non-Convective solar pond is termed Salinity Gradient Solar Pond (SGSP). The three layers of a SGSP are characterized by varying thickness, salinity, density and temperature which are summarized in Table-1.1.

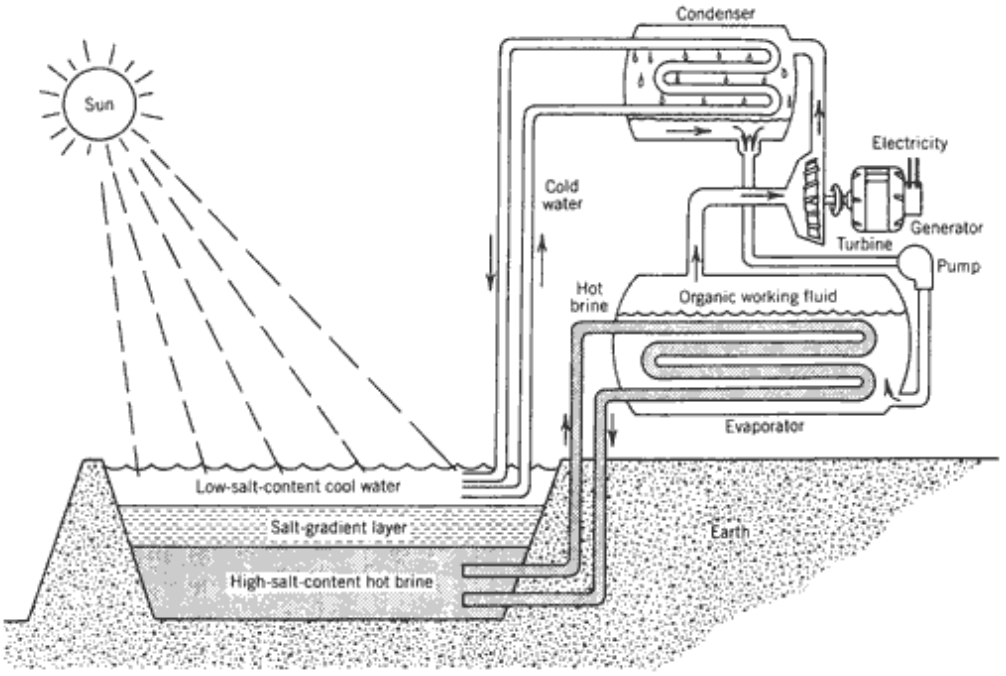

Fig-1.1: Schematic representation of a solar pond along with the electricity generating unit. (Source: https://www.kathirgugan.com/solar-pond.html)

Table-1.1: Summary of properties of different layers of a solar pond.

Zones	Thickness	Salinity	Density	Temperature	Property
Top Layer or Upper Convective Zone	0.1 to 0.4 m	2-3%	Low, Uniform	Same as ambient temperature	Convection
Middle Layer or Non-Convective Zone or Gradient Zone	~1 m	Variable	Variable	Variable	No convection, gradual increase toward bottom
Bottom Layer / Lower Convective Zone / Storage Zone	~1 m	Near sea	High, Uniform	High (50-90 °C)	Convection, heat storage

1.3. Types of solar ponds

There exist different other types of non-convective solar ponds which are-

Membrane Solar Pond- the zones are separated by thin and transparent membrane to suppress convection (Hull, 1980 as sited in Elsarrag et al., 2016).

Viscosity Stabilized Solar Pond- transparent polymer gel as non-convective zone to prevent environmental pollution and ease the maintenance (Shaffer, 1978 as cited in Elsarrag et al., 2016).

Partitioned Solar Pond- two transparent partitions preventing bacterial and algal growth, dirt and dust accumulation resulting a decrease in transparency and evaporative loss of water (Elsarrag et al., 2016).

Saturated Solar Pond- all layers are saturated, the temperature and the solubility of salt increases. Maintenance is minimal due to self-sufficiency (Shubhakar and Murthy, 1993 as cited in Elsarrag et al., 2016).

A convective solar pond is not layered and contains only a body of homogeneous fluid. A transparent cover prevents evaporative or conductive or convection heat loss, dust, and other pollutants (Elsarrag et al., 2016).

The size of solar ponds vary widely. They can be very small (less than 500 m^2, Solvay Minerals facilities in Granada, South Spain (Alcaraz et al., 2018)) or very big (more than 210000 m^2 (Beith Ha'Arava, West Bank, Israel (Tabor and Doron, 1990)). However, they are more economical from 10,000 to 100,000 m^2 (Egbe et al., 2013).

1.4. Some examples of artificial solar ponds

Solar pond may occur naturally or they can be built artificially. The earliest natural solar pond was detected in the Medve Lake in Transylvania (Hungary). The recorded temperatures of the lake bottom were as high as 70 °C caused by salinity gradient in the lake water (Tasdemiroglu, 1987). Lake Vanda and Lake Bonney in Antarctica and Castle Lake in California show similar characteristics (Binark et al., 2000). However, natural occurrences of solar ponds are not widespread and they may not be located at an optimum place for use. Thus, development of artificial solar ponds following the working principle of natural solar pond may be a viable option where the favorable conditions are met.

Notable solar ponds developed artificially include Beith Ha'Arava, Israel, El Paso, Texas and Bhuj, India.

- The Beith Ha'Arava is the largest solar pond built till date with an area of 210000 m^2 for generating 5 MW electricity (Garg, 1987).
- The El Paso solar pond was a research project of University of Texas which was a salinity gradient solar pond with a surface area of 3000 m^2 and depth of 3.2 m. It produced industrial process heat and was also used as a desalting facility (Lu and Swift, 2001).
- The Bhuj solar pond is 6000 m^2 in area and 3 m in depth with a temperature of 70 °C at the bottom. The heat was used for a dairy industry to heat up around 8000 l of milk in a day (Kishore and Kumar, 1996).

Other artificial solar ponds include-

- A 156 m^2 pond in Wooster, Ohio with a depth of 3 m built to provide heat for greenhouses. It produced about 20 GJ in less than two months of its operational period (Elsarrag et al., 2016).

- Al-Marafie constructed a solar pond at Kuwait Institute of Scientific Research. Its area is 1700 m^2 and depth is 3.5 m and was developed to produce 25 m^3 of fresh water using Multistage Flash Desalination unit. The storage zone temperature may attain a maximum of 58 °C (Al-Marafie et al., 1991).

- Ein Bokek solar pond near Dead Sea with an area of 7500 m^2 and depth of 2.6 m attained storage zone temperature of 92 °C. It could produce electricity of 150 to 170 kW (Elsarrage et al., 2016).

- Pyramid Hill solar pond with an area of 3000 m^2 producing up to 60 kW of heat for salt production in Australia (Elsarrag et al., 2016).

- Margherita Di Savoia solar pond in Southern Italy with an area of 25,000 m^2 and depth of 4 m to supply 500 kW of process heat (Elsarrag et al., 2016).

Some of the above mentioned solar ponds are not in operation any more due to various operational and maintenance issues arising from unfavorable environmental or economic conditions. Many solar ponds are built in the laboratory for experimental purposes, however, building artificial solar ponds in a particular geographic location are more complicated as they involve many factors. A geographic area should have some favorable geo-environmental characteristics to be suitable for the development of artificial solar pond. This research is focused on the assessment geo-environmental characteristics of a "Chott el Djerid" for its suitability of development of solar pond.

1.5. Geospatial aspect of solar pond development

Solar ponds have many aspects that can be related to different geographic phenomena. For example, since solar ponds work with solar energy, areas with high solar insolation should be suitable for their operation. The solar pond is essentially a saline pond and hence it is necessary to provide either saline water or salt. As a result, areas that have either saline water or salt deposits should be suitable for solar pond development. Suitable areas for pond development should be flat and hence areas with large parcels of flat land should be suitable for solar pond development. Large scale solar pond require large areas and hence already developed areas or areas already under use for different purposes may not be suitable for large scale solar pond development. Another important aspect for the stability of solar pond is the wind speed. Since solar ponds are shallow water bodies, high speed wind may disrupt the internal layering of the pond and hence may even destroy the pond. So it is very important that prospective areas for solar pond development have very low wind speed. Other factors may also influence the choice of land for solar pond development, but above mentioned factors are the most important and measures may need to be taken for solving issues of minor importance.

Thus, the problem of solar pond development can be treated as a geospatial problem and can be solved by geospatial methods. This research is about translating the problem of solar pond development as a geospatial problem and solve it by applying appropriate geoscientific approach.

1.6. Research objectives

The development of a solar pond is a broad task and involve many considerations. There are many aspects such assessment of potential, development of the actual pond, development of other facilities. Thus, the development of artificial solar pond may be broadly subdivided into four parts:

- Assessment of Potential- Preliminary investigation of the favorable conditions for solar pond development

- Design- Mathematical models, energy balance calculations, estimations of energy production.

- Construction- Actual civil engineering works to build a physical solar pond.
- Production, Supply and Maintenance- Industrial production and use.

The main objective of this research is to assess the potential of solar pond development in a specific location namely Chott el Djerid, by applying remote sensing and GIS data and techniques. This is an exploratory research conducted to make use of available online data and information to evaluate the factors and variables impacting the development of a solar pond.

1.7. Sub-objectives

The sub-objectives are as follows:

- Analyzing different geo-environmental factors affecting the efficiency of solar pond and select most suitable ones.
- Setting restrictions and evaluating potential areas.
- Identifying the most suitable areas regarding all aspect for the solar pond development.

1.8. Research questions

Are there any favorable condition for development of solar pond at Chott el Djerid? What would be the proper way to identify and evaluate most relevant variables according to the research objectives? What methodologies would be appropriate to analyze the data and come up with acceptable results?

2. LITERATURE REVIEW

2.1. Overview

Different researchers have worked on different aspects of solar pond. There are many literature available online and giving a full description of all of them would be a mammoth task. However, here the most important, relevant and easily available literature are highlighted in as much detail as possible based on the major aspects of a solar pond which are modelling and simulation, design and construction, performance and modification, and application of solar pond. However, there are few literature on the multi-criteria evaluation of potential site for solar pond. There are also very few literature on different geographic and environmental aspects of Chott el Djerid. The works can be broadly categorized as geo-environment and groundwater which are important for the assessment of solar pond development.

2.2. Modelling and simulation of solar pond

Many works can be found on the modelling and simulation of solar pond, the estimation of the heat storage capacity, and the estimation of electricity generation of a solar pond being most extensive.

Rao and Kaushika (1983) presented an analytical model of solar pond with heat exchanger with the result that the annual average efficiency of heat extraction exhibits asymptotic increase with the increase of length per unit pond area of heat exchange pipe.

Sogukpinar (2019) conducted a numerical investigation on temperature distribution using a seven layered model salinity gradient solar pond (SGSP) with square cross-section and insulated wall for the provinces in Turkey. He considered previously conducted experimental studies and ran Finite Element Method with a commercial software COMSOL including all possibility to calculate temperature distribution in different layers of SGSP and evaporative heat losses. Annual average values of temperature and solar radiation data were used for numerical calculation. The Maximum temperature was attained at the end of 600 hr during 720 hr of total simulation time and remained constant for the rest. Major heat loss was simulated at the top surface as the side wall and base were insulated with rock wool. The bottom temperature remained under 26.85 °C only in one place, under 36.85 °C in five places and over 46.85 °C in 31 places.

Mahdi and Jebbar (2019) used Finite Difference Method (FDM) to simulate incident radiation and the thermal transfer scenario in a solar pond in Kerbala city, Iraq. They used FORTRAN language for the numerical simulation and found a good agreement between various data for incident global solar radiation and NASA's published data. They also found that good similarity between obtained data of temperature inside the pond and the published experimental data given that the most effective factor affecting the amount of stored energy is the amount of amount of incidence GHI on the pond's location.

Amigo et al., (2017) developed a transient model to represent the thermal evolution of a SGSP and the surrounding ground. They evaluated the model under different contrasting scenarios such as buried and unburied ponds, artificially or naturally heated ponds and for deep or shallow groundwater tables. They calibrated and validated the model against the data collected from some indoor laboratory-scale and outdoor solar ponds and observed a good agreement between experimental and modelled result. They also found that dividing the ground into multiple layers contributes to the robustness of the model.

Chakrabarty et al. (2020) conducted an analysis based on transient model to investigate the effect of various parameters such as variations of the thickness of zones, ground conditions, and surface losses on the temperature development in a solar pond. They validated the numerical model with experimental result from two different locations and found that a phase difference between of nearly 42 days occurs between maximum values of solar radiation and temperature of Lower Convective Zone (LCZ), the evaporation loss is higher than convection and radiation loss, the impact of evaporation loss is highest in the temperature of Upper Convective Zone (UCZ) and LCZ, the change in LCZ temperature due to surface losses is minimal, and solar pond with larger area requires less duration to acquire high temperature. They suggested that shading area should be considered for the investigation of smaller area of pond.

Ding et al. (2016) explored the prospect of solar pond in electricity generation by thermoelectric generators (TEG) that convert the heat of LCZ into electricity. They discussed the effect of heat extraction, climatic variation, temperature polarization, and the conversion efficiency of TEG on the thermal performance and electrical performance of the system by analyzing the result produced by a transient model for different climatic zones. They found that the solar pond in Riyadh (Group B of Koppen climate classification) has the highest potential in generating electricity, which is about 4.834 kWh/year-m^2 at heat extraction of 15% of yearly average horizontal solar radiation (i.e. solar pond yearly efficiency of 15%) while having average LCZ temperature of 80 °C throughout the year. Overall, the thermal-electrical conversion efficiency, of this system is in the range of 1% - 1.5% from the heat extracted.

Ding et al. published a similar work in 2017 where they presented feasibility of a system of a combination of a solar pond and a thermoelectric module. They found that under ideal condition the system is at least 10 times costlier than other renewables like off-grid solar photovoltaic system with storage. However, they system has the advantage of reducing the annual carbon dioxide emission by 2.38 kg/m^2-year.

Ziapour et al. (2017) investigated the potential of thermoelectric generator as a power generation system using heat from SGSP by comparing two models: (1) without and (2) with heat exchanger. They improved the system by using thermoelectric generator instead of condenser of Organic Rankine Cycle (ORC) and evaluated the systems through computer simulation. They collected ambient conditions from beach of Lake Urmia in Iran. The results yields that the model 1 has higher performance than model 2 for identical conditions and for temperature of 90 °C in LCZ, the overall thermal efficiency of the power plant were 0.21% and 0.2% more than ORC without TEG, respectively.

2.3. Design and construction of solar pond

Tabor and Doron (1990) presented the design, construction and operation experiences of a 5 MW (e) solar pond power plant at Beith Ha'Arava, Israel. The pond size was estimated to be 1 km^2 and the output was estimated for 5500-6000 hours per year. The pond included new features which were extraction of pond surface water to an auxiliary pond for condenser cooling, a low-cost liner consisting of polyethylene and clay, and series of high-velocity, lower-fluid-volume jets for gradient formation and repair. They also presented measured plant efficiencies and total costs.

Baharin et al. (2017) described the construction and operation of the first salinity gradient solar pond in Malaysia which is an experimental SGSP to analyze the thermal storage capability. The solar pond is 2.4 m^2 in area and 1.4 m deep with sodium chloride as the salt solution. A diffuser was used to develop the

salinity gradient. The thickness of LCZ, NCZ and UCZ are 0.5 m, 0.8 m respectively and 10 cm and the density of LCZ is 1200 kg/m^3. Maximum recorded temperature of LCZ was 36.5 °C after four weeks with an upward trend.

Edesess et al. (1979) of Solar Energy Research Institute (SERI) published a report describing the methods for designing a solar pond. They provided formulas for surface area calculation, depth calculation, reflection calculation, temperature estimation and finding demand served for a given pond.

Dhindsa and Sokhal (2020) discussed the design and development of SGSP to enhance heat storage for solar still in India. They used a double glass cover along with reflector to increase the heat storage by reducing top losses. The reflector was used to enhance the solar radiation which position changed manually to track the sun to receive maximum beam radiation on the reflector. It was also used as cover during night to reduce surface heat loss. They proposed to minimize the bottom and side losses and maximize the volumetric storage of solar pond in order to be able to supply heat to basin water of still during night. Due to these designs the intensity of solar radiation and temperature of solar pond increased by 20% to 47% and 10 °C, respectively.

2.4. Performance and modificication of solar pond

Alcaraz et al. (2018) investigated the performance and efficiency of an industrial solar pond in Granada, Spain under extreme weather condition. They showed that the temperature of the storage zone of the 500 m^2 solar pond remained constant (40 °C) even when the ambient air temperature plummeted to as low as -2.4 °C due to snowfall. They concluded that the system responded positively to weather variations and the fundamental role of the salinity gradient as a thermal insulation layer was confirmed.

Dhindsa and Sokhal (2020) compared the performance of a solar pond for four test cases- 1: without glass cover and reflector, 2: with glass cover but without reflector, 3: with glass cover and reflector (fixed position) and 4: with glass cover and reflector (changing position). The best performance was obtained for case 4.

Vichare (2015) described the design procedure of a solar pond as an energy storage system for the Pasteurization process in dairy industry. He described three steps of solar pond construction: calculation of required area, fix the constructional dimensions including salt dissolution, and analyze the thermal behavior. He estimated that in a dairy industry where the daily production of milk is around 85000 litres, required pond area is 2172 m^2. If used a solar pond can reduce 160 and 90 tons of carbon dioxide emission from coal or natural gas boiler systems per month.

Aizaz (2013) discussed the basic principles of solar pond design, construction of a prototype solar pond, thermal energy extraction from the solar pond and cost benefit analysis for industrial sector in Pakistan.

Ganguly et al. (2017) discussed the effect of adding heat to solar pond from external source where he indicated that the process may actually cause heat loss if not applied with caution. He thus proposed a strategy to restrict the heat loss by using a flow controller with a temperature sensor to sense the temperature of LCZ and the fluid outlet temperature from the Evacuated Tube Solar Collector (ETSC) or from another heat source. The controller stops the flow of the heat addition when the temperature of

the LCZ is higher than the source. He observed that the optimum range of operation temperature for a solar pond with heat addition is between 70 °C and 80 °C.

Verma and Das (2019) experimented with different wall profile of solar pond for determining the maximum efficiency of the pond with reference to a given volume of water and top area. They found that vertical wall offers more output from the pond than an equal volume pond of any other geometry i.e. linear, concave parabolic and convex parabolic.

Murthy and Pandey (2002) conducted studies on the use of fertilizer salt instead of sodium chloride salt in India. They found that the fertilizer slat have similar properties to the sodium chloride and is cheaper. It is also better for environment and has the added value for the farm as crop nutrient. Since the sodium chloride salt is hazardous to environment and has no alternative use, the fertilizer salt may be a better alternative.

2.5. Application of solar pond

Solar pond has many applications the most interesting of them is the electricity generation. Other application fields has also been explored. However, not too many literature are available online on the application of solar pond.

The application of solar pond for desalination was discussed by Saifullah et al. (2012). They stated that the SGSP is the most eco- and environment-friendly among all solar energy systems for electricity generation, desalination, hot water applications in agriculture, green house heating, domestic hot water production and space heating and cooling of buildings. It is also more cost-effective as its collection cost is one-fifth of that of the flat plate collector per square meter. The cost of electricity generation by SGSP is one-fifth of that produced by photovoltaic cells per kWh. They also opined that a solar pond multi-stage flash distillation system (SPMSF) is very promising for Bangladesh as it can produce 6-60 $L/m^2/day$, in contrast to typical solar stills which is 3-4 $L/m^2/day$.

Elsarrag et al. (2016) provided a detailed review of the underlying principles of operation of desiccant cooling systems and its main components (dehumidifier, evaporative cooler and regenerator). They suggested that the solar pond as a thermal collector is an interesting option for energy requirements of the regenerator especially when large scale or storage capability is necessary.

Frederick and Riobo (2016) described a thermal model for describing the thermal dynamics of solar ponds. They used the thermal model for choosing heat exchangers and operating conditions for supplying process heat to an industry in Chile. They found that although the thermal efficiency of solar pond is low it can supply the required heat for almost half the operating time.

Rocca et al. (2017) analyzed a model of power generation from an SGSP by an Organic Rankine Cycle (ORC). They validated the model using climate data of an area near Palermo city (Italy).

2.6. Multi-criteria suitability assessment

Multi-criteria Decision Analysis method has been used extensively in geospatial science for complex decision making problems regarding suitable site selection. Many literature are available online on multi-

criteria analysis of suitability of different geographic aspects such as agriculture, groundwater recharge, retention pond, landfill, solar/wind power, astronomical observatory, natural hazard etc. However, GIS based multi-criteria assessment for solar pond suitability is rather scant. This may be due to the fact that this is rather a new area of geo-scientific interest awaiting further research. Only a couple of work have been found which are very recent. The Analytical Hierarchy Process (AHP) is also a well-used method for assigning appropriate weights to MCDA criteria or thematic layers.

Nower et al. (2020) conducted a GIS based multi-criteria analysis for suitable site selection for solar pond in Egypt. They assembled, reviewed, analyzed and categorized literature in the field of solar ponds and clean energy to deduce data about solar pond locations. They considered different variables such as roads, different countries, land cover as environmental parameter, and direct normal radiation (DNR), temperature, relative humidity as technical variables. They identified areas which have satisfactory requirements for solar pond in terms of efficiency and cost.

In another very recent article Elashaal et al. (2021) conducted similar study in Middle and North Africa (MENA) region. They calculated the mean of the technical parameters for thirty years for 65500 points. Based on the analysis they concluded that Morocco, Algeria, Libya, Egypt, Sudan, Syria, Iraq, Saudi Arabia, UAE, Oman, and Yemen satisfy the renewable energy potential.

Zolekar and Bhagat (2015) used AHP based multi-criteria suitability analysis for classifying suitable lands for agriculture in hilly region. They considered slope, land use land cover, soil depth, soil texture, soil moisture, maximum water holding capacity, soil erosion, soil organic carbon, potential of hydrogen, nitrogen, phosphorus, potassium to identify suitable agricultural lands.

Yalew et al. (2016) presented a Google Earth Engine (GEE) based online framework named AgriSuit to integrate various global data from different sources for detecting suitable agricultural land using analytical hierarchy based multi-criteria assessment. This framework uses remote sensing, GIS and computational power of GEE to perform data gathering, training and classifying of land cover classes. They used different data such as river/water bodies, towns, soil groups, slope, roads, land use, elevation, soil water content, soil stoniness, soil depth to assess the suitable land for agriculture.

Achu et al. (2020) Delineated groundwater potential zones by integrating remote sensing, GIS and AHP based multi-criteria decision analysis of geo-environmental conditions such as lithology, geomorphology, land use land cover, density of lineament and stream network, slope, and soil texture.

Diouf et al. (2017) assessed suitability to develop artificial basins and lakes in Senegal to store water where they considered fourteen criteria layers such as Land use, Elevation, Slope, Hydrogeology, Pedology, Locality and Drainage Density, Watershed average slope and elevation, Rainfall, Distance from the road, Gravelus index, Ecogeography areas and population density for multi-criteria analysis and Weighted sum overlay to aggregate layers. They first preprocessed the layers by georeferencing, projection and conversion into raster.

Ajibade (2019) integrated GIS and multi-criteria decision analysis to identify suitable sites for solid waste disposal and management by considering geo-environmental factors such as land use, slope, distance to drainage, distance to linear features, soil, geology, distance to the residence and road accessibility.

Islam et al. (2018) analyzed environmental (groundwater, surface water, vegetation, soil type and environmental sensitive areas), social (roads, slope), and economic (settlements, airports, railways) factors to identify suitable sites for landfill. They used AHP for the identification of the sites which have minimal influence on environment, ecology, economy and public health. They conducted ground truthing to select seven site out of initial twelve and least cost path to identify four most suitable sites out of the seven.

Nebey et al. (2020) identified and weighted factors that affect the suitability for solar PV and multiplied the weighted valued and reclassified values to produce the final suitability map for solar PV. They used nine criteria such as irradiance, roads, town, soil, slope, land use, forest, stream and schools.

Koc et al. (2019) used AHP and GIS to determine suitable site for solar-wind energy in Igdir, Turkey. The investigated possible locations for solar-wind power plant installation using a mapping method, GIS and then, AHP. They used elevation, land cover, aspect, inclination, geological rock type, solar irradiance, temperature, and transmission line for solar energy and elevation, land cover, aspect, inclination, geological rock type, average wind speed, and transmission line for wind energy.

Koc-San et al. (2013) selected astronomical observation site using multi-criteria decision analysis integrated with GIS and remote sensing by considering eleven factors (criteria) such as cloud cover, perceptible water, earthquake zones, geology, landslide inventory, active fault lines, Digital Elevation Model, city lights, mining activities, settlement areas, roads. They used AHP for determining the weights of criteria layers.

Sambah and Miura (2014) assessed tsunami vulnerability in Japan using elevation, slope, coastal proximity, river, and land use data by analytical hierarchy process and multi-criteria analysis.

Abija (2020) delineated potential landslide occurrence by using geotechnical boring and laboratory analysis, remote sensing analysis of SRTM-(DEM) and Landsat ETM imageries to extract slope and aspect, land use land cover, drainage and normalized vegetation index. They used AHP and multi-criteria decision analysis to identify three zones of low, high, and very high landslide susceptibility.

Since the multi-criteria analysis is a versatile tool and the selection of criteria may vary according to the research question in hand.

2.7. Geo-environmental condition of Chott el Djerid

The most important aspects of Chott el Djerid are ephemeral lake and salt playa which are very important with regard to solar pond development as they indicate two most important components of solar pond such as water and salt available in the area.

Abbas et al., (2019) studied flood events with MODIS-Terra time-series data and found maximum extent of 660 km^2 and maximum duration of 88 days among four different events in 2007, 2009, 2014 and 2015.

Bryant (1999) used Advanced Very High Resolution Radiometer (AVHRR; resolution 1·1 km at nadir) images to explore the application of high frequency temporal monitoring of Chott el Djerid. He complied 39 images (a short time series of 36 months between 1987 and 1990) with climate information from a weather station at Tozeur (a city at northern chott). He extracted lake areas using image histogram

manipulation from the time series and observed a good degree of agreement between recorded rainfall events and the presence of surface water on the playa. For a limited sample of large flood events significant relationships between rainfall, evaporation and estimated lake areas was found. He deduced temporal changes has major control over concurrent lake formation in the chott. The effect of flood events on sedimentary surfaces and their preservation can be derived from the coefficient of variation of the time series, and a combination of temporal reflectance profiles it gives (Bryant, 1999).

In a similar study, Bryant and Rainey (2002) used AVHRR data (2 images per month) with concurrent meteorological data to detect and monitor inundation events in the chott. They used reflectance profiles for each time-series to infer inundation processes for the playa and sequential image data to extract lake areas to determine the extent of inundation.

Abbas et al. (2018) described the endorheic nature of chott which is generally covered by evaporated during dry period (May to August) resulting from the desiccation of a post flood lake on a seasonal basis. They used optical multisource, multispectral, and multidate data of Landsat 4-5 TM, Landsat 8 OLI, SPOT 6, and Landsat Surface Reflectance (LSR) to map and monitor chott evaporates. They studied the central part of the chott and observed that the evaporites precipitated as concentric layers over the las 15 years where wind might play a critical role. They detected halite and gypsum by image interpretation combined with field data.

The importance of fluvial processes in sediment transport within the chott playa was revealed by multi-temporal thematic mapper images by Townshend et al. (1989) to monitor sediment transport systems. They identified large braided channels up to 1 km wide.

Bryant et al. (1994) studied an exceptional rainfall event which filled up the in the chott playa in January 1990 and in ten months the lake dried up. Chemical analysis of the major solutes in the lake brine sampled during March, May and September 1990 showed that with increased evaporation, gypsum and halite were precipitated and the most-concentrated brines were saturated with sylvite. By XRD analysis of salt crusts formed on the chott they found that gypsum, halite and carnallitite (carnallite with halite) were the constituent minerals. They concluded that the playa geochemistry was controlled mainly by the recycling of ancient marine evaporates suggested by the nature of both predicted and observed salt phases (Bryant et al., 1994).

Drake et al. (1994) applied linear mixture modelling to a sequence of seven Landsat TM images of the chott to calculate proportion maps of four surface materials such as gypsum, halite, clastic sediment and water. They could analyze their mean patterns and derive information on their spatial and temporal variability.

Millington et al. (1995) described semi-circular and crescent-shaped salt ramps in the chott playa. They formed in the late stages of the desiccation of shallow ephemeral lake by salt precipitation from brine. They are short lived and are destroyed by flooding with less saline water, rainfall and deflation.

2.8. Groundwater of Chott el Djerid

Groundwater may offer an alternative sources for the development of solar pond and thus the groundwater resource may be very important.

To test their hypothesis that "it is possible to infer the rates of evaporation of groundwater using radar backscatter measurements in arid playa", Wadge and Archer (2002, 2003) used an empirically derived relationship between backscatter and surface roughness and a model of how surface roughness changes with a continuous process of halite crystal efflorescence "to calculate the volume of groundwater that must have evaporated to produce that roughness effect". They used ERS-1 SAR sensor data from 1992-93. In the summer months the backscatter gradually rises but with the beginning of winter rains it reduces abruptly due to the dissolution of halite crust formed by evaporation. Thus the method is valid only for summer months (March to October). The found that the radar-derived evaporation rates are higher than the meteorological station measurements by factors of 2-3 probably due to recycling of sodium and chloride ions during dissolution of the halite crusts by winter rains.

Kraiem et al. (2012) carried out electrical imaging tomography survey to identify lateral and vertical salinity distribution in the oasis shallow aquifers of the Nefzaoua region in southwestern chott. They also determined the main factors and mechanism of the groundwater chemistry and salinity by using hydrochemical and isotopic data. They found that the increase in salinity nearby oasis is mainly due to the irrigation excess-water. The groundwater mineralization results from the dissolution of evaporates such as halite, anhydrite and gypsum as indicated by major element distribution, saturation indices and isotopic data.

Kamel (2013) studied the shallow depth Plio-Quaternary (PQ) water table aquifer which is present almost the entire chott basin and used for irrigation. Although the lithology is simple, the mineralization mechanism and origin of water is complex in this aquifer which he investigated with an approach combining the dissolved chemical species and isotopes. The chemical analysis showed that the mineralization occurs due to the dissolution of sulphate ($MgSO_4$ and Na_2SO_4) chloride (NaCl and MgCl) salts which is abundant in the gypsum crust both in the surface and subsurface. Evaporative dissolution was confirmed by positive correlations between anhydrite, gypsum, halite, mirabilite, and thenardite saturation indices with the respective mineral species. In addition to sporadic rainfall events, contribution from deeper aquifers was implied by the isotopic data. Moreover, evaporation partly affects the irrigation return flow before the recharge of shallow aquifer within oases limits.

Haj-Amor et al. (2017) evaluated how soil salinization and shallow groundwater properties are affected by excessive irrigation of date palms with low-quality water in a Saharan Tunisian oasis over a period of 10 years (2005-2015). The three phased study assessed the suitability of groundwater for irrigation, quantification of long term water use, and quantification of dynamic patterns of electrical conductivity of soil and shallow saline groundwater. The results indicated that the rapid rise of soil salinization within the oasis was due to the use of low-quality water under high evapotranspiration conditions coupled with rapidly rising shallow groundwater at critical depths (1.5 m). The electrical conductivity of soil exceeded date palms' salt tolerance level (4 dS m^{-1}). The salinity of groundwater is decreased by the dilution of irrigation water, but the rising water table increases the risk of soil salinity.

Elguedri (1999) and Chaibi (2005) reported geothermal waters of the aquifer systems of the chott.

3. STUDY AREA

3.1. General description

In this research the Chott el Djerid playa lake in Tunisia has been selected as the study area. While many geo-environmental factors are favorable for the development of artificial solar ponds here, it is necessary to conduct geospatial research to locate the prospective areas which are most suitable. The prospect for development of artificial solar pond in southern Tunisia due to high insolation (18 MJ/m2 day) and vast arid area was mentioned by Dah et al. (2005).

Chott el Djerid (also spelled Sciott Gerid and Shott el Jerid, https://geographic.org/) is quite often referred to as the closest thing to Mars on Earth. As the name translates "Lagoon of the Land of Palms" (Shceffel and Wernet, 1980), the chott is a seasonal or endorheic lake that stays dry for the most of the year. Since it is a playa lake, the surface is composed of hard crust of different salts. The area has vivid colour due to high iron content and the environment closely resembles layered deposits of chloride salts found at high latitudes of Mars (https://www.europlanet-society.org/chott-el-jerid-tunisia-the-closest-thing-to-mars-on-earth/).

3.2. Location

Chott el Djerid is one of a series of waterbodies belonging to the "Zone of Chotts" spanning over Tunisia and Algeria and one of the largest of its kind with an area of about 4600 km² (Abbas et al., 2018). The chott stretches in east-west direction dividing Tunisia into northern and southern parts, spanning between 33°22/ to 34°00/ N and 7°44/ to 9°40/ E. The eastern narrow arm of the chott is known as the Chott el Fejej (Fig-3.1). The area is sparsely populated and there are only some settlements around the chott. These are the city of Tozeur and town of Dguache on the north, municipality of Naftah on the northwest, the village of Fatnassa, the Island of Jeziret Mosbah, Governorate of Blidet on the south, the town of El Hamma on the east.

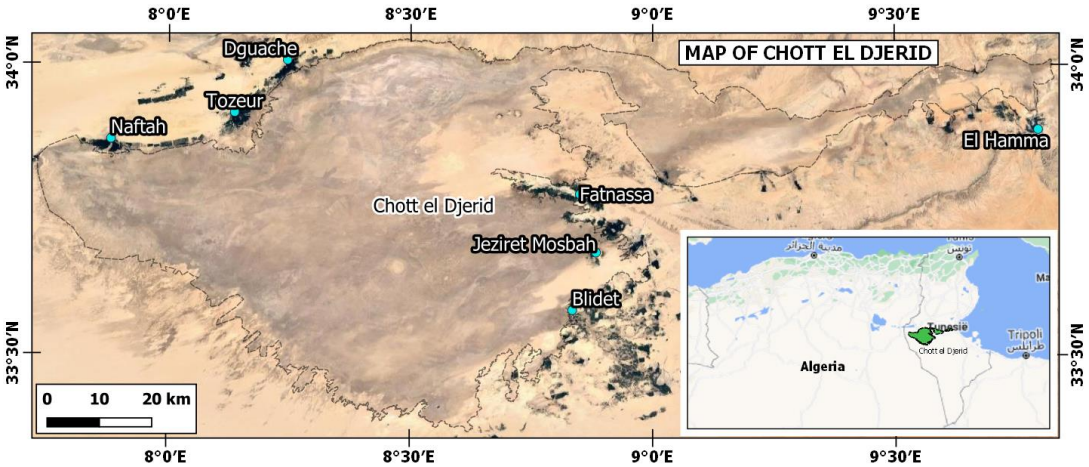

Fig-3.1: Map of Chott el Djerid (Inset: Location of Chott el Djerid in the Zone of Chotts and Tunisia, images acquired from GoogleMaps and GoogleEarth).

3.3. Geo-environmental conditions

Chott el Djerid has the characteristics of an ephemeral lake and salt playa/slat flat. An ephemeral lake is a basinal area that gets flooded for short time period during a year but the water does not persist for long. It may be stay dry for several years if there is not enough rainfall to produce flood (Whitford and Duval, 2020). As an ephemeral lake Chott el Djerid undergone flood events in 1990, 1995, 2003, 2006, 2007, 2009, 2010, 2011, 2014 and 2015 due to runoff from the surrounding relief and water resurgence. The desiccation of flood water results in the deposition of evaporite salts such as halite and gypsum during the dry period from May to August. Thus a large salt playa is formed in the northern part of the chott. (Abbas et al., 2019). There is also plenty of sunlight in the chott as it is located in southern Tunisia which is an arid region and is characterized by high insolation with annual average global solar radiation exceeding 2000 kWh/m^2/year (El Ouderni et al., 2013). The images in Fig-3.2 through 2.4 shows some aspects of the chott collected from image sharing site https://www.flickr.com/.

Fig-3.2: Flooding in the chott. (Photo Credit: David Stanley, Title: Chott el Djerid, License: https://creativecommons.org/licenses/by/2.0/, image was cropped and resized)

Fig-3.3: Drying up of the lake after flood. (Photo Credit: Marcin Grabski, Title: Before Sunrise, License: https://creativecommons.org/licenses/by/2.0/, image was cropped and resized)

Fig-3.4: Vast flat salt plane of the chott. (Photo Credit: Kamil Porembinski, Title: Chott el Djerid, https://creativecommons.org/licenses/by/2.0/, image was cropped and resized)

3.4. Hydrogeology

It is a low-lying flat area with mean elevation of only about 16 meter above mean sea level and saline water in the underlying sediments (Abbas et al., 2018). The chott basin is also characterized by large underground aquifer system. A detailed description of the aquifer system has been provided by Kamel et al. (2007) the summary of which is given in Fig-3.5 along with the associated geological units.

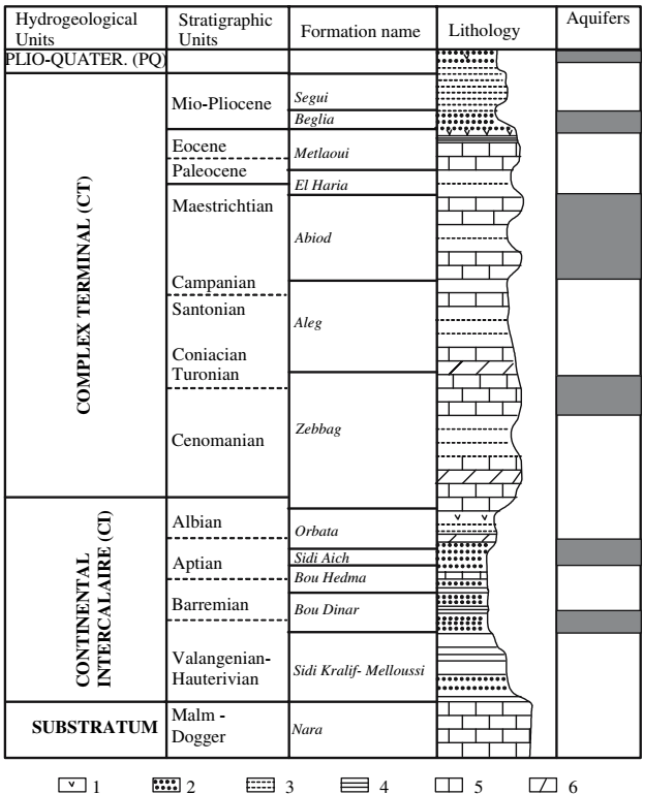

Fig-3.5: Aquifer system and associated geological units (1 gypsum, 2 sand and sandstone, 3 dayey sand, 4 day, 5 limestone, 6 dolomite) (Adopted from Kamel et al., 2007).

The lowermost aquifer system is termed as the Continental Intercalaire (CI) which is one of the largest confined aquifers in the world. The area of the aquifer is about 600000 km^2 and the thickness is between 120 and 1000 m (Castany, 1982). It contains the Bou Dinar Formation which is 60 m in thickness and forms an aquifer in the northern part of the chott. Another formation is the Sidi Aich which is the main

aquifer and is 150 m in thickness. It expanse the western part of the chott and forms an important geothermal fields with production ranging from 600 to 1000 l/s in different places (Kamel et al. 2007). The transmissivity ranges from 0.8 x 10^{-3} to 4.5 x 10^{-4} and storage coefficient ranges from 0.2 x 10^{-4} and 1.4 x 10^{-4}. The geothermal water is utilized for heating and irrigating greenhouses and for bathing purposes (Elguedri, 1999). The temperature of the geothermal water of the CI aquifer system may reach up to 70 °C (Chaibi, 2005).

Above the CI is the relatively homogeneous Complex Terminal aquifer system containing three main aquifers separated by semi-permeable to impermeable strata. The lowermost is Zabbag Formation with thickness varying from 120 to 150 m. The middle Abiod Formation is 100-200 m thick. The top most Beglia Formation is 250 to 300 m thick. The transmissivity of the Beglia Formation ranges from 0.1 x 10^{-2} to 4.5 x 10^{-2} m^2/s (Kamel et al., 2007). This aquifer system is also known as a source of geothermal water. The temperature is however lower than the CI ranging from 30-50 °C (Chaibi, 2005).

The topmost aquifer system i.e. Plio-Quaternary (PQ) water table aquifer system, present over almost the whole Djerid basin. It may locally contain a 0.5-1.5 m thick gypsum crust. The thickness of the aquifer may vary from 10 to 40 m to the south and 400 m to the north of chott. Water is withdrawn from this aquifer at about 4 millions m^3/year through more than 2000 dug wells below 50 m depth. The transmissivity of the PQ aquifer ranges from 3 x 10^{-3} to 5.5 x 10^{-4} m^2/s (Kamel, 2013).

Furthermore, the chott area is characterized by many oasis (about 30). The drainage network consists El Khanga wadi (about 50 l/s) and Melah and Tseldja non-perennial reivers. The El Khanga wadi originated from groundwater springs. Melah and Tseldja rives collect surface runoff from neighboring hills (Kamel, 2013).

3.5. Climatic condition

The climate of the chott is arid the precipitation is irregular and low. Annual average rainfall over a period of 1650-2004 is 91 mm and 101 mm recorded at two meteorological station in the northwestern part. The mean annual temperature is about 21 °C, evaporation is about 2102 mm/year (UNESCO, 1972) and evapotranspiration (by Thornthwaite, Turc and Penman methods) ranges from 1275 (in 1991) to 1806 (in 1989) per year between 1984 and 1991 (ONM, 2010; Kamel, 2013).

3.6. Geographic comparison with an existing solar pond

Since the research is focused on the assessment of geo-environmental condition of Chott el Djerid for the solar pond development, it would be logical to compare the conditions with an area where solar pond has already been developed. For that purpose, a location in Beith Ha'Arava, Israel where the largest solar pond was developed has been chosen. Both the places are near the shore of the Mediterranean Sea and belong to the same geographic belt (Fig-3.6) and hence should have similar geo-environmental conditions.

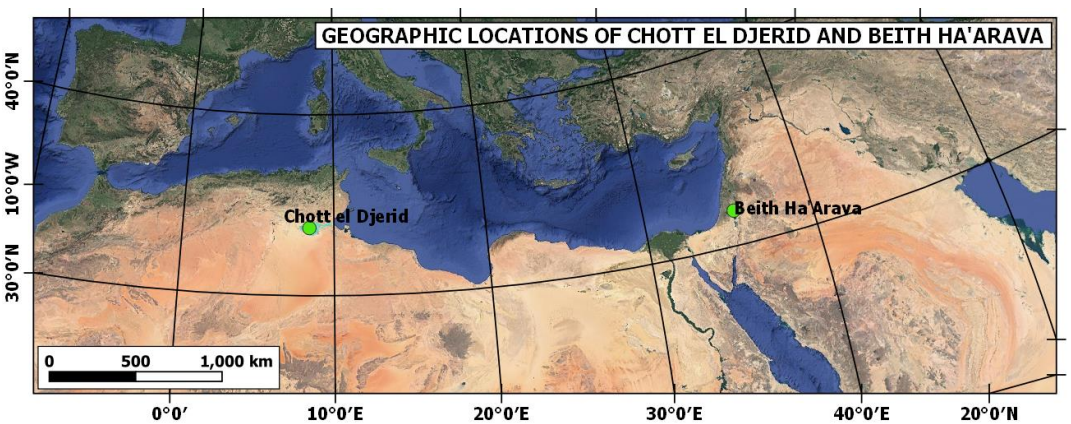

Fig-3.6: Relative geographic positions of Chott el Djerid and Beith Ha'Arava.

The Beith Ha'Aravas solar pond can be identified in the GoogleEarth image (Fig-3.7). A zoomed in view (Fig-3.8) shows the solar pond and the surrounding areas containing the operational facilities.

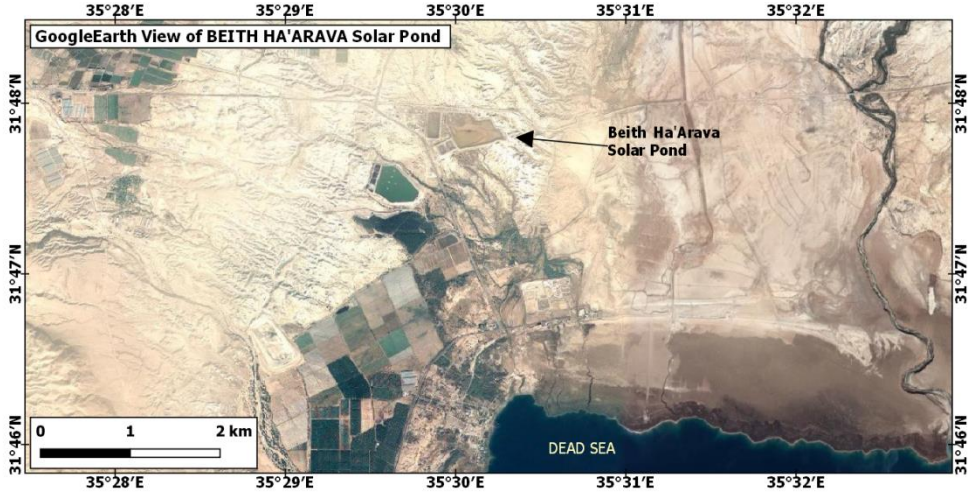

Fig-3.7: The Beith Ha'Arava solar pond in the GoogleEarth image.

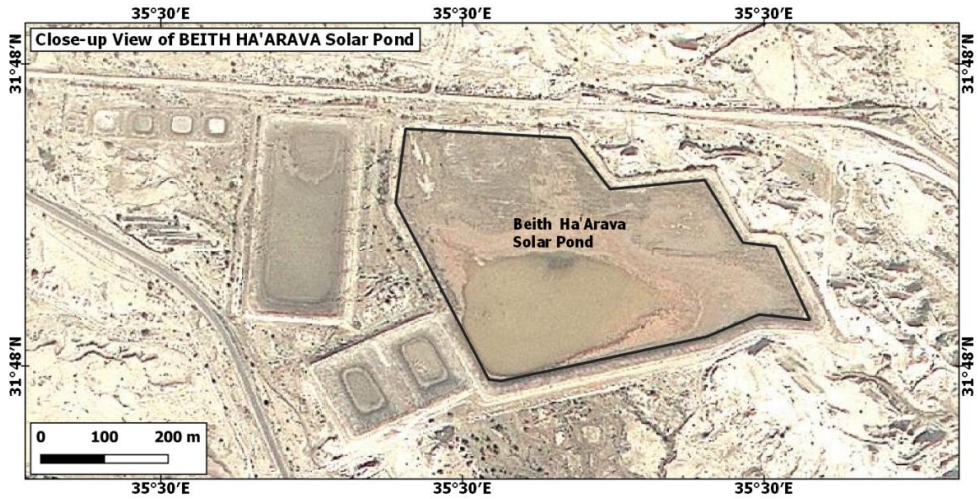

Fig-3.8: Zooermed in view showing the Beith Ha'Arava solar pond and surrounding facilities.

4. METHODOLOGY

4.1. Approaching the research question

In order to answer the question of identifying the suitable location for developing solar pond it is necessary to work with a different number of conditions. Some systematic approaches needed to be taken such as defining the working principle of a solar pond, selecting relevant and appropriate variables, collecting and generating necessary data, and analysing the data in a proper way. Nower et al. (2020) followed an approach of assembling, reviewing, analyzing and categorizing solar pond and clean energy related literature to evaluate and select relevant data and analysing such data for selecting suitable site for solar pond development. A similar approach has been followed in the current research.

An adequate understanding of the working principle of a solar pond is important to evaluate which aspects of the solar pond are geospatially important and should be considered for assessment of potential of artificial development. The working principle of a solar pond has been discussed in detail to achieve that. Based on that knowledge and the research objectives, the relevant variables have been identified and chosen for further analysis. This also determined the choice of data and for that different raw data and geospatial products have been selected and processed. The data have then been prepared for analysis and an appropriate analytical method has been chosen. Since, the selection of potential location for solar pond is a question of multiple variables, a multi-criteria analytical method has been chosen. The GIS based multi-criteria analysis has been applied in many geospatial decision problems and is a well-established analytical method for such decision problems where many variables are analyzed to find a better solution from a number of alternatives. The methodological approach has been portrayed by a flow chart (Fig-4.1) showing the relation of different parts.

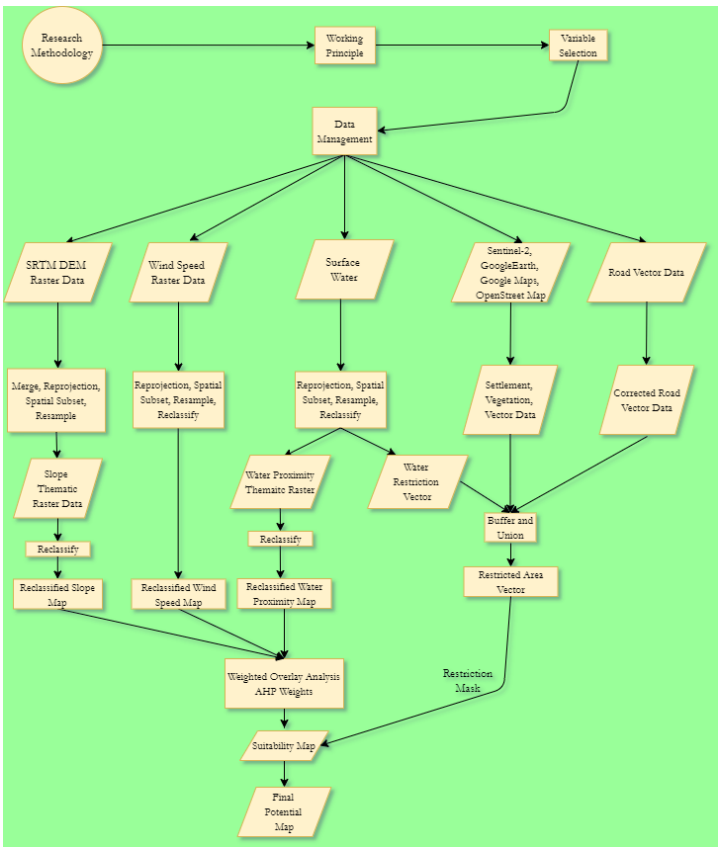

Fig-4.1: Flowchart representing the steps of the methodology.

4.2. Working Principle

4.2.1. Construction and energy balance

The building of large pond several meters deep it is not necessary to dig out a hole that big. The pond area can be flattened with conventional land-working machinery and the removed earth can be used to construct the walls. The walls should be 3-4 m wide to the top to allow vehicle movement on them. The slope may be 1 in be on the inside and 1 in 2 on the outer side. The pond geometry has small effect on the lateral temporal distribution and hence large pond can be of any shape following the natural topography rather than forced to be rectangular. A minimum depth of the storage zone is necessary to prevent high flow when withdrawing heat but more depth has no adverse effect and rather adds to the storage volume. Thus, it is not required to flatten the whole area only except ensuring that at every point the minimum depth has achieved. Thus a large earth working can be saved if the site is not naturally flat (Tabor and Doron, 1990).

The solar pond as an energy storage device stores solar energy, charging during high solar insolation months of the year, and make it possible to use the energy when needed. Part of the incident solar radiation is reflected from the surface of the pond while most of it is propagated downward. A fraction of it is rapidly absorbed in the Upper Convective Zone (UCZ) and is lost to the atmosphere by convection and radiation heat transfer. Part of the remained radiation is absorbed in the Non-Convective Zone (NCZ) in the middle before the rest of it reaches the bottom Lower Convective Zone (LCZ) where it is converted into heat and stored as sensible heat in the high concentration brine (Alcaraz et al., 2018; Valderrama et al., 2016).

The amount of incident sunlight on the water surface determines the efficiency of the solar pond hence it also determines the amount of heat gained. However, due to different heat losses the amount of gained heat may vary among solar ponds. The process of heat loss and gained can be formulized mathematically and there are many mathematical and numeric models for estimating the storage zone temperature. There are different types of one and two dimensional models describing both the static and dynamic behaviours of solar ponds. Different energy balance equations represents the internal heat generation and storage mechanism of a solar pond. The energy balance equations for the thin and least dense upper layer and the densest lower layer are the main working principle of solar pond Egbe et al. (2013). Different models aim to discuss absorption of heat from solar radiation, convection heat loss, radiation heat loss, evaporative heat loss, inlet heat flux, heat loss from the side walls, bottom losses, and outlet heat flux for the UCZ, NCZ and LCZ.

4.2.2. Storage zone temperature

The storage zone temperature can be determined from energy balance equations. However, since they are computationally extensive there is a method stated by Egbe et al. (2013) to estimate the storage zone temperature by comparing the solar radiation with an existing solar pond. For that purpose an existing solar pond in Riyadh has been compared with the chott (Table-4.1). The Riyadh data has been collected from Egbe et al. (2013) and the chott data has been collected from the https://ec.europa.eu.

The Fig-4.2 shows that the monthly average GHI values of Riyadh and the chot are very similar which implies that the storage zone temperature should also be similar. The storage zone temperature during a year in the Riyadh solar pond has been shown in Fig-4.3 where the maximum temperature may reach 75

°C during the summer months of June-August. The storage zone temperature of the chott may also be assumed from that.

Table-4.1: Monthly average solar irradiation in Riyadh and Chott.

Month	Riyadh Radiation (MJ/m²/day)	Chott Radiation (MJ/m²/day)
January	13.536	13.236
February	16.668	14.7084
March	19.368	19.8768
April	22.284	22.7436
May	25.74	29.3508
June	28.332	28.518
July	27.324	30.126
August	25.74	26.754
September	22.824	21.5508
October	19.692	16.9764
November	15.192	12.9744
December	12.672	12.7032

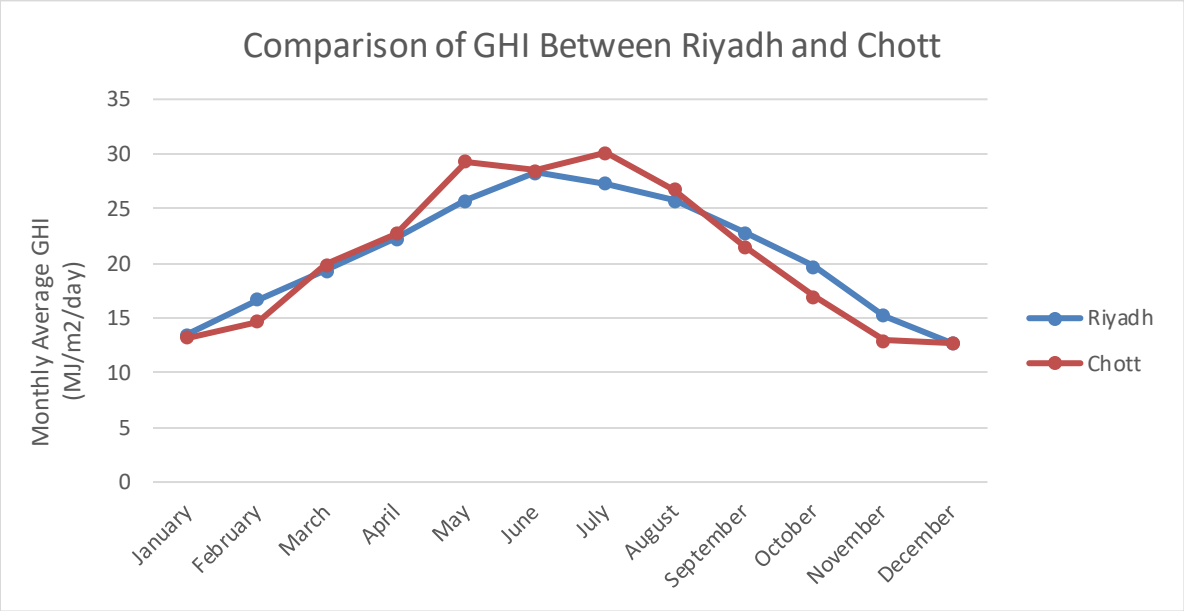

Fig-4.2: Comparison of monthly average solar irradiances in Riyadh and Chott.

The solar pond needs some time which is termed as phase difference to attain the maximum temperature after the start of the operation or reception of the maximum solar radiation since the heat is accumulating gradually. Baharin et al. (2017) reported a phase difference of four weeks for a small scale, experimental solar pond in Malaysia. Chakrabarty et al. (2020) reported a phase difference of 42 days for a solar pond

in Bhabnagar in India. They also mentioned that solar pond with larger areas require less phase difference to attain high temperature.

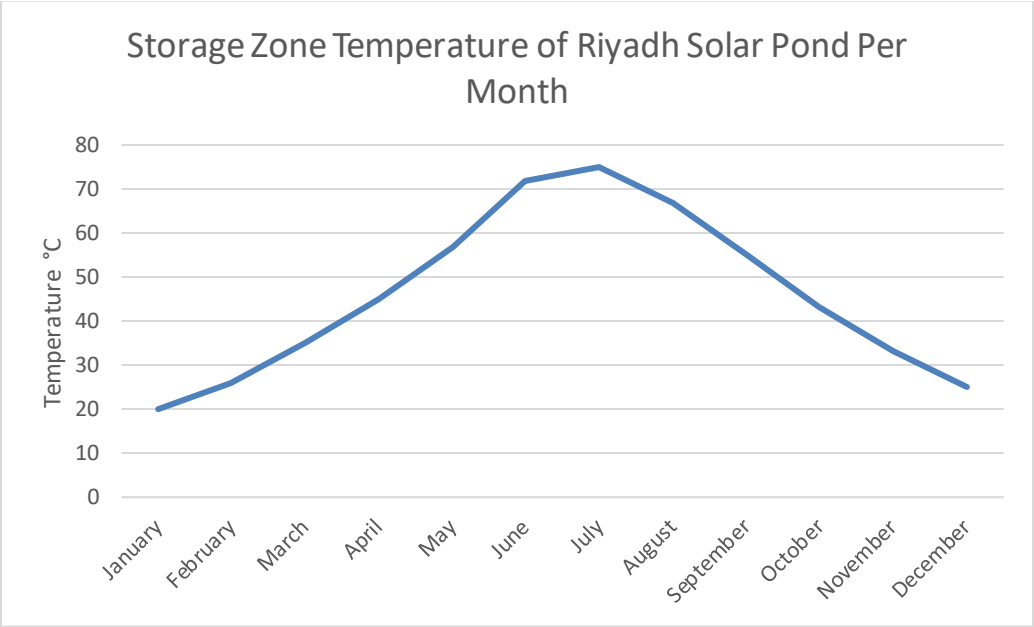

Fig-4.3: Monthly average storage zone temperature of Riyadh solar pond.

4.2.3. Other factors affecting the storage zone temperature

Egbe et al. (2013) presented the effect of different gradient zone depths on the storage zone (LCZ) temperature. It is found that 1 m is the optimum depth for gradient zone as it shows an increasing trend for the first 6 months and reached 105 °C after that period when the temperature starts to decrease again. He used different depths of 0.4, 0.6 and 0.8 m but the performance is best for 1 m as more and more solar radiation is absorbed by the gradient zone and less heat loss from the storage zone.

The storage zone temperature should increase with the increase of surrounding temperature but rather loss heat due to evaporation, radiation, conduction and convection. The evaporation heat loss of solar pond can be prevented by covering it with insulating material (Egbe et al., 2013).

The relationship between the radiation and storage zone temperature is influenced by the thickness of gradient zone. For example, at 1 m depth 36% of the radiation is available and 2 m depth it is only 30% (Egbe et al., 2013).

Increasing the density of the storage zone would increase the temperature as more heat will be trapped but there is an issue with that since more salt flushing would also be required in the UCZ. Moreover, if the density of the upper layer increases, the temperature of the LCZ would decrease and that would require more maintenance by removing the salted from the UCZ (Egbe et al., 2013).

Heavy rain and wind can cause instability of the solar pond system and can affect its efficiency (Alcaraz et al., 2018). However, if rainfall is not heavy, it may help maintaining the density of the UCZ at a low value. During raining there is no need for flushing the UCZ to maintain its low density. On the other hand, heavy monsoon rain may penetrate to the NCZ and dilute it and hence it would be needed to maintain a thicker surface zone in rainy season (Baharin et al., 2017). Wind velocity also influence the selection of the thickness of the UCZ since it may affect the stability of the zone (Chakrabarty et al., 2020) however, wind speed of up to 3-4 m/s would have no effect on UCZ beyond 30 cm from the surface (Ding et al., 2016). Algae may reduce transmission of energy through (Tabor and Doron, 1990) the pond and hence special measures may be needed to control them if not eliminated entirely.

4.3. Variable selection and data management

4.3.1. Evaluating relevant variables

As stated in the objective of the research the different geo-environmental aspects of Chott el Djerid would be studied to identify the optimum site for solar pond development. Thus it is necessary to identify the most relevant geo-environmental variables affecting the efficiency of solar pond. Different authors have discussed about different geo-environmental conditions that should be considered for selecting the site for solar pond development.

Date and Akbarzadeh (2014) described the optimum site for solar pond to be flat land with free draining and solid dry soil, easy supply of cheap saline water, high solar radiation, low wind speed, low sedimentation, and least heat loss to groundwater. Vichare (2015) emphasized on the accessibility to water and salt, low wind speed, relatively flat site, soil with good cohesion for walls. Thus, suitable areas for solar pond development should have some favorable geo-environmental conditions. Moreover, there may be some restrictions where it is not possible to develop solar ponds i.e. areas with existing land use such as settlements (cities, villages etc.), vegetation (agriculture, forests etc.), road, natural water body etc. The research is thus consists of exploration and analysis of available data that indicate the conditions that influence the development of solar pond.

In a recent work of selecting potential areas for solar pond in Egypt, Nower et al. (2020) chose only four variables namely direct normal radiation (DNR), monthly average wind speed at 10 meters height from the surface, temperature, and relative humidity data. They did not consider the slope which is very important in terms of solar pond development. Also the temperature is a redundant choice as it is resulting from the solar radiation. Same is true for humidity. Furthermore, the global horizontal irradiation is used for calculating the thermal efficiency of solar pond (Ding et al., 2016; Ding et al., 2017). They also mentioned other factors such as power line and stations, road networks and cities but did not include them in the analysis explicitly.

Thus from the literature review and from the educated judgement of the author the flowing variables and factors have been chosen for further analysis to find suitable locations-

- Surface flatness (slope) by analyzing elevation data. It is desirable that the land is already flat for solar pond development to minimize earth works. The flatter the land the more suitable it is for solar pond development.
- Distribution of solar energy over the area. It is very important since it is the only energy source of the solar pond. The more the solar energy in a location the better it is for solar pond development.

◆ Distribution of wind speed over the area. A very important variable is the wind speed since it influences several factors as evaporation, siltation, and agitation in the pond. The lower the wind speed is the better for solar pond development.

◆ Distribution of surface water. Since water is the main ingredient of the solar pond sufficient supply of water needed to be ensured. If the water is located nearby the availability of water would be higher and the location would be better. However, it would not be possible to develop solar pond in watery areas as water is considered as a resource especially in harsh environment like the chott and any water resource should be preserved and must not be destroyed.

◆ Surface salinity. The source of salt or saline water is very important for the successful operation of a solar pond and hence a nearby source of salt or saline water is desired. However, in natural condition it may not always be the case and salt may need to be supplied from other areas.

The analysis of restricted and potential areas is very important while considering a solar pond. It may not be possible to develop solar ponds in already developed areas such as settlements, roads, or used for other purposes such as agriculture, natural vegetation for various reasons. So places which are already in use should be avoided and only barren lands should be considered for solar pond development. For that reason careful mapping of these types of restricted areas re needed and safe distance should be applied. Thus-

◆ Identification and mapping settlements (cities, villages, and municipalities) and setting safe distance (100 m) and proximity.

◆ Identification of vegetation (agriculture and forest) setting safe distance (100 m).

◆ Identification and mapping of existing road and setting safe distance (100 m).

◆ Identification and mapping of surface water and setting safe distance (100 m) and proximity.

have been considered while assessing the potential for solar pond to avoid conflict with any other interests. Thus a restriction layer can be generated by combining all the restriction layers.

Relevant data have been collected and processed to analyze the variables which are described in the next sections. Since, there are many factors involved in the selection of suitable location for solar pond development it would be appropriate to solve this issue using GIS based multi-criteria suitability analysis. In order to perform the analysis it is necessary to create thematic maps and assign appropriate weights to each thematic layer by an appropriate method. Before that it is necessary to select best suited data for the analysis.

4.3.2. Description of raster data

Surface elevation data- Shuttle Radar Topography Mission (SRTM) DEM data have been collected from United States Geological Survey website Earth Explorer (https://earthexplorer.usgs.gov/) to analyze the topographic information. The data provider is NASA and contains digital elevation at 1 m vertical and 30 m spatial resolutions. Eight images cover the entire Chott area. The image resolution is sufficient for the study area and is of high quality. This is one of the best and easily accessible source of digital elevation data provided by highly reliable organization. The data is provided in EPSG:4326 - WGS 84 – Geographic which is also the co-ordinate system used in the thesis and hence further reprojection has not been necessary. The data have then been merged and clipped to the extent of the study area. Fig-4.5 shows a digital elevation model of the chott.

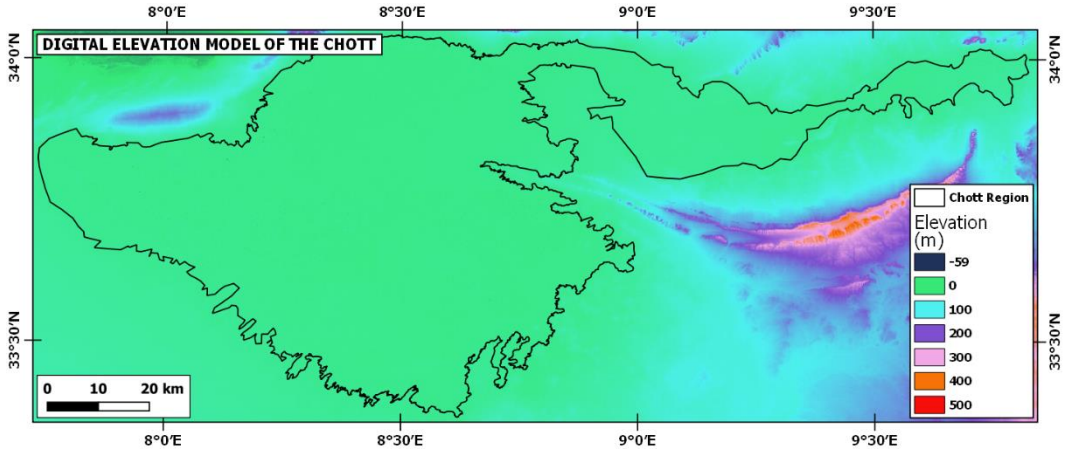

Fig-4.5: SRTM DEM of the chott area.

Solar energy data: The Global Horizontal Irradiation (GHI) (kWh/m²) data has been used to represent solar energy. This long term yearly average data ranging for a period of 1994 to 2018 is a combined effort of the World Bank Group, Energy Sector Management Assistance Program (ESMAP) (funding) and SolarGIS. The data covers the Middle East and North Africa disseminated through the website named Global Solar Atlas (https://globalsolaratlas). The purpose of the data is to assess the solar heating technologies (e.g. hot water) as well as flat-plate PV (photovoltaic). This product is an output from the SolarGIS global solar model. The spatial resolution is normally 9 arcsec (275 m). However, the data intended for introductory-level suitable for preliminary analysis.

The data is provided in EPSG:4326 – WGS 84 – Geographic coordinate system, and the spatial resolution is 0.0025 x -0.0025. The data has been reprojected to the EPSG:32632 – WGS 84 / UTM zone 32N coordinate system, resampled to 10 x 10 m resolution and clipped to the extent of 381520, 578320, 3691380, 3768420 (Fig-4.6). The data values range from 1900 to 2100 kWh/m².

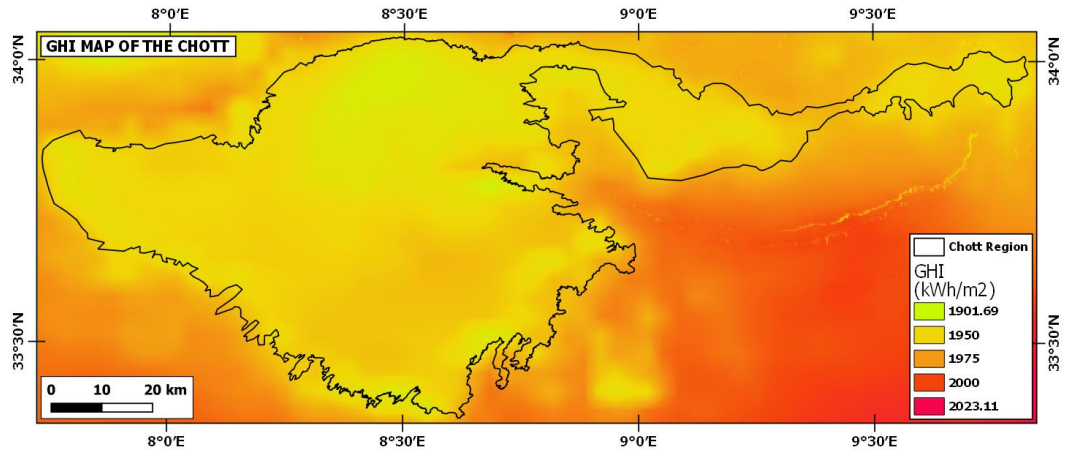

Fig-4.6: Distribution of global horizontal irradiation over the chott (Source: Global Solar Atlas).

Fig-4.7 shows the GHI distribution map of the Beith Ha'Arava solar pond and surrounding area. The Beith Ha'Arava solar pond area is characterized by GHI between 1986 and 2017 kWh/m² which is also similar to the chott area.

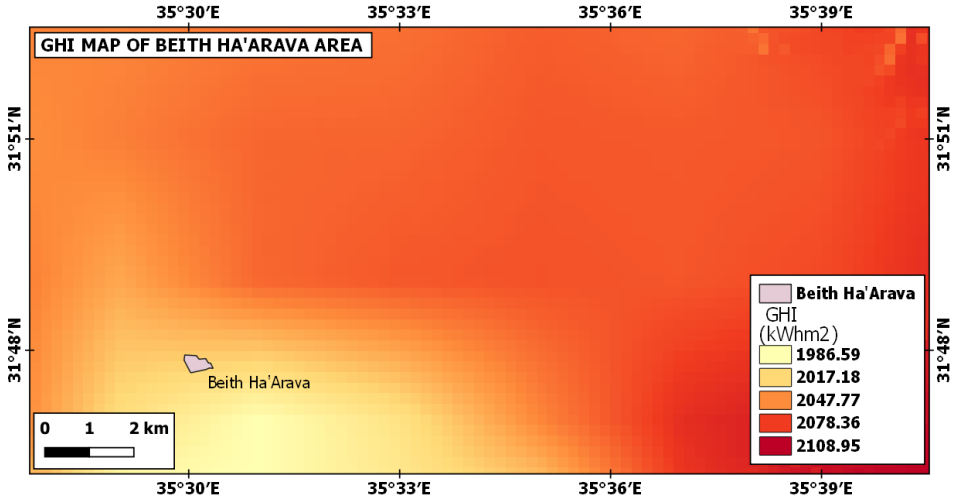

Fig-4.7: Distribution of GHI in the Beith Ha'Arava area (Soure: Global Solar Atlas).

Wind Speed: The wind speed data of the chott has been collected from the website named Global Wind Atlas (https://globalwindatlas.info). The data is a result of partnership between the Department of Wind Energy at the Technical University of Denmark (DUT Wind Energy), the World Bank Group, Energy Sector Management Assistance Program (ESMAP) (funding), and Vortex (a leading commercial provider of wind resource data analysis) and is provided for policymakers, planners, and investors for the purpose of wind power generation and perform preliminary calculations. The data and maps are freely obtainable for use in GIS tools at the global, country, and first-administrative unit (State/Province) levels.

The long term data from 2008-2017 is produced by downscaling of large-scale wind climate data to microscale wind climate data. The large-scale data is provided by atmospheric re-analysis data, in GWA version 3, the ERA5 dataset from the European Centre for Medium-Range Weather Forecasts (ECMWF) is used for the simulation for the period 2008-2017 (https://globalwindatlas.info/about/method).

The spatial resolution of the data is 230 m. The yearly average wind speed within 10 m height has been used. The data is provided in the EPSG:4326 – WGS 84 – Geographic coordinate system with pixel size of 0.0025 x -0.0025. The data has been reprojected to EPSG:32632 – WGS 84 / UTM zone 32N coordinate system, resampled to 10 x 10 m resolution and clipped to the extent of 381520, 578320, 3691380, 3768420. Fig-4.8 shows the wind speed distribution over the chott which varies from 2.3 to 8.31 m/s.

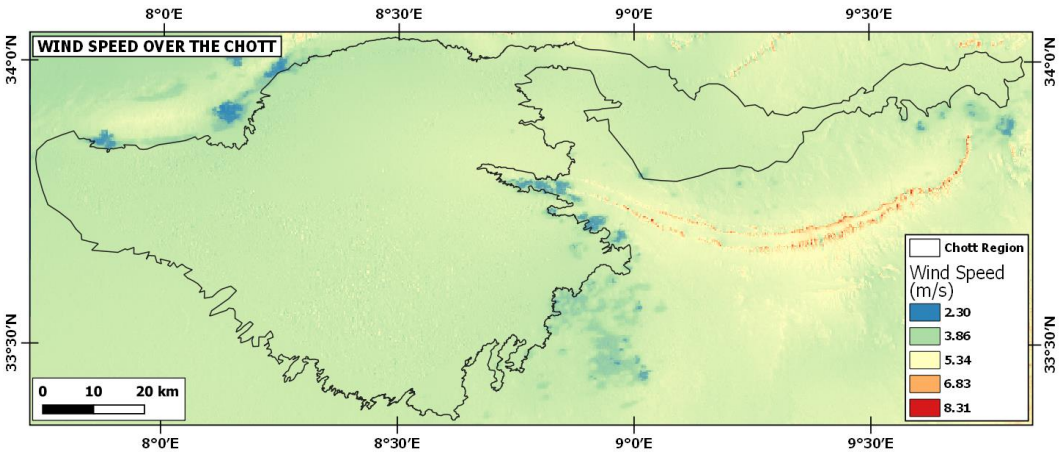

Fig-4.8: Wind speed distribution over the chott (Source: https://globalwindatlas.info).

Fig-4.9 shows the wind speed distribution of the Beith Ha'Arava solar pond and surrounding area. The pond and neighbouring area is characterized by wind speed range of 3. The wind speed in the chott is also near this range.

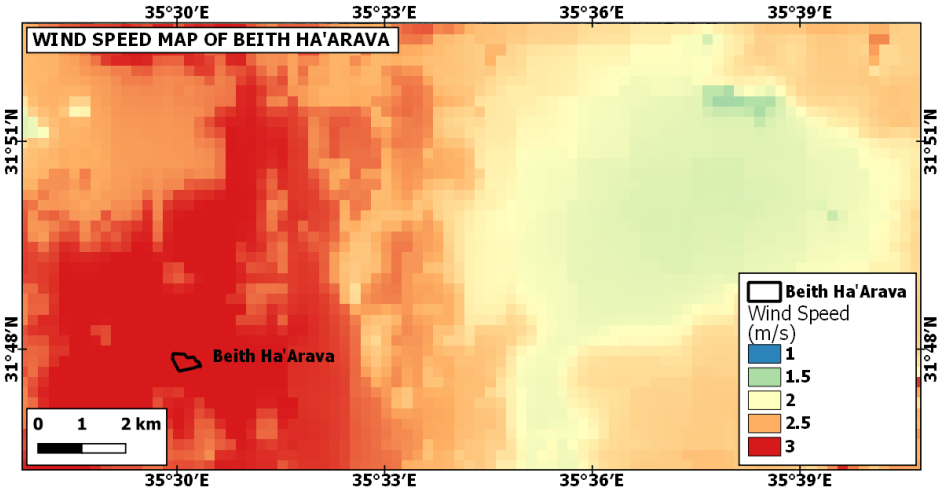

Fig-4.9: Wind speed map of the Betih Ha'Arava (Source: https://globalwindatlas.info).

Surface water data: For surface water the data provided by the Global Surface Water Explorer website (https://global-surface-water.appspot.com/) have been used. The data and maps show the spatial and temporal distribution of surface water of the last 37 years. The statistics on the extent of the water surface is also available. The data is provided under the Copernicus Programme by the Joint Research Centre, European Commission and is free to use. The data can be explored and downloaded from Global Surface Water Explorer which is a web-mapping tool that shows all type of surface coverage of water globally.

There are several types of data among which the water transitions data has been used for this research. The data can be downloaded in tiles 10° x 10° from the global map, the location of tile for the chott is 30-40N, 0-10E. The data is provided in EPSG:4326 – WGS 84 – Geographic coordinate system, with pixel size of 0.00025 and -0.00025. The data has been reprojected to EPSG:32632 – WGS 84 / UTM zone 32N coordinate system, resampled to 10 x 10 m resolution and clipped to the extent of 381520, 578320, 3691380, 3768420.

Fig-4.10 shows the surface water distribution map over the chott with several types of water occurrences such as unchanging permanent water surfaces; new permanent water surfaces (conversion of land into permanent water); lost permanent water surfaces (conversion of permanent water into land); unchanging seasonal water surfaces; new seasonal water surfaces (conversion of land into seasonal water); lost seasonal water surfaces (conversion of a seasonal water into land); conversion of permanent water into seasonal water; and the conversion of seasonal water into permanent water. All these areas indicate inundation for a certain time. So, all these water areas should be considered as protected and restricted areas. On the other hand, only except the lost permanent and lost seasonal water, all the other water areas may be considered as potential source of water (Fig-4.11).

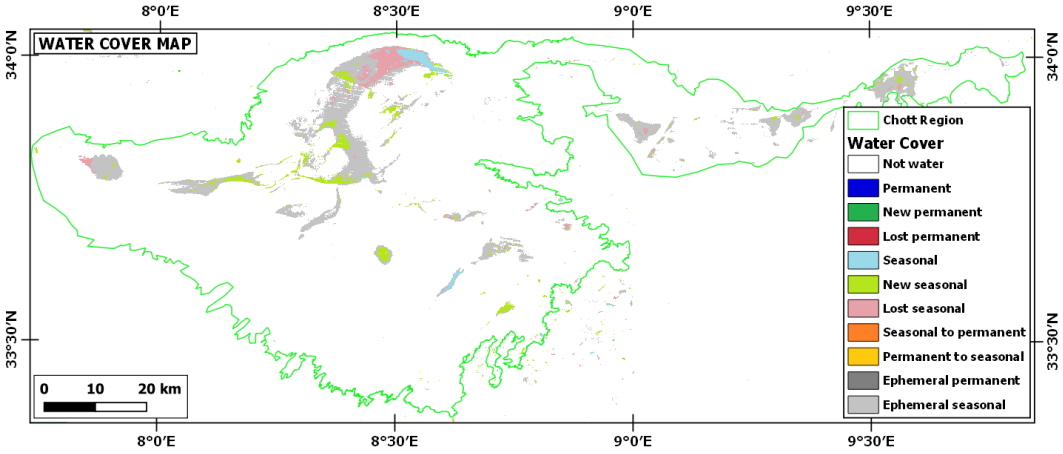

Fig-4.10: Surface water occurrence map over the chott (Source: Global Surface Water Explorer).

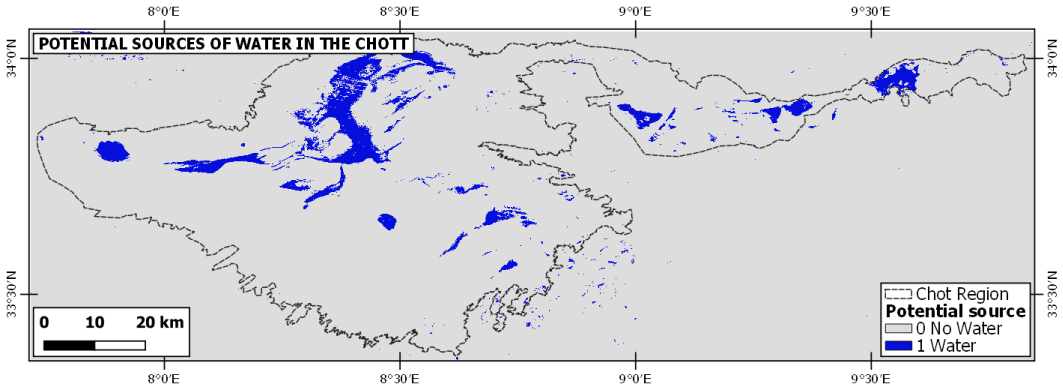

Fig-4.11: Potential sources of water represent permanent water bodies (Source: Global Surface Water Explorer).

Spectral data: Sentinel-2 imagery has been used as spectral data of the various surface features to identify vegetation, settlement, road, barren lands, and settlements. Two sets of data have been collected from Copernicus website (https://scihub.copernicus.eu/) representing wet and dry periods. The data provider is European Union/ESA/Copernicus which is of high temporal, spatial and spectral resolutions. Sentinel-2 is a constellation of two satellites (A and B) operated by European Space Agency (ESA). The sensor is called Multi Spectral Instrument (MSI) and has 13 bands. Band B2 is Blue, B3 is green and B4 is Red, B8 is NIR, are all 10 m spatial resolution and have been used to calculate various indices. Other bands are of higher resolution and have been resampled to 10 m resolution if used. Here the Level-2 images have been used. Level-2 is surface (bottom of the atmosphere [BOA], top of canopy [TOC]) reflectance, which is atmospherically corrected, band B10 is excluded, reflectance is calculated and land cover classification band is added.

The wet period spans from September to April and dry period from May to August. Images from January, 2020 and July, 2019 used as representative of the wet and dry periods respectively to observe the peak of the two seasons. Three images of Sentinel-2 required for covering the whole area. For wet period, the images
S2B_MSIL1C_20200114T101259_N0208_R022_T32SLC_20200114T121102.SAFE,
S2B_MSIL1C_20200114T101259_N0208_R022_T32SMC_20200114T121102.SAFE, and
S2A_MSIL1C_20200116T100341_N0208_R122_T32SNC_20200116T110013.SAFE have been used.
Fig-4.12 shows a true colour composite for the wet period.

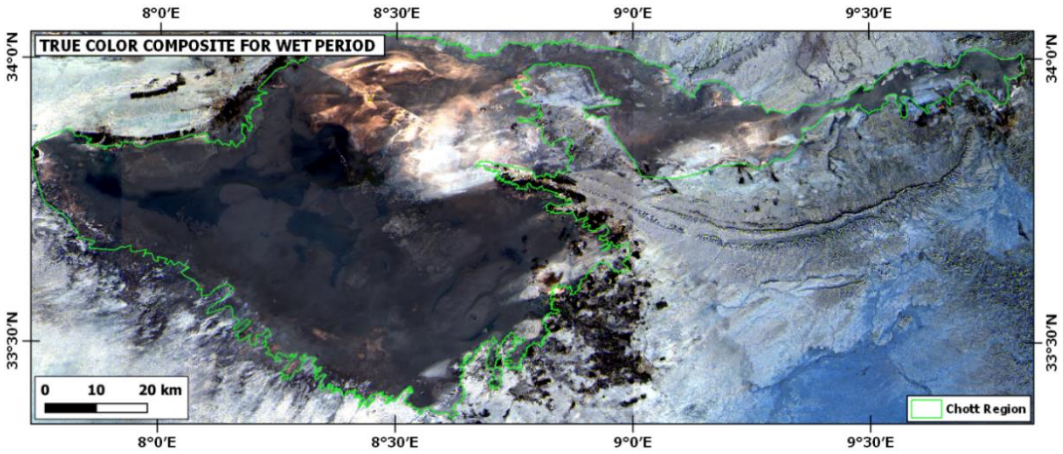

Fig-4.12: True colour composite image of the wet period (consisting of three adjacent Sentinel-2 images).

For dry period, the images
S2B_MSIL1C_20190708T101039_N0208_R022_T32SLC_20190708T125653.SAFE,
S2B_MSIL1C_20190708T101039_N0208_R022_T32SMC_20190708T125653.SAFE and
S2A_MSIL1C_20190710T100031_N0208_R122_T32SNC_20190710T120330.SAFE have been used.
Fig- 4.13 shows a true colour composite for the dry period.

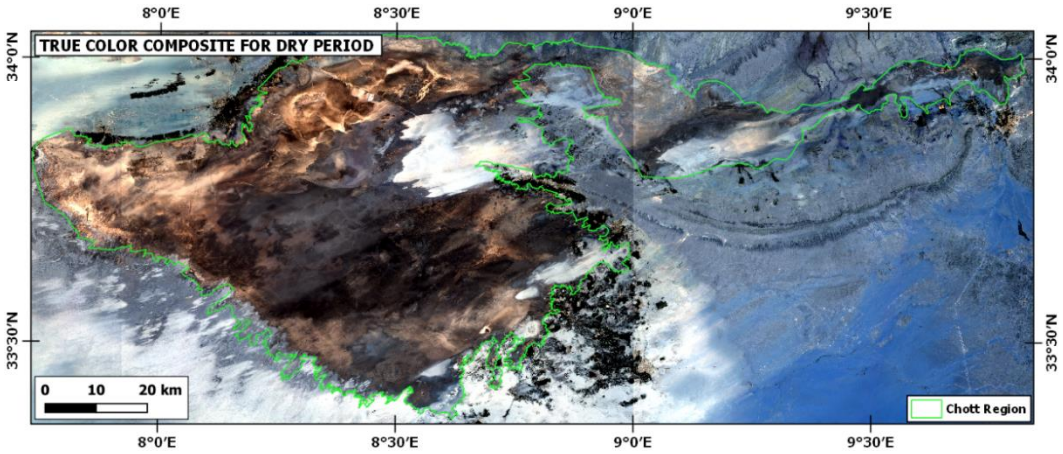

Fig-4.13: True colour composite image of the dry period (consisting of three adjacent Sentinel-2 images).

The images are from both Sentinel-2A and 2B missions with 0-5% cloud cover. The images have been downloaded as Level-1C products and has later been atmospherically corrected to Level-2A products using Sen2Cor tool provided by ESA in command line environment.

Surface salinity Data: No salinity data of the chott has been found. Several salinity indices have been tried on but with not very satisfactory results. Although there are salt deposits and saline water in the chott, it is not very convenient with satellite data alone to have a complete and high quality estimation of the salinity here. The lack of field verification have made the issue even more acute. Salt can be imported from outer sources, and hence it may not mandatory to have salt in the area. However, since there are reports that the chott has salt deposits or saline water, detail information on salinity may help the evaluation the importance of salinity in the assessment possible.

A laboratory experiment was conducted to understand the spectral behavior of salt. For the experiment different desert minerals such as quartz (pure sand), kaolinite, gypsum, halite and water were used as both

individual and mixtures to replicate the desert condition. The samples were analyzed with XRD, SPECIM, and ATR instruments for both dry and wet conditions (the detail reports have been provided in Appendix A, Appendix B, Appendix C respectively). However, the wet samples could not be analyzed due to high water content. Thus, it was dried and after drying it resembled the desert condition with a hard crust. The sample was homogenized by crushing and thus it became same as the dry sample again. But interestingly enough the results of these two samples were somewhat different. From the experiment a conclusion was made that the dissolution and recrystallization of salts changed the spectral behavior of the bulk sample and hence make the detection of desert salts very complicated by remote sensing. This is even more complex in the real situation due to the unlimited number of combination of different proportions of the mixture.

4.3.3. Description of vector data

Different vector data have been collected and created for the purpose of mapping and analyzing. The country boundary vector data of Tunisia has been downloaded from the site https://map.igismap.com/gis-data/tunisia/administrative_outline_boundary. Polygon vectors of the chott, the beith, the settlements, and the vegetation; the line vector of roads, the point vectors of the chott, the beith and settlements have been created by the author using different web map services such as such as GoogleEarth, Google Maps, OpenStreetMap as base layers using Qgis. The settlement, vegetation, road and water vectors have been used for creating the restricted area.

Settlement vector: There are some settlements around the chott such as small cities and villages. Since settlements are already developed areas it is not possible to develop solar ponds there. Moreover, the solar pond development should not be within a certain distance (safe distance) from the boundary of the settlements. To fulfil these conditions, the settlements have been identified and mapped. The safe distance has been chosen to be 100 m.

The settlements can be identified easily by their distinct patterns (Fig-4.15). Thus boundaries of the settlements could be manually digitized and a polygon layer of them has been generated (Fig-4.16). After creating the polygon layer a 100 m buffer layer has been generated thus indicating all the areas within a safe distance. Thus, all the other areas are potential in terms of settlements.

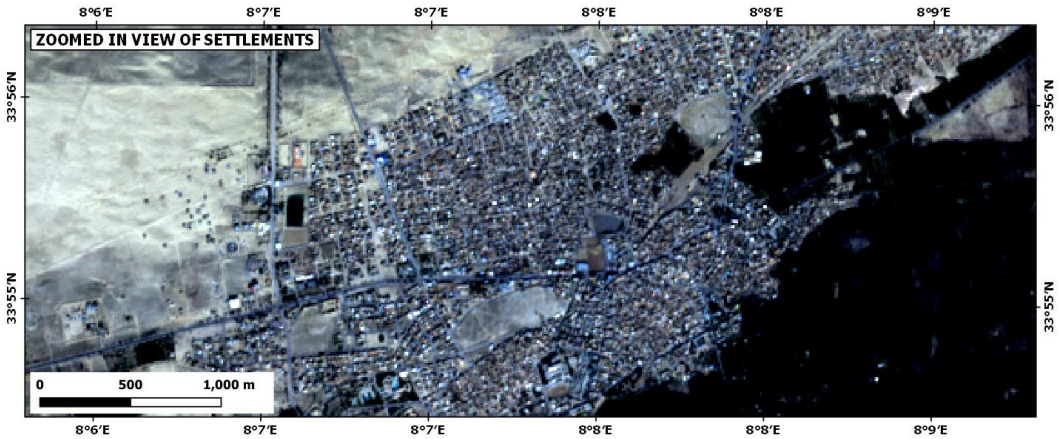

Fig-4.15: View of settlements in Sentinel-2 imagery.

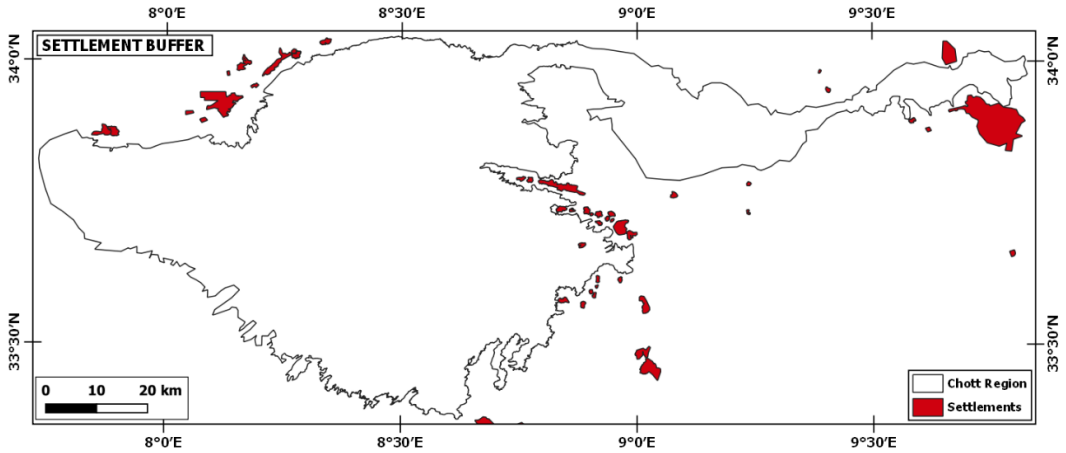

Fig-4.16: 100 m buffer of settlements polygon vector.

Vegetation Vector: Vegetation includes all the areas which are both forested and agricultural. Also the lands which are used for agriculture have been considered. The vegetation should be excluded from the development of solar pond as they are very important from environmental and economic point of view. As the study area is arid with desert landscape, vegetation is very scarce and only localized in the areas where surface water such as oases are available. So, they are not to be disturbed by the solar pond development and maintenance activities. Thus a safe distance should also be considered.

The identification of vegetation is very easy and straightforward by using false colour composite of high resolution imagery (Fig-4.17), spectral indices such as NDVI ([B8-B4]/[B8+B4]) (Fig-4.18), and GoogleEarth image (Fig-4.19). The imagery of wet period has been used since this is the time when vegetation can flourish fully and may be detected easily.

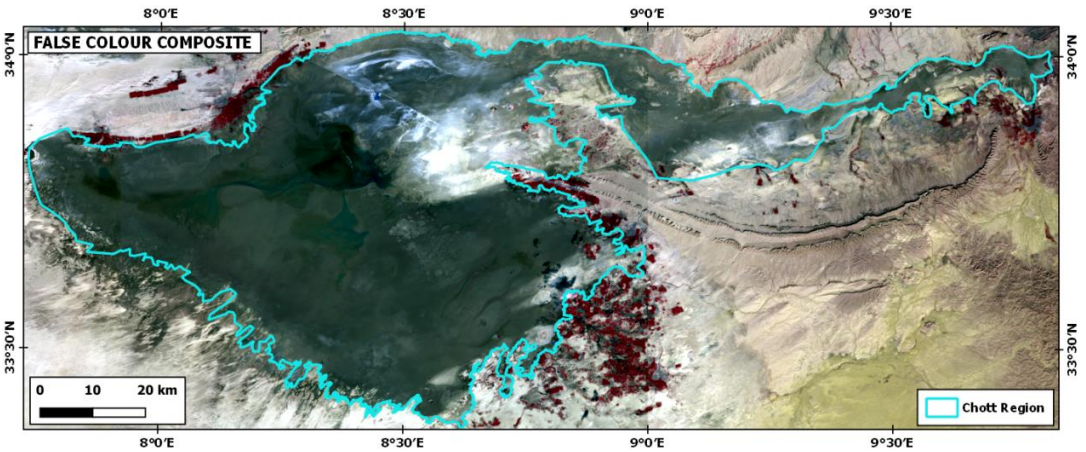

Fig-4.17: False colour composite of satellite imagery showing vegetation in dark red colour.

The only difficulty is to identify the arable lands. For that reason a visual identification method has been applied to identify those areas based on their distinct rectangular pattern (Fig-4.20) resulting from cultivation activities. A vegetation polygon layer has been created by manual digitization and applied a buffer of 100 m (Fig-4.21).

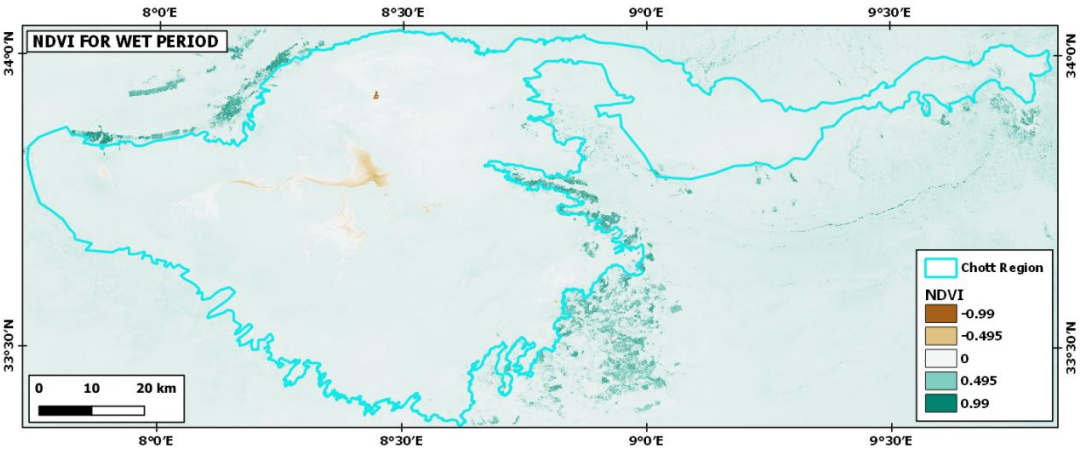

Fig-4.18: NDVI for wet period showing vegetation in green colour.

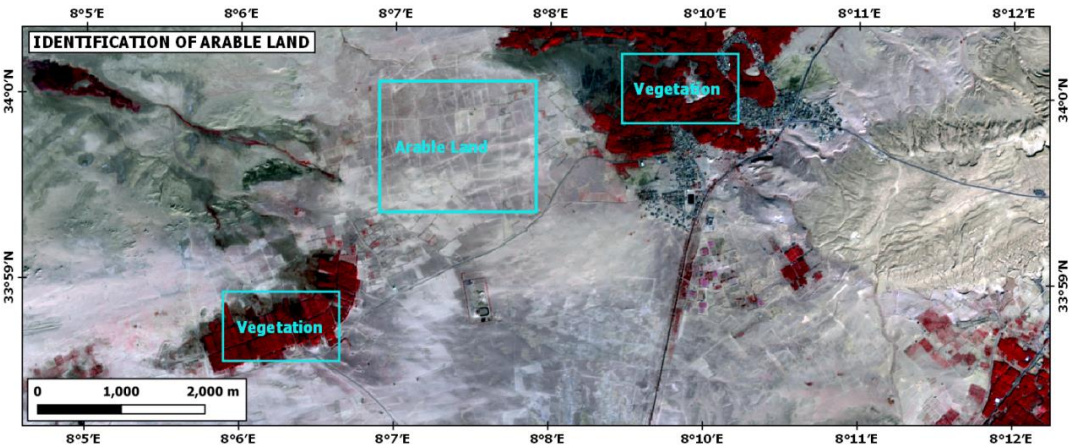

Fig-4.19: GoogleEarth image showing patches of green vegetation in a brown background.

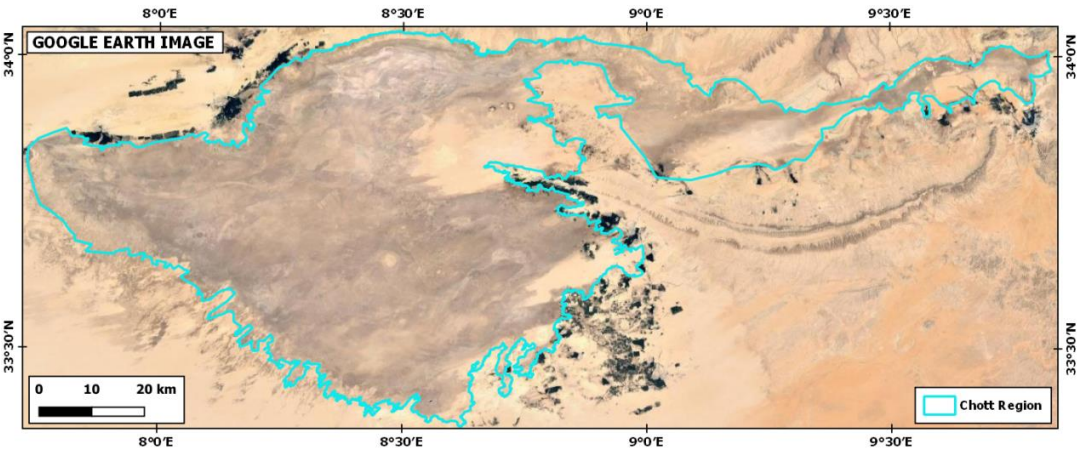

Fig-4.20: Visual identification of arable lands which are not identifiable by image analysis.

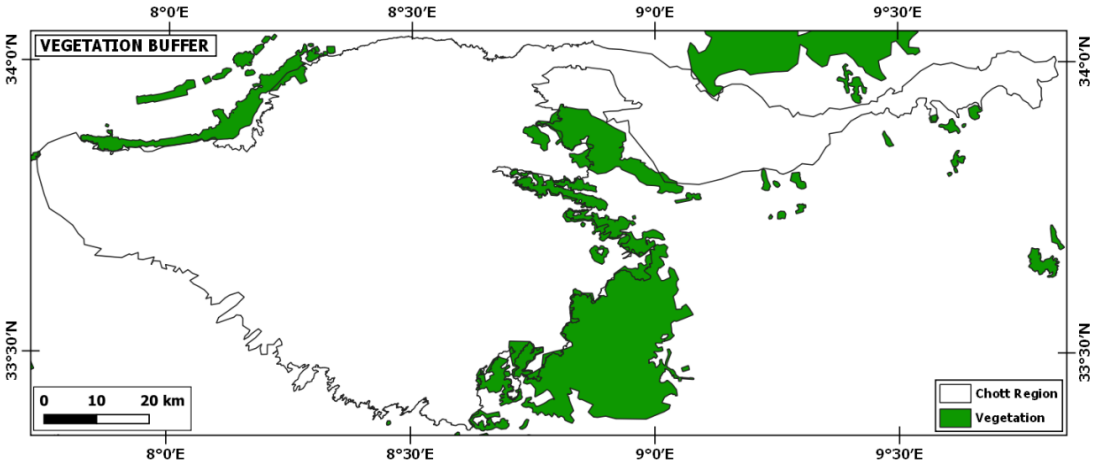

Fig-4.12: 100 m buffer of vegetation polygon vector.

Roads vector: Roads are important features that should be preserved. There are few roads around the chott that provide valuable connectivity around the chott and thus are also important from solar pond development point of view for transportation of materials needed for the construction works. As a result accurate mapping of the roads is very important. Also a minimum safe distance should be assigned to the roads so as not to interfere transportation and roadside activities.

Vector data representing roads in the chott region has been collected from the site https://geonode.wfp.org/layers/geonode:tun_trs_roads_osm which provide free vector data in shape file format. The collected vector data of the road network is not very accurate as revealed by the comparison with the GoogleEarth image (Fig-4.22), also many roads are missing (Fig-4.23).

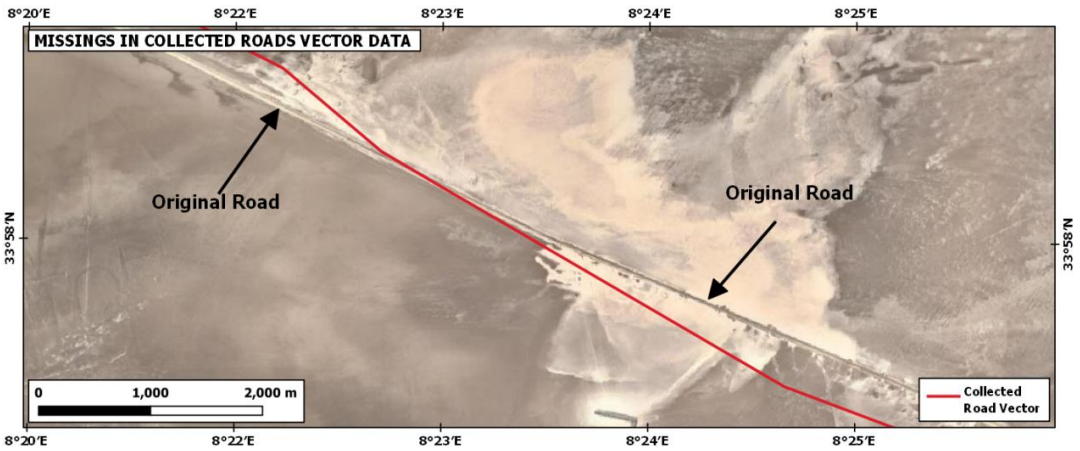

Fig-4.22: Inaccuracy in collected vector data.

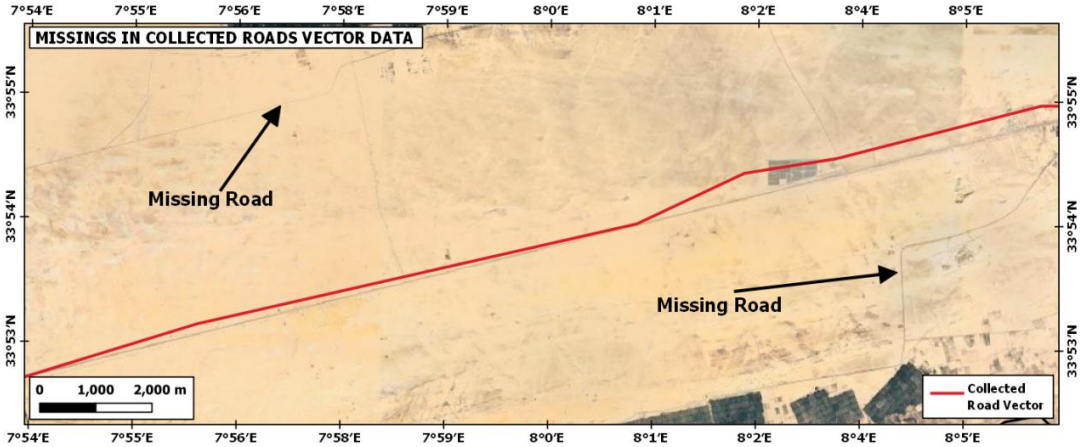

Fig-4.23: The collected vector misses some important roads.

The data has been corrected and missing roads have been updated using the GoogleEarth image as a base map and a road vector has been created and assigned a 100 m buffer (Fig-4.24).

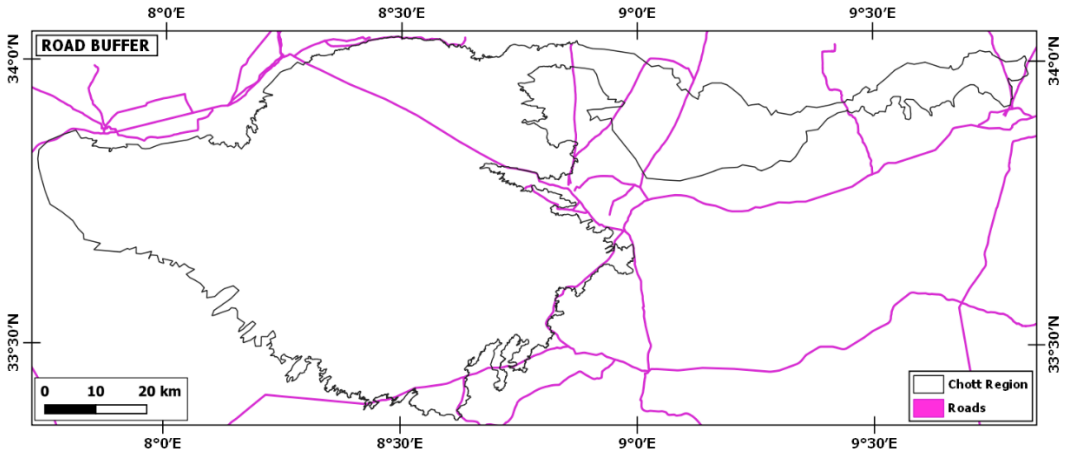

Fig-4.24: 100 m buffer road polygon vector.

Water polygon: As mentioned earlier, all the water areas should be preserved and hence it is included in the restriction layer. A polygon vector of all water areas has been created by converting the transition water raster layer in to a vector layer in Qgis and a 100 m buffer has been applied (Fig-4.25).

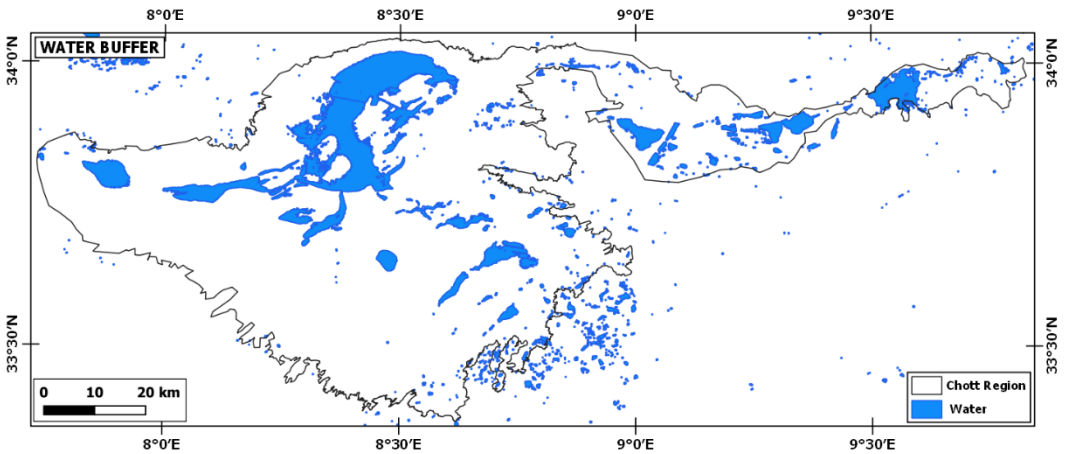

Fig-4.25: 100 m buffer water polygon vector.

4.4. Data analysis

4.4.1. Selection of data and analytical methods

The methodology consists of multi-criteria analysis of the data to get the outcome showing most suitable areas for solar pond development. The multi-criteria analysis consists of creation of thematic maps/layers (criteria layers) of the relevant data, reclassification of the thematic maps to a common scale, assign weightage by analytical hierarchy process (AHP), and running the weighted overlay operation. The thematic layers consists of slope data, wind speed data, water proximity data, and settlement proximity data. Since the solar energy value range is very low it can be considered constant over all the area and hence it has been left out of the analysis since it spatial influence would also be constant over the area. The thematic layers have been reclassified to a scale of 1-4, where 4 represents the most and 1 the least suitable areas. After that weights for each layer has been derived by AHP according to their relative importance. And finally, the weighted overlay operation can be applied to the layers by their relative weights to derive the suitability map. After that the suitability map has been multiplied by the potentiality map to get the final map of potential areas.

4.4.2. Creation of thematic/criteria layers

Four thematic maps have been created- slope map, wind speed map, settlement proximity map and water proximity map. The slope map (Fig-4.26) has been generated from the elevation data to demarcate the study area based on the flatness of the slope. The "Raster > Analysis > Slope" tool in Qgis has been used for generating the slope map.

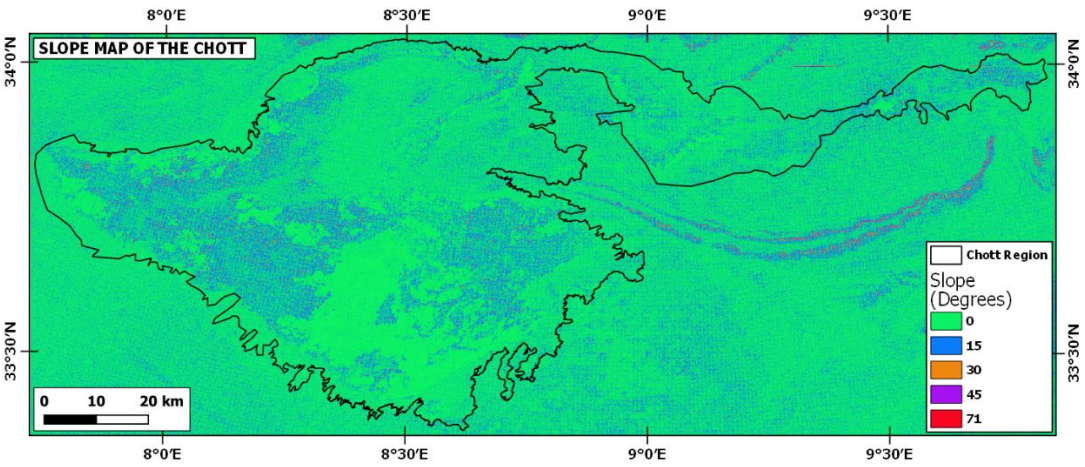

Fig-4.26: Slope map of the study area.

The wind speed map (Fig-4.27) has been created from the wind speed data within the height of 10 m from the ground. The wind speed varies from 2 to 8.5 m/s. Lower wind speeds are better for solar pond development.

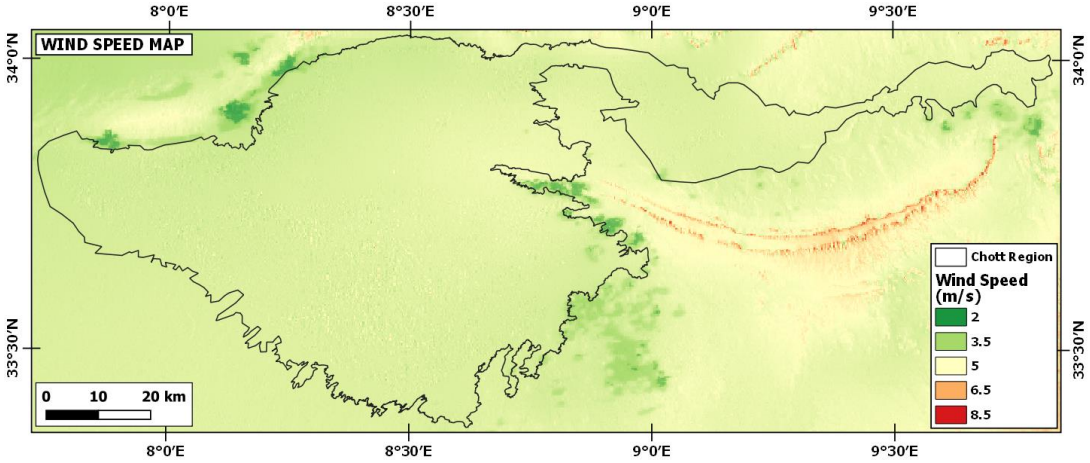

Fig-4.27: Wind speed map of the study area.

The prospective solar pond should be close to water bodies to ensure easy supply of water. Thus, proximity to water body is an important factor. A water proximity thematic map has been created using the water potential data (Fig-4.28).

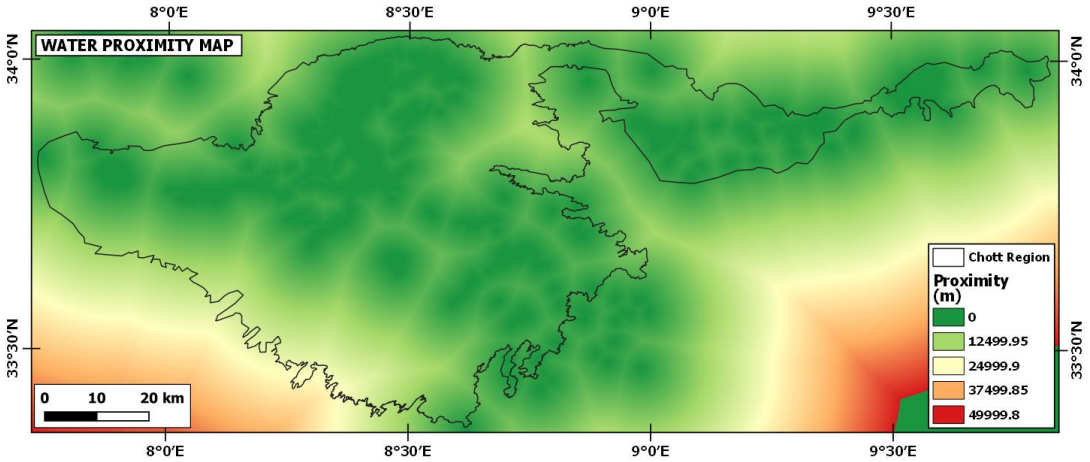

Fig-4.28: Water proximity thematic layer of the area.

The potential user of the solar energy would be the settlement areas so the prospective solar pond should be as close to the settlements as possible. Moreover, the distance should not be beyond a certain limit, which in this case has been considered 50 km. Thus, a settlement proximity has been created (Fig-4.30) from the Settlement Buffer layer (Fig-4.16) by first rasterizing (Fig-4.29) the layer and then running the Proximity (raster distance) tool in Qgis.

The following parameters has been used for rasterization: A fixed value to burn = 1, Output raster size units = Georeferenced units, Width/ Horizontal resolution = 10, Height/ Vertical resolution = 10 m, Output extent = 381531.1964, 578311.1964, 3691374.8678, 3768404.8678 [EPSG:32632], Nodata value = Not set, Output data type = float32.

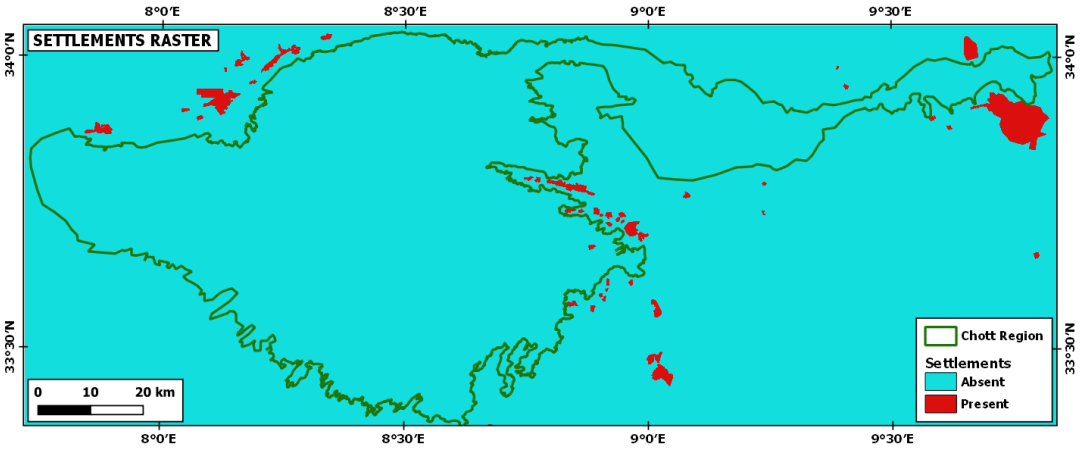

Fig-4.29: Settlement raster layer.

The following parameters have been used for generating the proximity map: Settlement_Buffer_Rasterized, A list of pixel values in the source image to be considered target pixels: 1, Distance units: Georeferenced coordinates, The maximum distance to be generated: 50 km, Value to be applied to all pixels that are within the -maxdist of target pixels: NotSet and Nodata value to use for the destination proximity raster: NotSet.

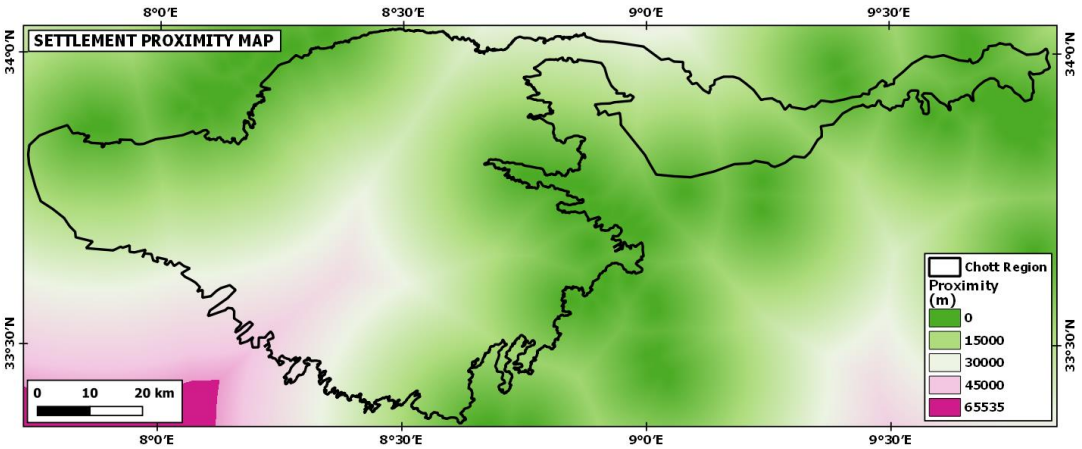

Fig-4.30: Settlement proximity map.

4.4.3. Reclassification of thematic layers

In order to perform the weighted overlay analysis it is necessary to reclassify the thematic criteria layers into a common scale for sake of comparison. Since, different data come in different formats and units, reclassifying them into a common scale enable them to be analyzed. For the purpose of reclassifying all the different thematic criteria layers in a common scale, a common range of 4 to 1 has been chosen indicating highest to lowest degree of suitability. The range of values of each thematic layers and their scale of reclassification is presented in Table-4.2. All the values that are outside the range has been given a "NoData" value. The reclassified maps are shown in Fig-4.31 through Fig-4.34.

Table-4.2: Re-scaling of the range of values of different thematic criteria.

Thematic Criteria Layers	Re-scaling of Ranges				Comments
	4	3	2	1	
Slope (Degrees)	0-5	5-10	10-15	15-30	Lower slope has higher suitability and best suitable land for solar pond should be flat or nearly flat
Wind Speed (m/s)	2-4	4-6	6-8	8-10	Lower wind speed has higher suitability, and solar pond best operate under low wind speed condition below 4 m/s
Proximity to Settlements (m)	0-10000	10000-20000	20000-30000	30000-50000	Closer areas are more suitable for potential user in the settlements.
Proximity to Water Bodies (m)	0-10000	10000-20000	20000-30000	30000-50000	Water areas close to water body is more suitable due to better accessibility to water source

Nower et al. (2020) used many classes for a rather narrow range of values. For example, they divided DNR values (5.5-8.85 kWh/m²/day) into 6 classes, temperature values (18-27 °C) into 9 classes, wind speed values (3.5-5.5 m/s) into 8 classes, and relative humidity values (20-65) into 9 classes. While it is reasonable to divide these values into further classes considering large area of a country, still the number of classes are too many considering the narrow range of values of the geo-environmental variables. Compared to that the chott is a smaller area where the range of variable values are even narrower and hence the GHI values (1900-2100) have been entirely discarded from the analysis as the variation is very small over the entire area and can be considered as a single class and hence would not have any effect in the analysis. Other values have been reclassified in a logical way acknowledging their significance on the analysis.

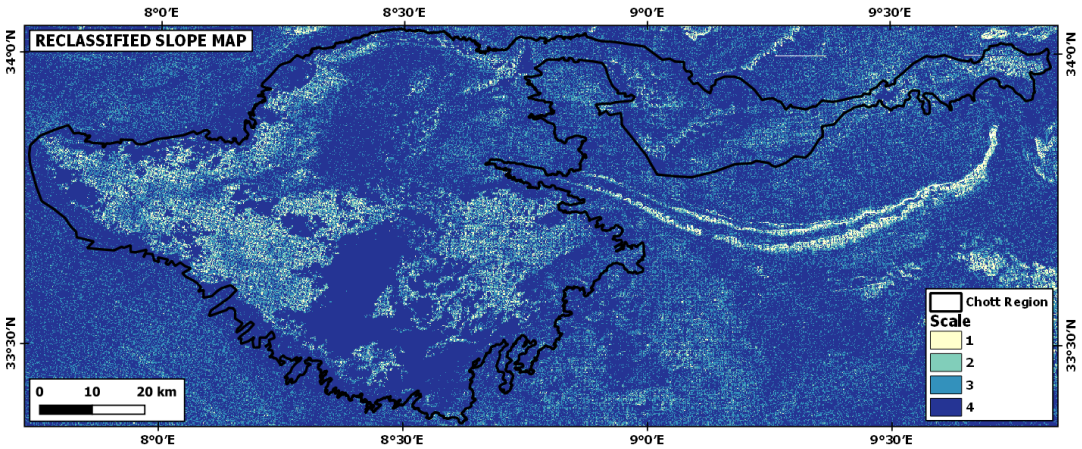

Fig-4.31: Redassified slope map.

Most of the area of the chott is characterized by gentle slope of 0-5 degrees as indicated by the scale of 4 in the reclassified slope map (Fig-4.31). There are also some areas of high slope which are indicated by 1 and are not suitable for solar pond development. These areas mostly represent the hilly areas surrounding the chott.

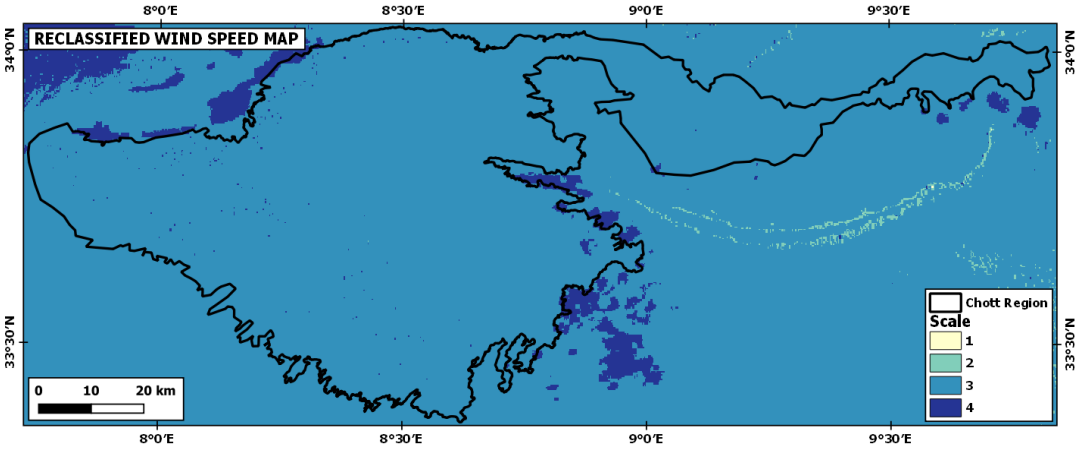

Fig-4.32: Redassified wind speed map.

Most of the chott area is characterized by higher wind speed (scale value of 3) that the lowest (scale of 4). The highest wind speed (scale value of 1) is near the hilly areas (Fig-4.32).

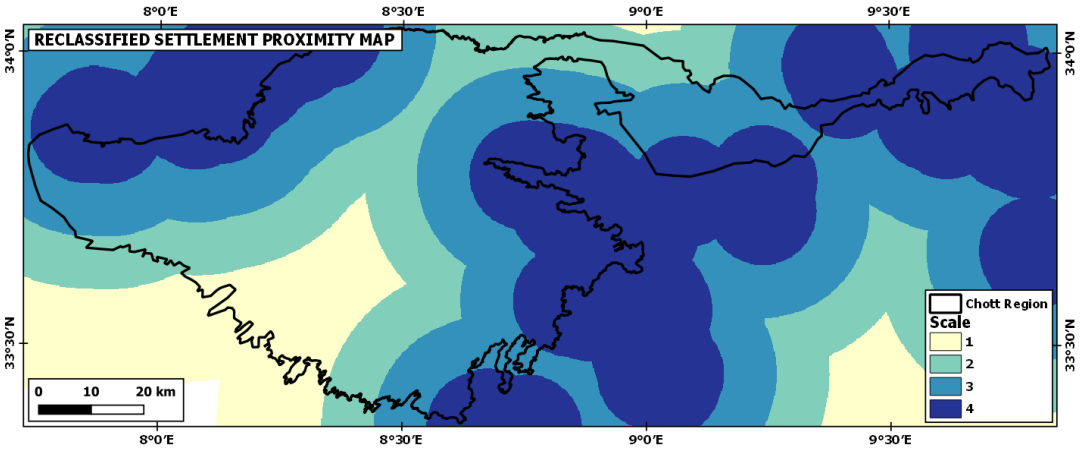

Fig-4.33: Redassified settlement proximity map.

The most suitable areas (4, closest to settlements) are near the north-western, central, southern and north-eastern parts of the chott (Fig-4.33). A small area in the southwest if beyond 50 km distance from the nearest settlement.

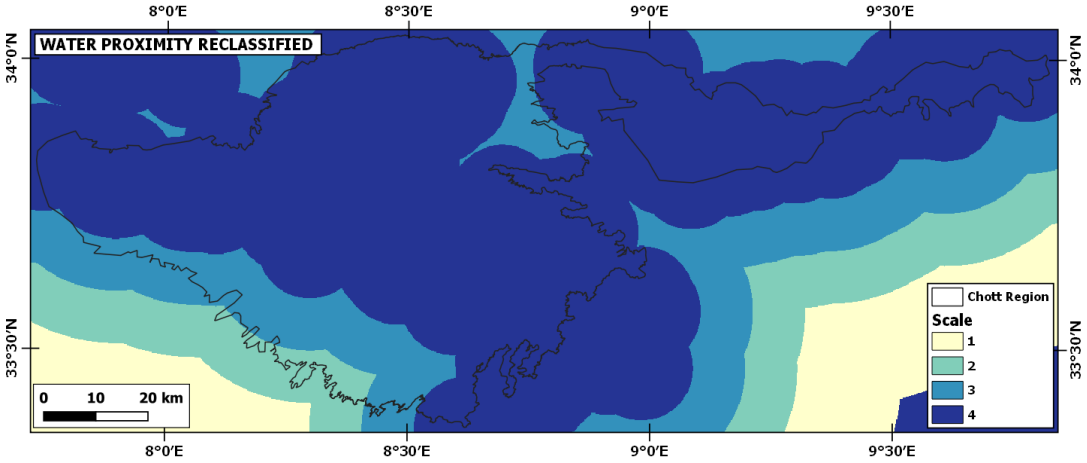

Fig-4.34: Redassified water proximity map.

The reclassified water proximity map (Fig-4.34) shows that most of the chott are is suitable in terms of proximity to water source.

4.4.4. Deriving weights by analytical hierarchy process (AHP)

Determining the weights of each criteria layer in an effective manner is very important step of the multi-criteria analysis. In this research the weights of each criteria have been determined by applying the AHP. The AHP is a well-accepted and highly used method in different studies for this purpose. Determining the weights of the thematic layers is dependent on the importance of each layer relative to each other. The derivation of the importance of the thematic layers is a matter of prior knowledge and expertise and hence it is generally done by taking the opinion of the experts of the particular field for which is multi-criteria assessment is done into consideration (Zolekar and Bhagat, 2015). Since, the present research topic is very new and there is hardly any expert for this particular topic, the knowledge gained from literature review have been used.

As mentioned in the Multi-criteria suitability assessment section of the Literature Review chapter, there may be differences in the selection of criteria for a particular geospatial problem and different workers may select and weight the variables differently based on the understanding of the problem and prior knowledge. Hence, there is no specific rule for the selection of criteria and assigning of the weights. However, the advantage of the method is that one can experiment with different choices and can verify different result to come up with the best solution for any particular case. In this research, an educated judgement has been used for deriving relative importance of the criteria layers and derive the individual weights. It is open to experiment with other combination of relative importance to see the change in the final outcome.

Since the land should be flat for solar pond development the slope map has been given the most importance. Then for the sustainable operation of the solar pond the wind speed should be suitable and hence the wind speed map get the next rank. Since, the solar pond should be close to the user, the settlement proximity map should be the next important layer. Lastly, the water source should also be very

close to the pond. However, since, water can be supplied from other sources such as sea, groundwater, or nearby rivers it may be given the least important and hence placed last in the ranking.

The relative importance of one layer to another is done by following the pairwise comparison scale of Saaty (1980), Saaty (2008). The intensity of the relative importance and their definition of the pairwise comparison scale are given in Table-4.3.

Table-4.3: Pairwise comparison scale (Saaty 1980, Saaty 2008).

Intensity of Importance	**Definition**	**Explanation**
1	Equal importance	Two criteria contribute equally
2	Weak or slight	
3	Moderate importance	Experience and judgement slightly favor one
4	Moderate plus	
5	Strong importance	Experience and judgement strongly favor one
6	Strong plus	
7	Very strong or demonstrated importance	A criteria is favored very strongly over another; its dominance demonstrated in practice
8	Very, very strong	
9	Extreme importance	The evidence favoring one criteria over another is of the highest possible order of affirmation

Then a pairwise comparison of the criteria layers has been done. For that a web-based tool has been used (https://bpmsg.com/ahp/ahp-calc.php) the names of the criteria layers and their relative importance have to be provided as input in the Pairwise Comparison calculator. The tool then calculates the Priorities and Decision Matrix from where the weights of each criteria layer can be found. The Consistency Ratio should be within 10%.

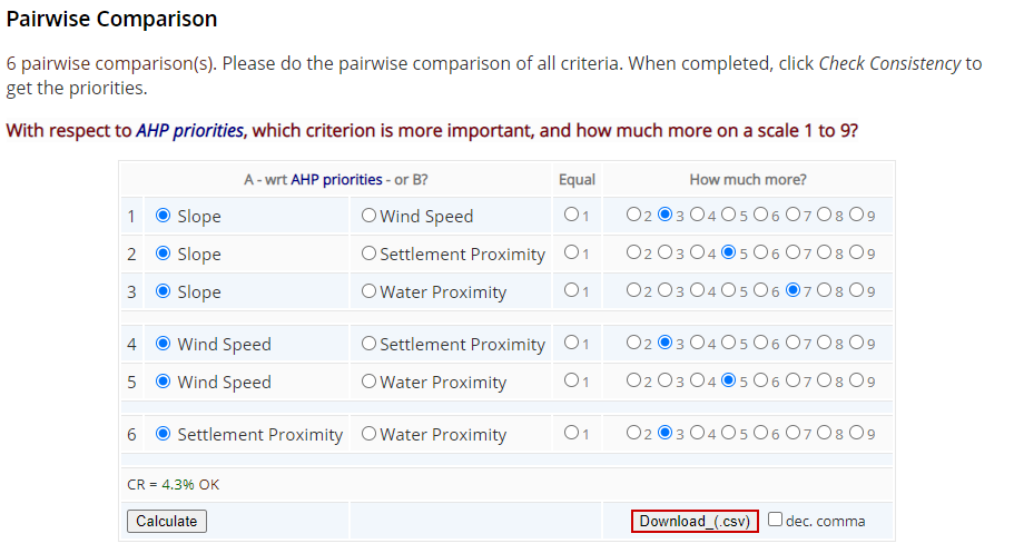

Fig-4.35: Pairwise Comparison of the criteria layers.

Here, the Slope layer is 3, 5, and 7 times more important than the Wind Speed, the Settlement Proximity and the Water Proximity layers. The Wind Speed layer is 3 and 5 times more important than the Settlement Proximity and the Water Proximity layers. Lastly the Settlement Proximity is 3 times more important than the Water Proximity layer. The pairwise comparison is shown in Fig-4.35 and the derived priorities and decision matrix are shown in Fig-4.36. The Consistency Ratio for this pairwise comparison is 4.3%.

Priorities

These are the resulting weights for the criteria based on your pairwise comparisons:

Cat		Priority	Rank	(+)	(-)
1	Slope	56.5%	1	15.9%	15.9%
2	Wind Speed	26.2%	2	6.5%	6.5%
3	Settlement Proximity	11.8%	3	3.2%	3.2%
4	Water Proximity	5.5%	4	1.7%	1.7%

Decision Matrix

The resulting weights are based on the principal eigenvector of the decision matrix:

	1	2	3	4
1	1	3.00	5.00	7.00
2	0.33	1	3.00	5.00
3	0.20	0.33	1	3.00
4	0.14	0.20	0.33	1

Fig-4.36: Priorities and Decision Matrix of the pairwise comparison of the criteria layers.

Thus the weights of the criteria layers are 56.5%, 26.2%, 11.8% and 5.5% for Slope, Wind Speed, Settlement Proximity and Water Proximity layers respectively. The weights can then be used in the Weighted Overly tool in ArcMap to derive the suitability map.

4.4.5. Weighted Overlay Analysis

The multi-criteria analysis has been performed by the Weighted Overlay tool of ArcGIS 10.7.1 by assigning the derived weights to each thematic layer to obtain suitable locations. Fig-4.37 shows the resulting suitability map with the most suitable areas in green and least suitable areas in red. The most suitable areas with a value 4 indicates that all these areas have fulfilled all the criteria to be best candidate for solar pond development while the lower values indicate that not all criteria are fulfilled. However, this suitability map does not consider the restricted areas. Thus a restriction mask has been applied to discard the areas that are not suitable for solar pond development and to obtain a resultant potentialty map.

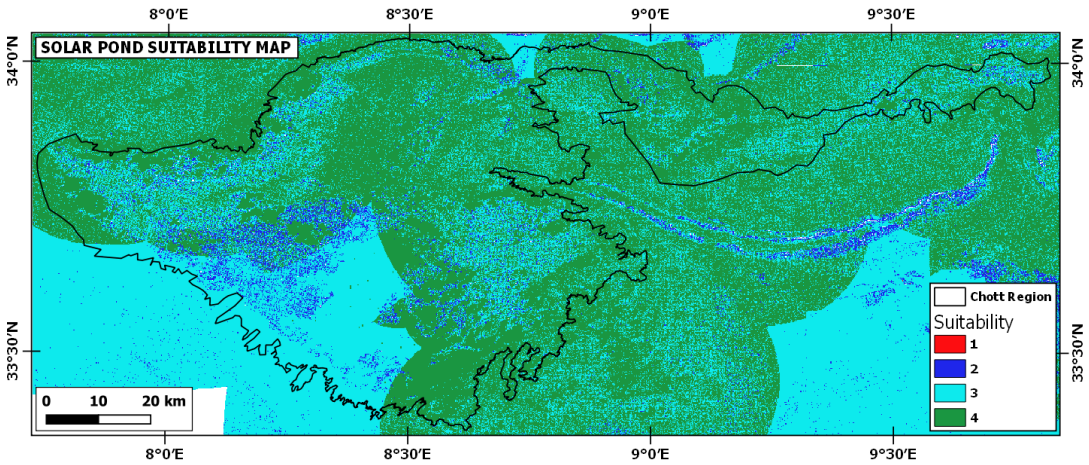

Fig-4.37: Solar pond suitability map of the chott area.

4.4.6. Creation of restriction mask

A restriction mask layer (Fig-4.38) has been created by adding all the buffer polygons of settlement, vegetation, road and water areas.

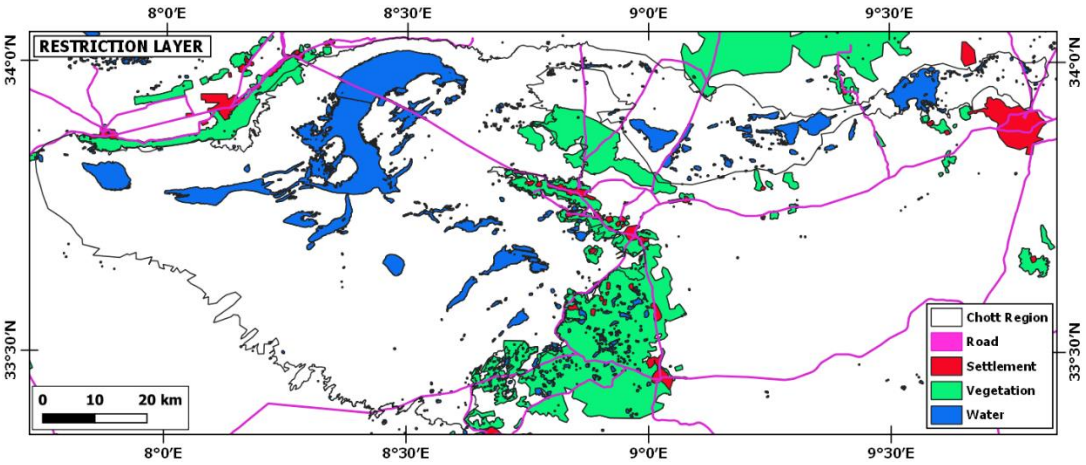

Fig-4.38: Restriction mask by combining restriction layers.

4.4.7. Creation of final potential map by applying restriction mask

The restriction layer has been used to mask the restricted areas in the suitability map of Fig-4.37. Thus all the other areas can be considered as potential for solar pond development. The potential map is shown in Fig-4.39.

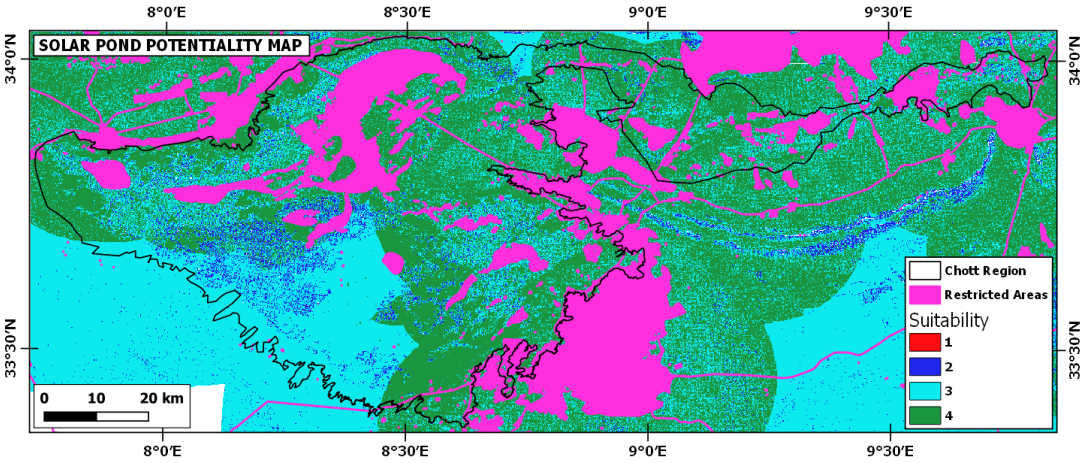

Fig-4.39: Potentiality map of solar pond development in the Chott el Djerid.

Thus, the Fig-4.39 is the final product of the multi-criteria suitability analysis for solar pond development in the Chott el Djerid showing best suitable areas (value 4) in green, and least suitable areas (in red) and restricted ares in pink. The best suitable areas indicate that all the conditions are favourable there and lesser values imply that two or more condition are not suitable. The restricted areas in pink indicate that these areas need preservation and they are not suitable for solar pond development.

5. RESULTS AND DISCUSSION

5.1. Estimation of area, generated power and served household of solar pond

As referred to the Beith Ha'Arava solar pond it follows that a 210000 m² solar pond can generate 5 MW electric power. This information can be used to estimate how much electricity can be generated and how many person or households can be served from ponds of different sizes in Chott el Djerid, Tunisia given that the geo-environmental conditions are similar to the beith.

Estimation of power generation for different sizes of solar pond:

Since, 500 m X 500 m (= 250000 m²) pond should produce 5 MW electricity, the production of 1 m² area would be (5/250000=) 0.00002 MW or 20 watt/m². Thus, the power production of different sizes of solar pond is a multiple of 0.00002 MW.

Energy demand per household in Tunisia:

The per capita energy consumption in Tunisia is 1306 kWh per year (www.worlddata.info). Thus, the consumption of one person per hour derived from yearly consumption a person is-
1306 kWh/year per person = 1306 kWh / 8760 h per person
0.15 kW per person per hour = 0.00015 MW per person per hour
Assuming each household has 5 persons in average, the hourly total consumption of power per household would be-
0.00015 MW * 5 = 0.00075 MW per household per hour
Thus, 1 MW of power can serve (1/0.00075) = 1333 household per hour

The power generation capability and number of household served for a number of different size of solar ponds has been given in Table-5.1.

Table-5.1: Estimated power and served household per hour for different pond sizes.

Area (m^2)	Power (MW)	Household (#)
5000	0.1	133
10000	0.2	266
50000	1	1333
100000	2	2666
250000	5	6666
500000	10	13333
750000	15	20000
1000000	20	26666

5.2. Prospective solar pond in the chott and their properties

From the potentiality map (Fig-4.39) for solar pond development of the chott it can be found that there are many areas that have full potential represented by consistent colour. However, in many of the places

there are irregularities which may vary from low to very high (Fig-5.1). While the highly irregular areas may not be very suitable, low irregular areas may be used with some facilitations. However, in this research only some of the very big consistent areas have been highlighted as prospective areas (Fig-5.2).

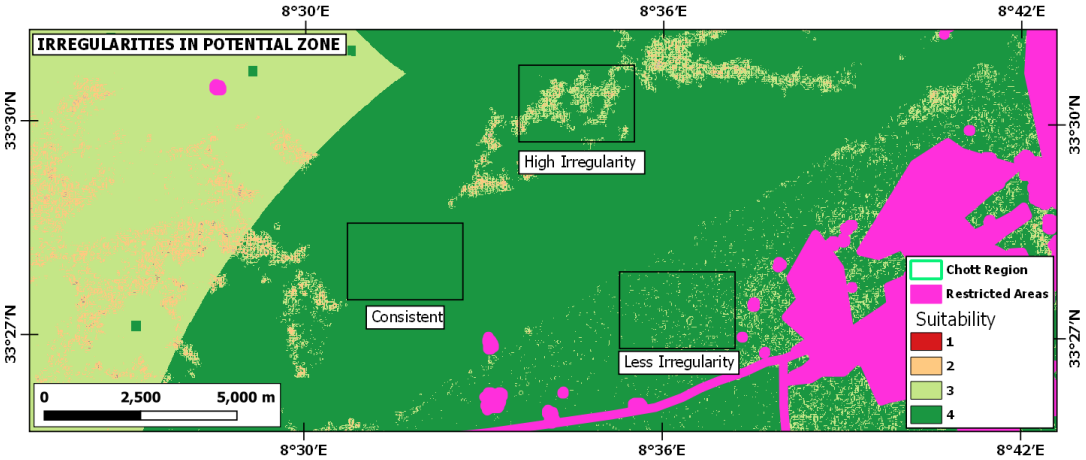

Fig-5.1: Consistent and irregular areas in the potential zone.

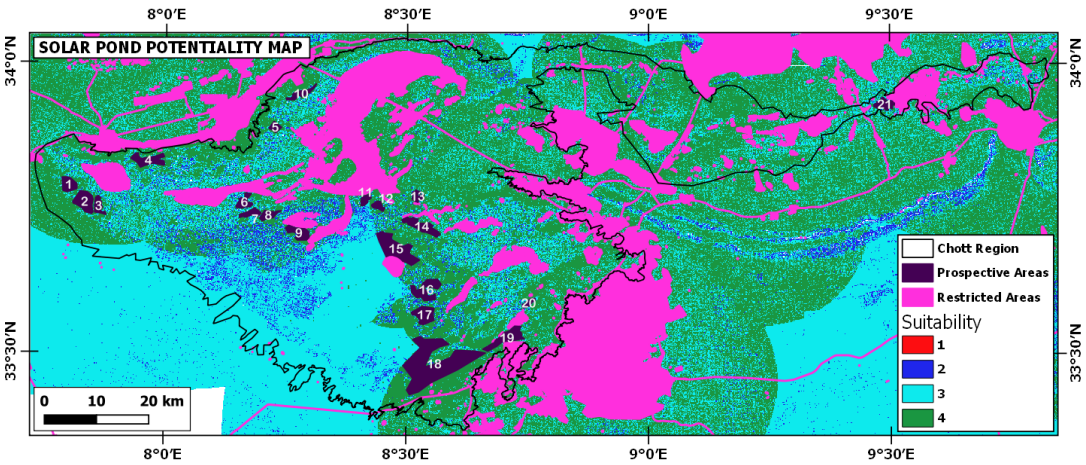

Fig-5.2: Prospective areas for solar pond development.

A total of 21 large prospective areas have been identified. Although small areas and less irregular areas are ignored, these areas are prospective for small scale solar pond. As such it is possible to develop many small scale solar pond all over the chott. The area, power generation capability and possible number of household served have been shown in the Table-5.2. The largest prospective area is 10194320.09 m^2, with a potential power generation of 204 MW and a total number of 272000 household served.

The close up view of each of the prospective areas has been shown in Appendix D showing the underlying topography as viewed in GoogleEarth image.

Thus, the multi-criteria analysis shows that there are many potential areas in the Chott el Djerid where the prospect for solar pond development is very high. Almost all the resources are available in the chott. Especially the chott water which is known for its high salinity and is referred to as brine indicating high salt concentration. Some very old texts exists on the salinity of the chott stating that the water salinity of the chott water "increases from few grams near the edges of the chott towards to a maximum value of

about 390 g/L in the center" (Gueddari et al., 1983). However, detailed field work is necessary to determine the suitability of the water for its use in solar pond.

Table-5.2: The prospective solar ponds, their areas, estimated power and number of household served.

id	Area (m^2)	Power (MW)	Household (#)
1	207	126	168000
2	10901296	218	290667
3	4083934	82	109333
4	9122461	182	242667
5	2708602	54	72000
6	4835818	97	129333
7	3801946	76	101333
8	4162439	83	110667
9	7146108	143	190667
10	4101120	82	109333
11	2576188	52	69333
12	2644906	53	70667
13	3041559	61	81333
14	10194320	204	272000
15	22341439	447	596000
16	11476179	230	306667
17	9999183	200	266667
18	69090025	1382	1842667
19	11808357	236	314667
20	2100000	42	56000
21	5054780	101	134667
Total	**207,479,229**	**4151**	**5,534,668**

Given that the per capita power consumption of Tunisia is 1306 kWh/year and the current population of Tunisia is 11,944,258 as of Friday, July 9, 2021 (Google.com, Fig-5.3), the current total household of Tunisia is 2,388,851.6 (11944258/5). Thus if all the potential areas could be developed into solar pond in Chott el Djerid alone, it would be possible to provide more than double power than required per household. However, it may not be practically feasible to develop all the prospective area in the chott and hence the real power production would be significantly lower than the potential.

Fig-5.3: Current population of Tunisia (a screen capture from Google search)

Due to its location in a desert environment the chott may experience lack of surface water. In this case other sources of water should also be considered such as groundwater. As discussed earlier, the chott is characterized by very big aquifer system which may provide sufficient water for the operation of solar pond in the chott. Further research on water cycle may be of great use in this regard.

The low rainfall in the chott may have positive impact on the operation of solar pond by maintaining the low density of fresh upper convective zone (UCZ) and there is no need for flushing (Baharin et al., 2017). However, high evaporation may cause the water to dry up and get saltier and needs to be prevented. There are different techniques to prevent or compensate for evaporative loss. For example the use of polystyrene top cover may be useful for preventing evaporative loss of surface layer. Another measure is to increase the salinity of the UCZ to prevent evaporative loss. Furthermore, water can be flashed to the upper layer to replenish the loss due to evaporation (Egbe et al., 2013; Ding et al., 2016; El-Sebaii et al., 2011; Ines et al., 2019). This is a part of maintenance of solar pond and should not be a major concern for the development of solar pond.

6. CONCLUSION AND RECOMMENDATION

The research is about finding suitable locations for the development of artificial solar ponds in the study area of Chott el Djerid. Due to the multiplicity of the variables and their complex interplay, a multi-criteria analysis method has been applied. The most important variables relevant to the conceptual framework of solar pond has been identified. The best of the sites should be flat land, with high solar irradiation and low wind speed. The site should be close to existing settlements i.e. the consumer and water bodies i.e. for ease of water supply and at the same time at a safe distance from settlements, vegetation, water and roads. Other factors may also be considered and hence the method is flexible for modification with regard to the criteria that has to be incorporated.

The research outcome shows that there are quite a few prospective sites for solar pond development around the chott basin. However, the analysis is based only on data available online and no field data has been used. No field verification has been carried out which is very important to ensure the accuracy of the result. Thus, it is highly recommended to conduct detailed field check before any further decision based on the result.

Another important aspect is the saline water or raw salt in the chott area which is an essential ingredient for the solar pond. Detailed field work is very important in order to assess the effect of these variable i.e. what type of salt is available at what quantity and if the quality is good enough for use or it needs refining. Most importantly the impact assessment on the environment could be a very interesting topic for further research.
Spatial multi-criteria decision analysis is multi-disciplinary in nature and hence participation of experts and stakeholders with different background is highly desirable. The opinion of local people and businesses may also play a critical role in determining the weightage of the variables. As mentioned earlier the research focuses on the first step of solar pond development but the following steps are based on the results in this step. Hence, it is the most important phase of solar pond development and detailed design, application and estimation of production are all based on the outcome of this step. As a result, more detailed and accurate study including field surveys and laboratory analysis are of utmost importance.

Thus a full and accurate assessment of all the environmental factors such as surface water, groundwater, salt, fresh/saline water, solar irradiation, wind speed are all essential for the accuracy of the estimate of land areas suitable for solar pond development.

LIST OF REFERENCES

Abbas, K., Deroin, J. P., & Bouaziz, S. (2018). Monitoring of playa evaporites as seen with optical remote sensing sensors: case of Chott El Jerid, Tunisia, from 2003 to present. *Arabian Journal of Geosciences*, *11*(92), 1-14. https://doi.org/10.1007/s12517-018-3410-0

Abbas, K., Deroin, J. P., & Bouazia, S. (2019). Multitemporal remote sensing for monitoring high dynamic phenomena: Case of the ephemeral lakes in the Chott El Jerid, Tunisia. *H. M. El-Askary et al. (eds.), Advances in Remote Sensing and Geo Informatics Applications, Advances in Science, Technology & Innovation,* 101-103. https://doi.org/10.1007/978-3-030-01440-7_24

Abija, F. A., Nwosu, J. I., Ifedotun, A. I., & Osadebe, C. C. (2020). Landslide susceptibility assessment of Calabar, Nigeria using geotechnical, remote sensing and multi-criteria decision analysis: Implications for urban planning and development. *Journal of Earth Sciences & Environmental Studies, 4*(6), 774-788. http://dx.doi.org/10.25177/JESES.4.6.RA.617

Achu, A. L., Thomas, J., & Reghunath, R. 2020. Multi-criteria decision analysis for delineation of groundwater potential zones in a tropical river basin using remote sensing, GIS and analytical hierarchy process (AHP). *Groundwater for Sustainable Development, 10*, 1-11. https://doi.org/10.1016/j.gsd.2020.100365

Ajibade, F. O., Olajire, O. O., Ajibade, T. F., Nwogwu, N. A., Lasisi, K. H., Alo, A. B., Owolabi, T. A., & Adewumi, J. R. (2019). Combining multicriteria decision analysis with GIS for suitably siting landfills in a Nigerian state. *Environmental and Sustainability Indicators, 3*(4), 1-14. https://doi.org/10.1016/j.indic.2019.100010

Alcaraz, A., Montala, M., Valderrama, C., Cortina, J. L., Akbarzadeh, A., & Farran, A. (2018). Thermal performance of 500 m² salinity gradient solar pond in Granada, *Spain under strong weather conditions. Solar Energy, 171*, 223-228. https://doi.org/10.1016/j.solener.2018.06.072

Al-Marafie, A., Al-Homoud, A. Al-Kandari, A. & Abou-Seido, E. (1991). Performace of 1700 m² solar pond operation in arid zone. *International Journal of Energy Research, 15*, 535-548.

Amigo, J., Meza, F., & Suarez, F. (2017). A transient model for temperature prediction in a salt-gradient solar pond and the ground beneath it. *Energy, 132,* 257-268. http://dx.doi.org/10.1016/j.energy.2017.05.063

Baharin, N. A., Yazit, I. F. M., Singh, B., Singh, B. Remeli, M. F., & Oberoi, A. (2017). Construction and Operation of First Salinity Gradient Solar Pond in Malaysia. *Journal of Mechanical Engineering, 4*(5), 217-235.

Kurt, H., Halici, F., & Binark, A. K. (2000). Solar pond conception – Experimental and theoretical studies. *Energy Conversion & Management, 41,* 939-951.

Bryant, R. G., Drake, N. A. & Millington, A. C. (1994). The chemical evaluation of the brines of Chott el Djerid, Southern Tunisia, after an exceptional rainfall event in January 1990. *Sedimentology and Geochemistry of Modern and Ancient Saline Lakes, SEPM Special Publication No. 50,* 3-12.

Bryant, R. G. (1999). Applications of AVHRR to monitoring a climatically sensitive playa. Case study: Chott el Djerid, Southern Tunisia. *Earth Surface Processes and Landforms, 24,* 283-302.

Bryant, R. G., & Rainey, M. P. (2002). Investigation of flood inundation on playas within the Zone of Chotts, using a time-series of AVHRR. *Remote Sensing of Environment, 82 (2-3)*, 360-375. https://doi.org/10.1016/S0034-4257(02)00053-6

Castany, G. (1982). Bassin se´dimentaire du Sahara septentrional (Alge´rie-Tunisie)—Aquife`res du Continental intercalaire et du Complexe Terminal. *Bulletin Bureau Recherches Ge´ologiques Minie`res (BRGM), 2(3)* 127–147.

Chaibi, M. T. and Bourouni, K. 2005. Geothermal Water Cooling Systems in Tunisia - Design and Practice. Proceedings World Geothermal Congress. Antalya, Turkey.

Chakrabarty, S. G., Wankhede, U. S., Shelke, R. S., & Gohil, T. B. (2020). Investigation of temperature development in salinity gradient solar pond using a transient model of heat transfer. *Solar Energy, 202,* 32-44. https://doi.org/10.1016/j.solener.2020.03.052

Dah, M. M. O., Ouni, M., Guizani, A., & Belghith, A. (2005). Study of temperature and salinity profiles development of solar pond in laboratory. *Desalination, 183*, 179-185. https://doi.org/10.1016/j.desal.2005.03.034

Date, A., & Akbarzadeh, A. (2014). Salinity gradient solar ponds. In: Enteria, N., Akbarzadeh, A, (Eds)., *Solar energy sciences and engineering applications (1st ed.).* CRC Press. https://doi.org/10.1201/b15507

Dhindsa, G. S., & Sokhal, G. S. (2020). Design and development of salt gradient solar pond to enhance heat storage for solar still. *International Journal of Advance Science and Technology, 29*(10S), 5553-5560. http://sersc.org/journals/index.php/IJAST/article/view/22277

Ding, L. C., Akbarzadeh, A., & Date, A. (2016). Transient model to predict the performance of thermoelectric generators coupled with solar pond. *Energy, 103*(C), 271-289. https://doi.org/10.1016/j.energy.2016.02.124

Ding, L. C., Akbarzadeh, A., Singh, B., & Remeli, M. F. (2017). Feasibility of electrical power generation using thermoelectric modules via solar pond heat extraction. *Energy Conversion and Management, 135*, 74-83. http://dx.doi.org/10.1016/j.enconman.2016.12.069

Diouf, R., Ndiaye, M. L., Traore, V. B., Sambou, H., Giovani, M., Lo, Y., Sambou, B., Diaw, A. T., & Beye, A. C. (2017). Multi criteria evaluation approach based on remote sensing and GIS for identification of suitable areas to the implantation of retention basins and artificial lakes in Senegal. *American Journal of Geographic Information System, 6*(1), 1-13.

https://doi.org/10.5923/j.ajgis.20170601.01

Drake, N. A., Bryant, R. G., Millington, A. C., & Townshend, J. R. G. (1994). Playa sedimentology and geomorphology: Mixture modeling applied to Landsat thematic mapper data of Chott el Djerid, Tunisia. *Sedimentology and Geochemistry of Modern and Ancient Saline Lakes, SEPM Special Publication No. 50.*

Edesess, M., Henderson, J., & Jayadev, T. S. (1979). A simple design tool for sizing solar ponds. *Solar Energy Research Institute. U.S. Department of Energy. U.S. Government Printing Office.*

Egbe, J. G., Khan, A. H., & Wisatesajja, W. (2013). Design of Solar Pond calculation and technique in Africa. *IOSR Journal of Mechanical and Civil Engineering (IOSR-JMCE), e-ISSN: 2278-1684, 6*(1), 22-32.

Elguedri, M. (1999). Assessment of scaling and corrosion problems in the Kebili geothermal field, Tunisia. *Geothermal Training in Iceland, 1*, 1–40.

El Ouderni, A. R., Maatallah, T., El Alimi, S., & Nassrallah, S. B. (2013). Experimental assessment of the solar energy potential in the gulf of Tunis, Tunisia. *Renewable and Sustainable Energy Reviews, 20*, 155-168. https://doi.org/10.1016/j.rser.2012.11.016

Elashaal, A., Embaby, M., & Nower, M. (2021). Potential for solar pond as source of thermal energy to sustain the development in MENA region. *International Journal of Applied Science and Engineering Review, 2*(2), 103-122. http://dx.doi.org/10.52267/IJASER.2021.2203

Elsarrag, E., Igobo, O. N., Alhorr, Y., & Davies, P. A. (2016). Solar pond powered liquid desiccant evaporative cooling. *Renewable and Sustainable Energy Reviews, 58,* 124-140. https://doi.org/10.1016/j.rser.2015.12.053

El-Sebaii, A. A., Ramadan, M. R. I., Aboul-Enein, S., & Khallaf, A. M. (2011). History of the solar ponds: A review study. *Renewable and Sustainable Energy Reviews, 15*(6), 3319-3325. https://doi.org/10.1016/j.rser.2011.04.008

Frederick, R. L., & Riobo, C. (2016). Heat exchangers for solar pond applications. *WIT Transactions on Engineering Sciences, 106,* 151-161. https://doi.org/10.2495/HT160151

Ganguly, S., Jain, R., Date, A., & Akbarzadeh, A. (2017). On the addition of heat to solar pond from external sources. *Solar Energy, 144,* 111-116. https://doi.org/10.1016/j.solener.2017.01.012

Garg, H. P. (1987). Advances in solar energy technology: Collection and storage systems. *Springer, 1,* XIX, 666. https://doi.org/10.1007/978-94-017-0659-9

Gueddari, M., Monnin, C., Perret, D., Fritz, B. & Tardy, Y. (1983). Geochemistry of brines of the chott El Jerid in southern Tunesia-Application of Pitzer's equations. *Chemical Geology, 39*(1-2), 165-178. https://doi.org/10.1016/0009-2541(83)90078-5

Haj-Amor, Z., Toth, T., Ibrahimi, M. K., & Bouri, S. (2017). Effects of excessive irrigation of date palm on soil salinization, shallow groundwater properties, and water use in a Saharan oasis. *Environmental Earth Sciences, 76*(590), 1-13. https://doi.org/10.1007/s12665-017-6935-8

Hull, J. R. (1980). Membrane stratified solar ponds. *Solar Energy, 25*, 317-325.

https://doi.org/10.1016/0038-092X(80)90344-8

Ines, M., Paolo, P., Roberto, F., & Mohamed, S. (2019). Experimental studies on the effect of using phase change material in a salinity-gradient solar pond under a solar simulator. *Solar Energy, 186*, 335-346. https://doi.org/10.1016/j.solener.2019.05.011

Islam, A., Ali, S. M., Afzaal, M., Iqbal, S., & Zaidi, S. N. F. (2018). Landfill sites selection through analytical hierarchy process for twin cities of Islamabad and Rawalpindi, Pakistan. *Environmental Earth Sciences, 77*(72), 1-13. https://doi.org/10.1007/s12665-018-7239-3

Kamel, S. (2013). Salinisation origin and hydrogeochemical behaviour of the Djerid oasis water table aquifer (southern Tunisia). *Arabian Journal of Geosciences, 6*, 2103-2117. https://doi.org/10.1007/s12517-011-0502-5

Kamel, S., Younes, H., Chkir, N., & Zouari, K. (2007). The hydro geochemical characterization of ground waters in Tunisian Chott's region. *Environmental Geology, 54*, 843-854. DOI:10.1007/s002254-007-0867-7

Kishore, V. V. N. & Kumar, A. (1996). Solar pond: an exercise in development of indigenous technology at Kutch, India. *Energy for Sustainable Development, III*(1), 17-28. https://doi.org/10.1016/S0973-0826(08)60177-5

Koc, A., Turk, S., & Sahin, G. (2019). Multi-criteria of wind-solar site selection problem using a GIS-AHP-based approach with an application in Igdir Province/Turkey. *Environmental Science and Pollution Research, 26*, 32298-32310. https://doi.org/10.1007/s11356-019-06260-1

Koc-San, D., San, B. T., Bakis, V., Helvaci, M., & Eker, Z. (2013). Multi-criteria decision analysis integrated with GIS and remote sensing for astronomical observatory site selection in Antalya province, Turkey. Advances in Space Research, 52, 39-51. http://dx.doi.org/10.1016/j.asr.2013.03.001

Kraiem, Z, Chkir, N., Zouari, K., Parisot, J. C., Agoun, A. & Hermitte, D. (2012). Tomographic, hydrochemical and isotopic investigations of the salinization processes in the oasis shallow aquifers, Nefzaoua region, southwestern Tunisia. *Journal of Earth System Science, 121*(5), 1185-1200. https://doi.org/10.1007/s12040-012-0221-7

Lu, H., & Swift, A. H. (2001). El Paso solar pond. *Journal of Solar Energy Eng, 123*(3), 178. https://doi.org/10.1115/1.1384572

Mahdi, J.T., & Jebbar, Y. A. (2019). A theoretical investigation of solar radiation and heat transfer in a solar pond in Kerbala city. *AIP Conference Processing 2144(1).* https://doi.org/10.100163/1.5123089

Millington, A. C., Drake, N. A., White, K. & Bryant. R. (1995). Salt ramps: wind-induced depositional features on Tunisian playas. *Earth Surface Process and Landforms, 20,* 105-113. https://doi.org/10.1002/esp.3290200202

Murthy, G. R. R., & Pandey, K. P. (2002). Scope of fertilizer solar ponds in Indian agriculture. *Energy, 27*, 117-26. https://doi.org/10.1016/S0360-5442(01)00059-7

Nebey, A. H., Taye, B. Z., & Workineh, T. G. (2020). Site suitability analysis of solar PV power generation in South Gondar, Amhara Region. *Hindawi Journal of Energy, 2020*, 1-15. https://doi.org/10.1155/2020/3519257

Nower, M., Embaby, M., Elashaal, A., & El-serafy, S. 2020. Mapping solar pond by GIS and Analytic Hierarchy Process. International Journal of Engineering and Advanced Technology (IJEAT), 9(4), 270-275. https://doi.org/10.35940/ijeat.D6757.049420

ONM (Office National de la Météorologie: monthly bulletins of climatological records in Tunisia of 1950 to 2010). Tozeur and Nefta Meteorological Stations. Tunisia

Rao, S. K., & Kaushika, N. D. (1982). Analytical model of solar pond with heat exchanger. *Energy Conversion and Management, 23*(1), 23-31. https://doi.org/10.1016/0196-8904(83)90004-3

Rocca, V. L., Morale., M., Peri. G., & Scaccianoce, G. (2017). A solar pond for feeding a thermoelectric generator or an organic Rankine cycle system. *International Journal of Heat and Technology, 35*(1), 435-441. https://doi.org/10.18280/ijht.35Sp0159

Saaty, T. L. (2008). Relative measurement and its generalization in decision making why pairwise comparisons are central in mathematics for the measurement of intangible factors the analytic hierarchy/network process. *RACSAM - Revista de la Real Academia de Ciencias Exactas, Fisicas y Naturales, Serie A. Mathematics, 102*(2), 251-318.

Saaty, T.L. (1980). The Analytic Hierarchy Process. *Open Journal of Social Sciences, 4*(12), 287.

Saifullah, A. Z. A. Iqubal, A. M. S., & Saha, A. (2012). Solar pond and its application to desalination. *Asian Transactions on Science & Technology, 02*(03).

Sambah, A. B., & Miura, F. (2014). Remote sensing and spatial multi-criteria analysis for tsunami vulnerability assessment. *Disaster Prevention and Management, 23*, 271-295. https://doi.org/10.1108/DPM-05-2013-0082

Shaffer, L. H. (1978). Viscosity stabilized solar pond. *In: Sun: Mankind's future source of energy; Proceedings of the International Solar Energy Congress, 2,* 1171-1175

Shubhakar, D., & Murthy, S. S. (1993). Saturated solar-ponds: 1. Simulation procedure. *Sol Energy, 50(3)*, 275-82.

Sogukpinar, H. (2019). Numerical study for estimation of temperature distribution in solar pond in diverse climatic conditions for all cities of Turkey. *Environmental Progress & Sustainable Energy, e13255*, 1-12. https://doi.org/10.1002/ep.13255

Suarez, F., Tyler, S. W., & Childress, E. (2010). A fully coupled, transient double-diffusive convective model for salt-gradient solar ponds. *International Journal of Heat and Mass Transfer, 53(9-10)*, 1718-1730. https://doi.org/10.1016/j.ijheatmasstransfer.2010.01.017

Tabor, H. Z., & Doron, B. (1990). The Beith Ha'Arava 5 MW (e) Solar Pond Power Plant (SPPP) – Progress Report. *Solar Energy, 45*, 247-253.

Tasdemiroglu, E. (1987). Salt availability in Turkey and its potential use in solar ponds. *Resources and Conservation, 15*(3), 215-228. https://doi.org/10.1016/0166-3097(87)90004-6

Townshend, J. R. G., Quarmby, N. A., Millington, A. C., Drake, N., Reading, A. J., & White, K. H. (1989). Monitoring playa sediment transport systems using thematic mapper data. *Advances in Space Research, 9*(1), 177-183. https://doi.org/10.1016/0273-1177(89)90483-3

UNESCO. (1972). Etude des ressources en eau du Sahara Septentrional. Projet ERESS. Nappe du Complxe Terminal Tech Rep 6:44

Valderrama, C., Cortina, J. L., & Akbarzadeh, A. (2016). Solar Ponds. Storing Energy: With Special Reference to Renewable Energy Sources, 273-289. http://doi.org./10.1016/B978-0-12-803440-8.00014-2

Verma, S., & Das, R. (2019). Wall profile optimization of a salt gradient solar pond using a generalized model. *Solar Energy, 184*, 356-371. https://doi.org/10.1016/j.solener.2019.04.003

Vichare, R. V. (2015). Design of a solar pond as an energy storage system for the pasteurization process in dairy industry. *International Journal of Science and Research (IJSR), 6*(11), 267-271. https://www.ijsr.net/search_index_results_paperid.php?id=ART20177872

Wadge, G., & Archer, D. J. (2002). Remote measurement of the evaporation of groundwater from arid playas. European Space Agency, (Special Publication) ESA SP, Issue 475, 165-169.

Wadge, G. & Archer, D. J. (2003). Evaporation of groundwater from arid playas measured by C-band SAR. *IEEE Transaction on Geoscience and Remote Sensing, 41*(7), 1641-1650. https://doi.org/10.1109/TGRS.2003.813747

Whitford, W. G., & Duval, B. D. (2020). Chapter 4 – Wind and Water Processes. *In: Ecology of Desert Systems (Second Ed.)*, 73-107.

Yalew, S. G., van Griensven, A., van der Zaag, P. (2016). Agrisuit: A web-based GIS-MCDA framework for agricultural land suitability assessment. *Computers and Electronics in Agriculture, 128*, 1-8. https://doi.org/10.1016/j.compag.2016.08.008

Ziapour, B. M., Saadat, M., Palideh, V., & Afzal, S. (2017). Power generation enhancement in a salinity-gradient solar pond power plant using thermoelectric generator. *Energy Conversion and Management, 136*, 283-293. http://dx.doi.org/10.1016/j.enconman.2017.01.031

Zolekar, R. B. & Bhagat, V. S. (2015). Multi-criteria land suitability analysis for agriculture in hilly zone: Remote sensing and GIS approach. *Computers and Electronics in Agriculture, 118*, 300-321. https://doi.org/10.1016/j.compag.2015.09.016

APPENDIX A

Title: X-Ray Diffraction Pattern of Materials Commonly Found in Desert Environment

Authors: Mohammad Omer Faruk Khan, s2292505, WREM, ITC, University of Twente,
Caroline Lievens, Head of the Geoscience laboratory and VGMC, ITC, University of Twente

Keywords: XRD, Desert, Halite, Gypsum, Kaolinite, Sand

Introduction: In this assignment the X-ray diffraction pattern of different materials commonly found in the desert environment has been analyzed. The materials are pure sand, halite, gypsum, and kaolinite. They have been analyzed both as pure sample and mixture. The mixture is intended to approximate the desert condition in Chott el Djerid playa in Tunisia.

Materials and Methods: The materials consist of samples and scientific equipment. As samples, both pure and mixed powders of quartz sand, common table salt (halite), gypsum, and kaolinite have been used. The mixture has been prepared based on the literature (Drake et al., 1994) describing the proportion of different constituents of the surface materials in the Chott el Djerid area, which is a desert playa lake in Tunisia. The samples have been in powered form which have been homogenized by mortar and pestel. Two mixtures to represent the two-extreme conditions in the desert i.e., dry and wet have been prepared. For the dry mixture 10% sand, 40% halite, 40% gypsum 10% kaolinite, and for the wet mixture 5% sand, 20% halite, 20% gypsum 5% kaolinite and 50% ultrapure water have been mixed. A sample matrix has been provided in Table-01.

Table-01: Sample matrix for the selected materials found in the desert environment.

No	ID	Sand (g)	Halite (g)	Gypsum (g)	Kaolinite (g)	Water (ml)
1	OK-01	5	20	20	5	50
2	OK-02	10	40	40	10	0
3	OK-03	100	0	0	0	0
4	Ok-04	0	100	0	0	0
5	OK-05	0	0	100	0	0
6	OK-06	0	0	0	100	0
7	OK-07	0	0	0	0	100

The wet sample has too much water content for analysis in XRD. So, it has been dried overnight in microwave oven at 105° C temperature and a thin crust has been formed which may resemble the desert condition after desiccation (Figure-1). However, the sample has been pulverized and homogenized for XRD analysis.

Figure-01: Wet sample after drying.

Instruments- Bruker D2 Phaser X-Ray Diffractometer.

Software- DIFFRAC.MEASUREMENT for measuring the data with the following parameters: Rounds: 30, 2θ (o) Start = 6, 2θ (o) Stop = 80, increment = 0.012, Duration [s] = 655, Divergent slit = 0.6, Knife (mm) = 3, Detector Slit (mm) = 8, Repeat = Y. The Cu tube width is 1.54184 [Å].
DIFFRAC.EVA for data analysis with Guinier Table for each mineral.

Results and Discussion: The diffraction pattern of X-ray shown by different minerals have been shown in the Figure-2.

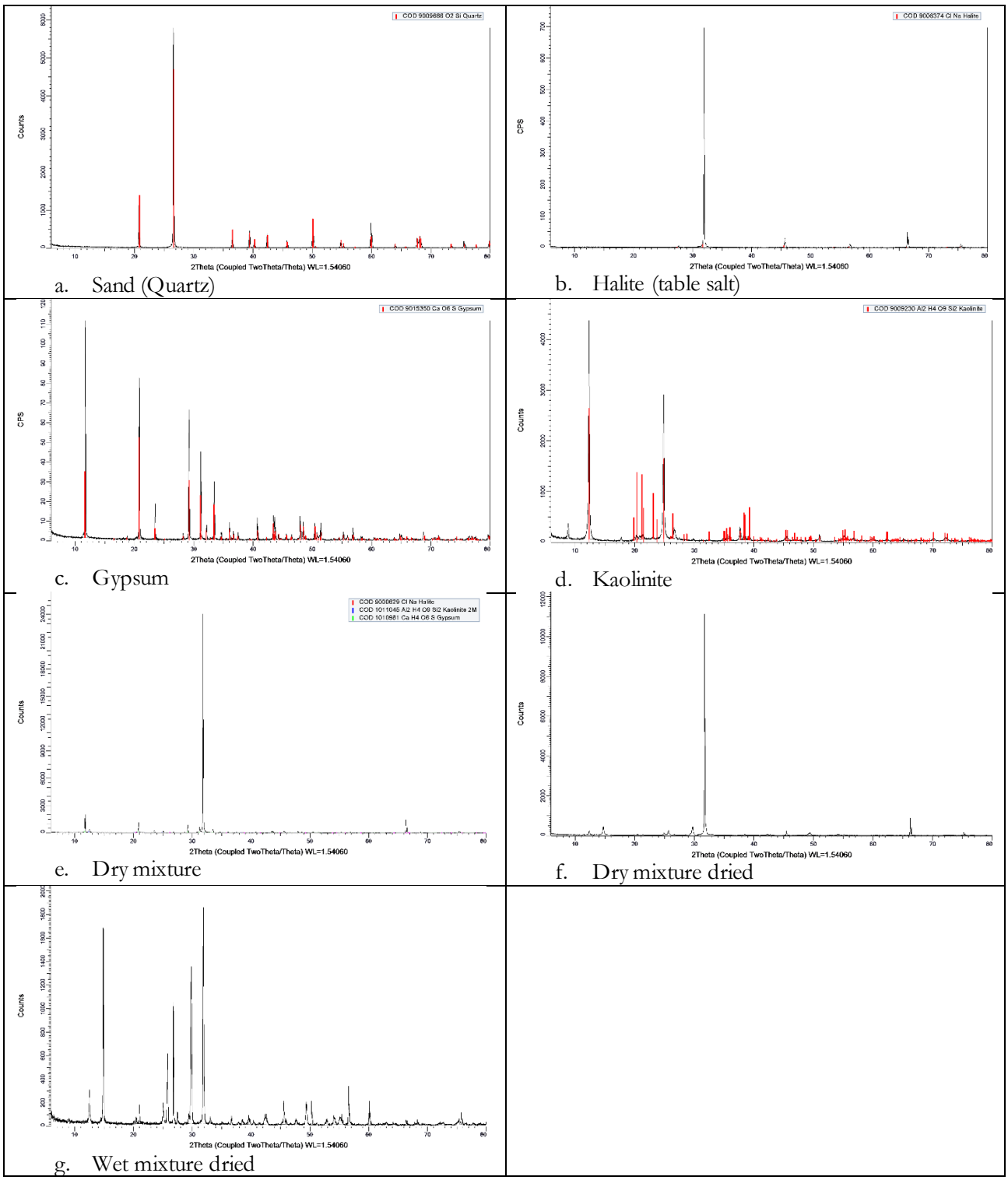

Figure-02: X-Ray diffraction pattern for different materials.

Figure-02 -a, -b, -c, and -d represent sand (quartz), halite (table salt), gypsum and kaolinite respectively. The x-ray diffraction pattern for sand is typical of quartz which means the sample is pure quartz sand. The halite is characterized by a large peak of 700 CPS at 32. The gypsum and kaolinite are characterized by large peaks.

Both the dry mixtures (Figure-02 -e and -f) show very similar patterns with minor differences which may be due to absorbed moisture in the dry sample. The gypsum and kaolinite may absorbed some ambient moisture which have been removed after drying. The other signals have been subdued by the very large peak at 32, which may be due to the presence of halite which has much stronger effect on other minerals. Lastly, the dried wet mixture (Figure-02 -g) has a much more informative x-ray pattern representing most of the minerals somewhat appropriately. This may be due to the dissolution of halite and saturation of gypsum and kaolinite by the added water which helped reduce the effect of halite over the other minerals.
Conclusion: In this study two extreme conditions of the desert environment viz. dry and wet have been analyzed by X-ray diffraction method by comparing the patterns with the pure samples. This is a very useful method to analyzing and identification the behavior of different materials. The interaction of different materials and the effect of one on the other can be effectively studied.

References

Drake, N.A., Bryant, R.G., Millington, A.C. and Townshend, J.R.G. 1994. Playa sedimentology and geochemistry: mixture modelling applied to Landsat Thematic Mapper data of Chott el Djerid, Tunisia. Sedimentology and Gechemistry of Modern and Ancint Saline Lakes, SEPM Special Publication No. 50, ISBN 1-56576-014-X, DOI: 10.2110/pec.94.50.0125

APPENDIX B

Title: Analysis of SWIR Characteristics of Materials Found in Desert Environment by SPECIM

Authors: Mohammad Omer Faruk Khan, s2292505, WREM, ITC, University of Twente,
Camilla Marcatelli, Specialist- SPECIM, ITC, University of Twente

Keywords: XRD, Desert, Halite, Gypsum, Kaolinite, Sand

Introduction: In this assignment the SWIR characteristics of different materials commonly found in the desert environment has been assessed. The materials are pure sand, halite, gypsum, and kaolinite. They have been analyzed both as pure sample and mixture. The mixture is intended to approximate the desert condition in Chott el Djerid playa in Tunisia.

Materials and Methods: The materials consist of samples and scientific equipment. As samples, both pure and mixed powders of quartz sand, common table salt (halite), gypsum, and kaolinite have been used. The mixture has been prepared based on the literature (Drake et al., 1994) describing the proportion of different constituents of the surface materials in the Chott el Djerid area, which is a desert playa in Tunisia. The samples have been in powered form which have been homogenized by mortar and pestel. Two mixtures to represent the two-extreme conditions in the desert i.e., dry and wet have been prepared. For the dry mixture 10% sand, 40% halite, 40% gypsum 10% kaolinite, and for the wet mixture 5% sand, 20% halite, 20% gypsum 5% kaolinite and 50% ultrapure water have been mixed. A sample matrix has been provided in Table-01.

Table-01: Sample matrix for the selected materials found in the desert environment.

No	ID	Sand (g)	Halite (g)	Gypsum (g)	Kaolinite (g)	Water (ml)
1	OK-01	5	20	20	5	50
2	OK-02	10	40	40	10	0
3	OK-03	100	0	0	0	0
4	Ok-04	0	100	0	0	0
5	OK-05	0	0	100	0	0
6	OK-06	0	0	0	100	0
7	OK-07	0	0	0	0	100

The wet sample has too much water content for analysis in SPECIM. So, it has been dried overnight in microwave oven at 105° C temperature and a thin crust has been formed which may resemble the desert condition after desiccation (Figure-1). However, the sample has been pulverized and homogenized for the analysis.

Figure-01: Wet sample after drying.

Instruments- ASD and SPECIM. The ASD has been used for preliminary assessment of the spectra for analysis in SPECIM. After the preliminary assessment the analysis in SWIR has been chosen.

Software- Excel, ENVI 5.5, and Hyppy. The images have been resized specially and spectrally in ENVI. The spectral signatures have been captured in Hyppy.

Results and Discussion: The spectral pattern of materials found in ASD has been given in Figure-2.

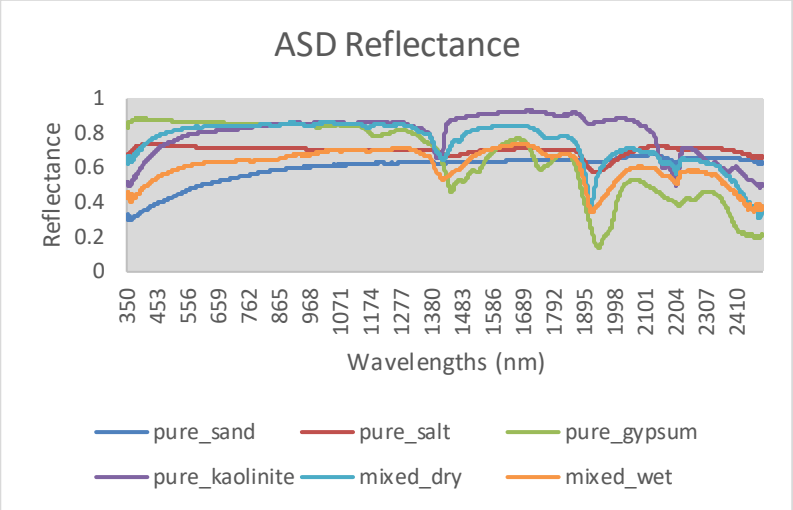

Figure-2: Spectral pattern of materials found in ASD showing that the SWIR range is more interesting for SPECIM analysis.

Figure-3 shows the SWIR reflectance pattern of pure samples from SPECIM.

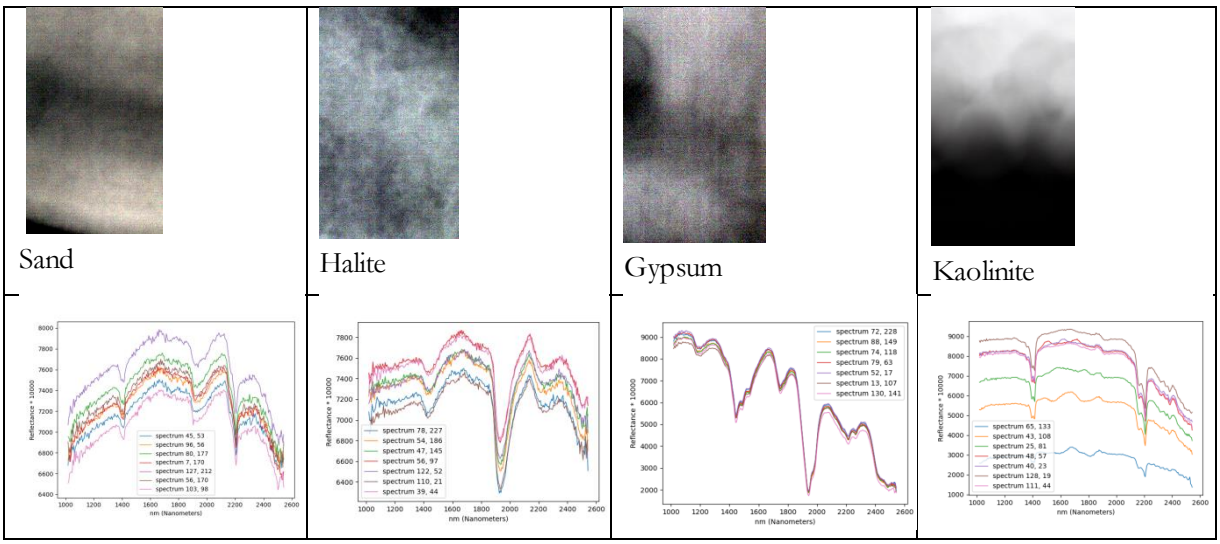

Figure-3: Images and spectral characteristics of pure samples in SPECIM.

The pure sand (quartz) sample shows a variable reflectance over the wavelengths. High reflectances are between 1500 and 1900 nm and 2000 and 2150 nm. The curves show a dome shape with sharp grooves at 1400, 1900 and 2200 nm, the last one being the sharpest. The halite sample shows clustered distribution of the reflectance values with very low amplitude dome shape the highest values being between 1600 and 1800 and 2100 and 2200 nm. There is a large groove at about 1950 nm. The gypsum sample shows a very even distribution of reflectances values with very low variation. The overall reflectance shows a decreasing trend towards the higher wavelengths with large grooves at about 1400 and 1950 nm. The highest values are in the 1000 to 1100 nm range and higher values are between 1200 to 1300 and at 1600, 1800, 2100 nm. The kaolinite sample has the most varied distribution of the reflectance values from 2000 to 9000. All the reflectance curves show similar pattern, an overall dome shape with grooves at 1400 and 2200 nm. The highest values are between 1000 and 1300 and 1500 and 2100. However the values show a steady decrease towards the larger wavelengths. Overall, the reflectance pattern of halite and gypsum and the reflectance pattern of sand and kaolinite are very similar in SWIR.

Figure-4 shows the SWIR reflectance patterns for mixed samples from SPECIM.

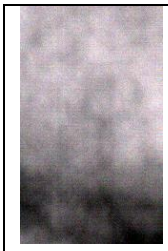

Dry Mix

Wet Mix

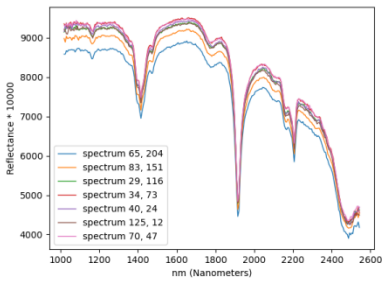

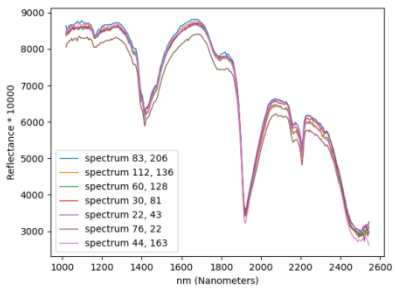

Figure-4: The images and reflectance patterns of dry and wet mixtures.

Both the dry and wet mixtures are highly influenced by the presence of kaolinite having very similar reflectance pattern to kaolinite. However, the wet sample is much more influenced of the two and indicates the high influence in the reflection in the wet period.

Conclusion: The reflectance pattern of the materials in SWIR is both influenced by the type and condition of the materials present. The presence of kaolinite has very high influence in all conditions. However, in the wet condition it is more indicating a homogeneous mixture by the presence of water.

References

Drake, N.A., Bryant, R.G., Millington, A.C. and Townshend, J.R.G. 1994. Playa sedimentology and geochemistry: mixture modelling applied to Landsat Thematic Mapper data of Chott el Djerid, Tunisia. Sedimentology and Gechemistry of Modern and Ancint Saline Lakes, SEPM Special Publication No. 50, ISBN 1-56576-014-X, DOI: 10.2110/pec.94.50.0125

APPENDIX C

Title: Analysis of Absorption Spectra of Materials Commonly Found in Desert Environment

Authors: Mohammad Omer Faruk Khan, s2292505, WREM, ITC, University of Twente,

Caroline Lievens, Head of the Geoscience laboratory and VGMC, ITC, University of Twente

Keywords: ATR, Desert, Halite, Gypsum, Kaolinite, Sand

Introduction: In this assignment attenuation of different spectra of different materials commonly found in the desert environment has been analyzed and interpreted. The materials are pure sand, halite, gypsum, kaolinite and water. They have been analyzed both as pure sample and mixture. The mixture is intended to approximate the desert condition in Chott el Djerid playa in Tunisia.

Materials and Methods: The materials consist of samples and scientific equipment. As samples, both pure and mixed powders of quartz sand, common table salt (halite), gypsum, kaolinite and water have been used. The mixture has been prepared based on the literature (Drake et al., 1994) describing the proportion of different constituents of the surface materials in the Chott el Djerid area, which is a desert playa in Tunisia. The samples have been in powered form which have been homogenized by mortar and pestel. Two mixtures to represent the two-extreme conditions in the desert i.e., dry and wet have been prepared. For the dry mixture 10% sand, 40% halite, 40% gypsum 10% kaolinite, and for the wet mixture 5% sand, 20% halite, 20% gypsum 5% kaolinite and 50% ultrapure water have been mixed. A sample matrix has been provided in Table-01.

Table-01: Sample matrix for the selected materials found in the desert environment.

No	ID	Sand (g)	Halite (g)	Gypsum (g)	Kaolinite (g)	Water (ml)
1	OK-01	5	20	20	5	50
2	OK-02	10	40	40	10	0
3	OK-03	100	0	0	0	0
4	Ok-04	0	100	0	0	0
5	OK-05	0	0	100	0	0
6	OK-06	0	0	0	100	0
7	OK-07	0	0	0	0	100

The wet sample has too much water content for analysis in ATR. So, it has been dried overnight in microwave oven at 105° C temperature and a thin crust has been formed which may resemble the desert condition after desiccation (Figure-01). The dry mixture has also been dried the same way.

Figure-01: Wet sample after drying.

Instruments- Bruker Vertex 70 - ATR.

Software- Bruker OPUS with following parameters MIR save data from 4000 to 600 cm^{-1}, Sample scan time: 16 scans, Background scan time: 16 scans, Resolution: 4 cm^{-1}, Result Spectrum set to: Absorbance.

Results and Discussion: The attenuation of different spectra by different bonds have been shown in the Figure-02.

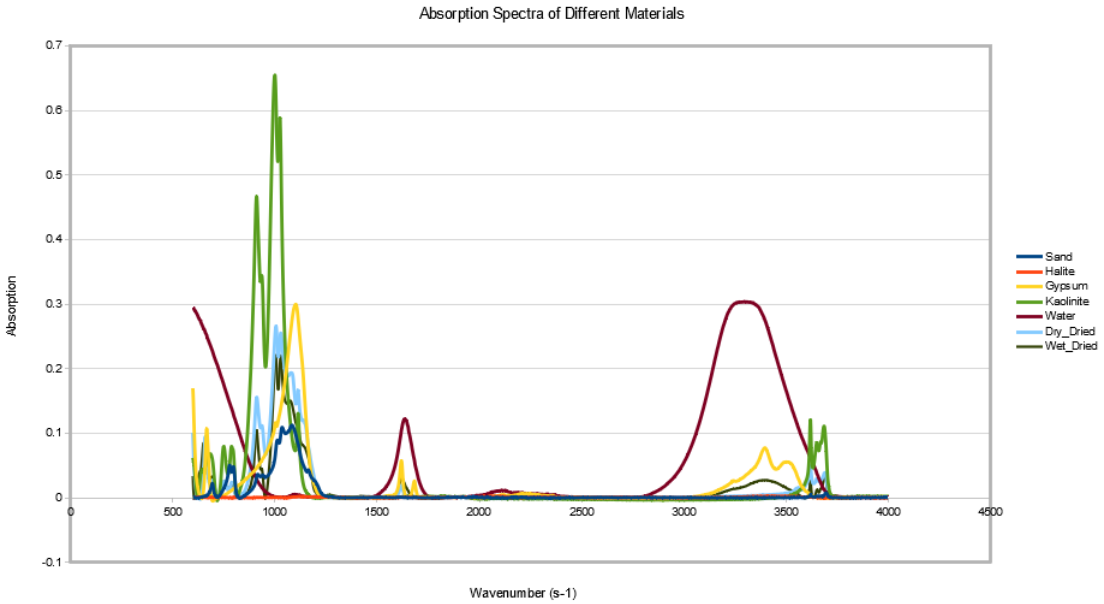

Figure-02: Absorption spectra of different materials.

Sand (quartz) shows significant absorption at 700 and 1100 (0.5 and 0.12 respectively). Halite shows very low absorbance only in the range of thousandths (ranging from 0 to 0.003). Gypsum shows absorbance at 650, 700, 1100, 1650 and 3400 (0.17, 0.12, 0.3 and 0.07). Kaolinite shows very high absorbance at 1000 and 900 (0.67 and 0.47) at lower absorbance at 750 and 3700 (0.075 and 1.2). Water shows high absorbances at 600, 1650 and 3300 (0.29, 0.125 and 0.32). The dried dry mixture shows absorbances at 900, 1000 and 3700 (0.16, 0.27 and 0.04). The dried wet mixture shows absorbances at 700, 800, 900, 1000 and 3600 (0.07, 0.08, 0.48, 0.67, 0.125). The absorbance characteristics of different bonds have been summarized in Table-02.

Table-02: Wavenumber and assigned bonds

Wavenumber (cm^{-1})	Bond
900-1100	Silicates (strong)
3500	Halite (very weak)
1100	Suphate (Gypsum) (strong)
900-1100	Silicates (Kaolinite) (very strong)
600, 3300	H-O-H (Water) (broad)

Conclusion: The absorption spectra of different materials found in the desert environment have been analyzed both in pure and mixed conditions. The spectral absorption of these materials are characteristics of their bonds which can be used to identify them. The dried wet and dry samples show similar pattern, however, the value of wet dried is lower than the dry dried mixture.

References

Drake, N.A., Bryant, R.G., Millington, A.C. and Townshend, J.R.G. 1994. Playa sedimentology and geochemistry: mixture modelling applied to Landsat Thematic Mapper data of Chott el Djerid, Tunisia. Sedimentology and Gechemistry of Modern and Ancint Saline Lakes, SEPM Special Publication No. 50, ISBN 1-56576-014-X, DOI: 10.2110/pec.94.50.0125

APPENDIX D

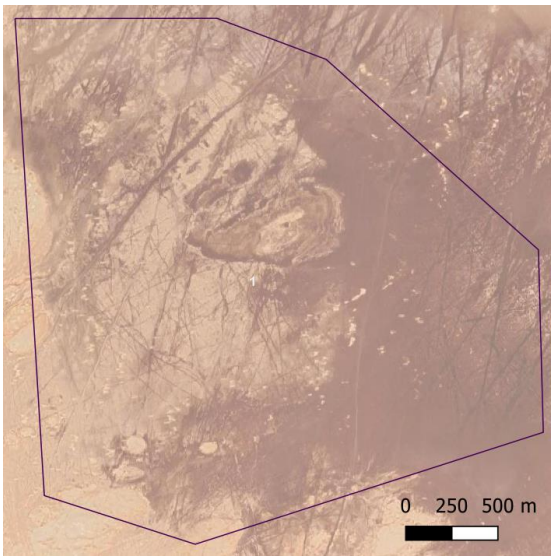

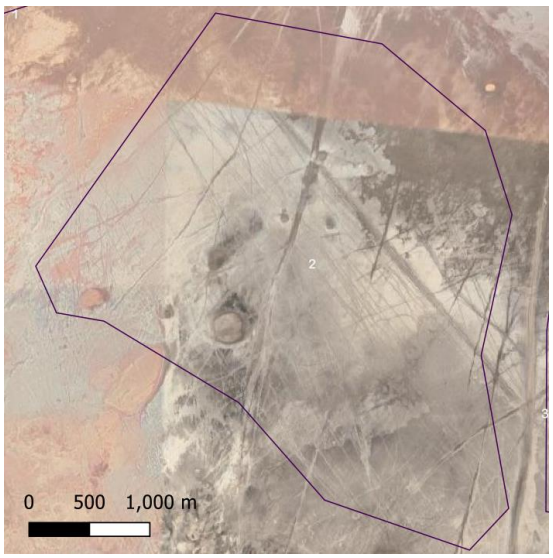

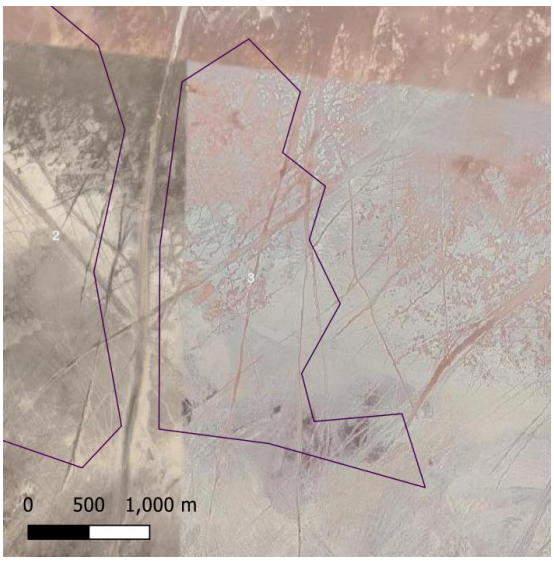


4
0 500 1,000 m

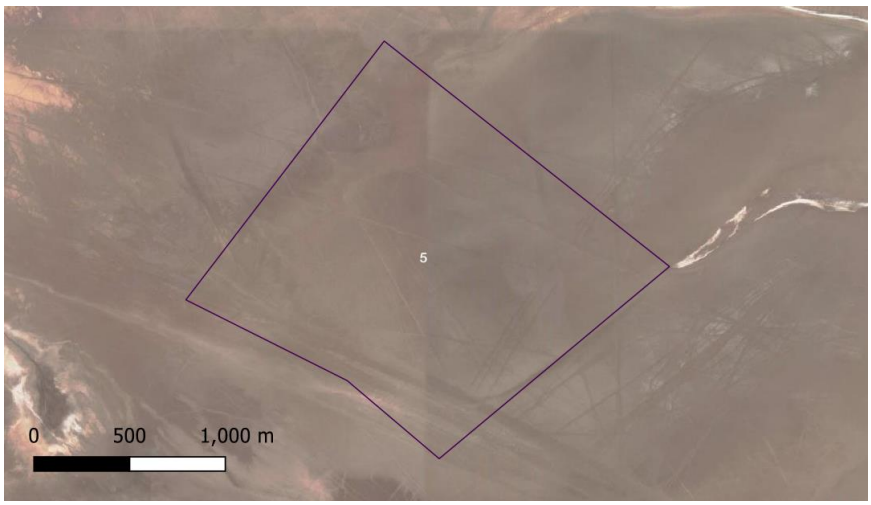
5
0 500 1,000 m

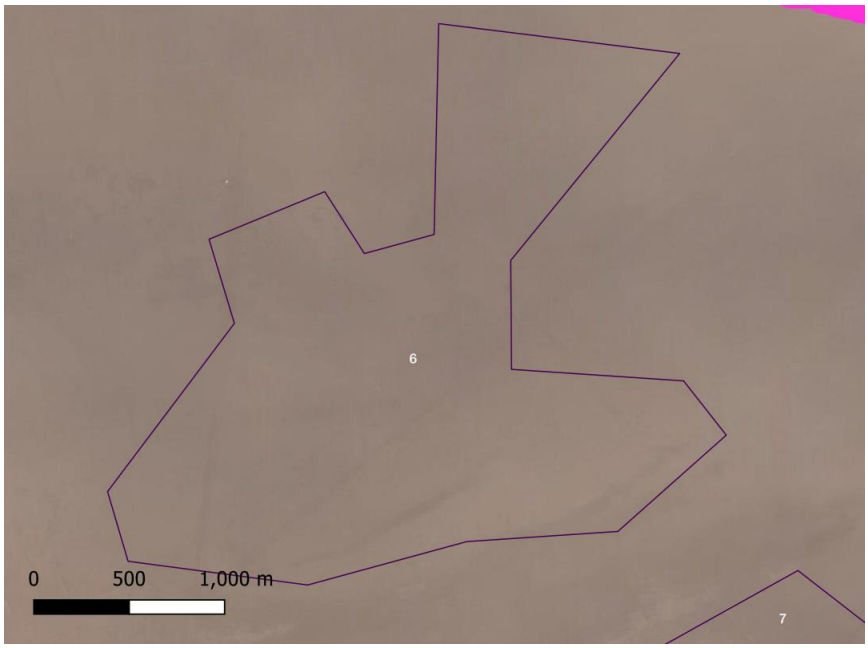
6
0 500 1,000 m
7

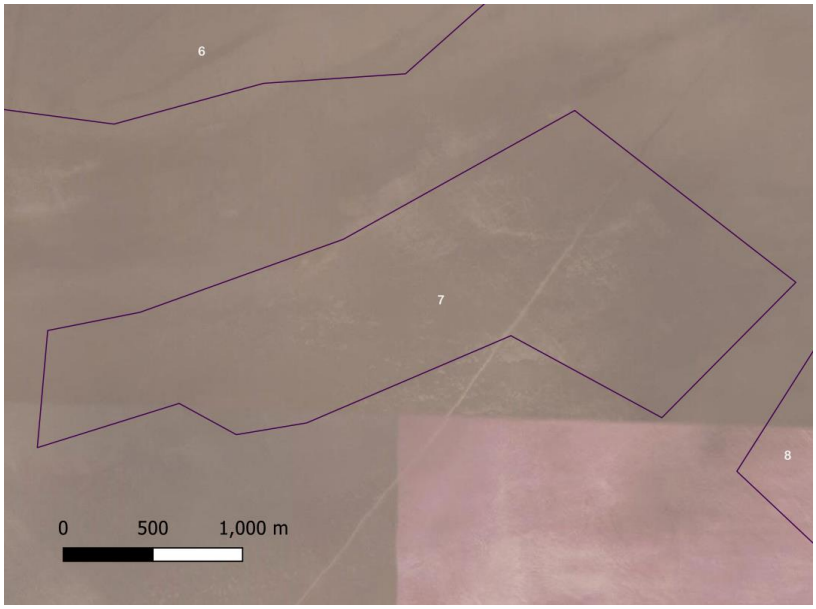
6
7
8
0
500
1,000 m

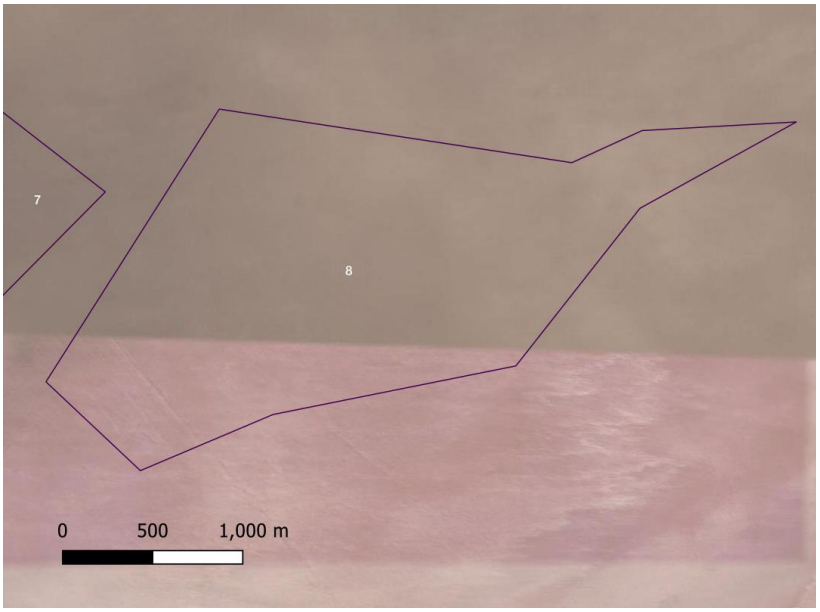
7
8
0
500
1,000 m

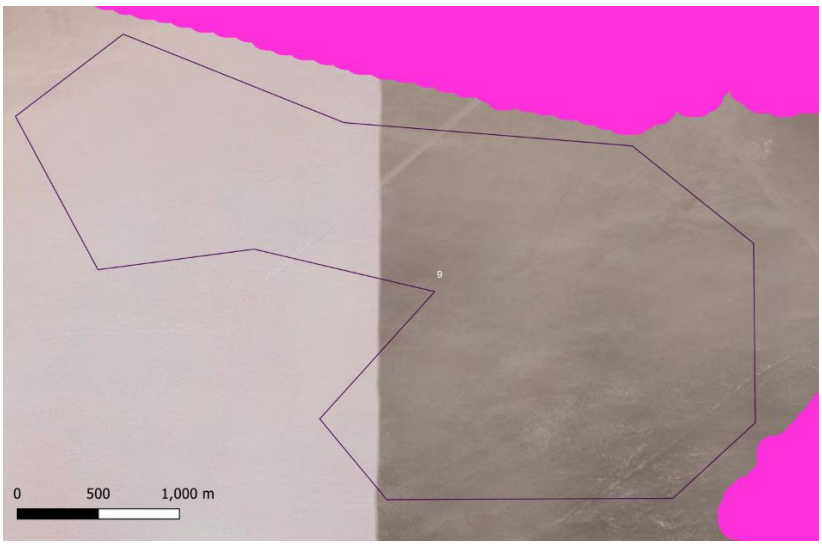
9
0
500
1,000 m

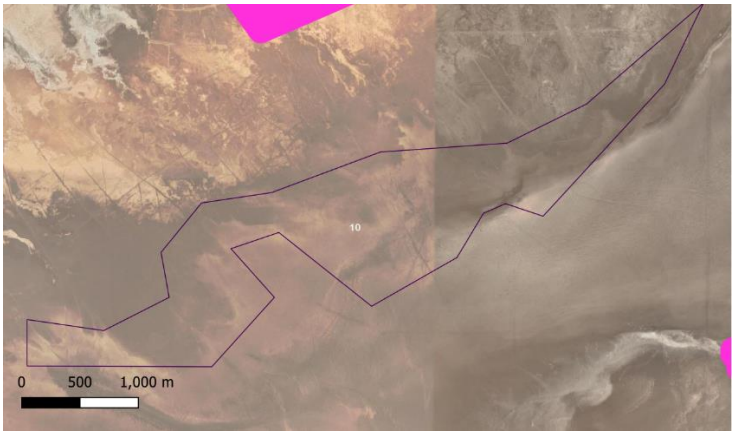
10
0
500
1,000 m

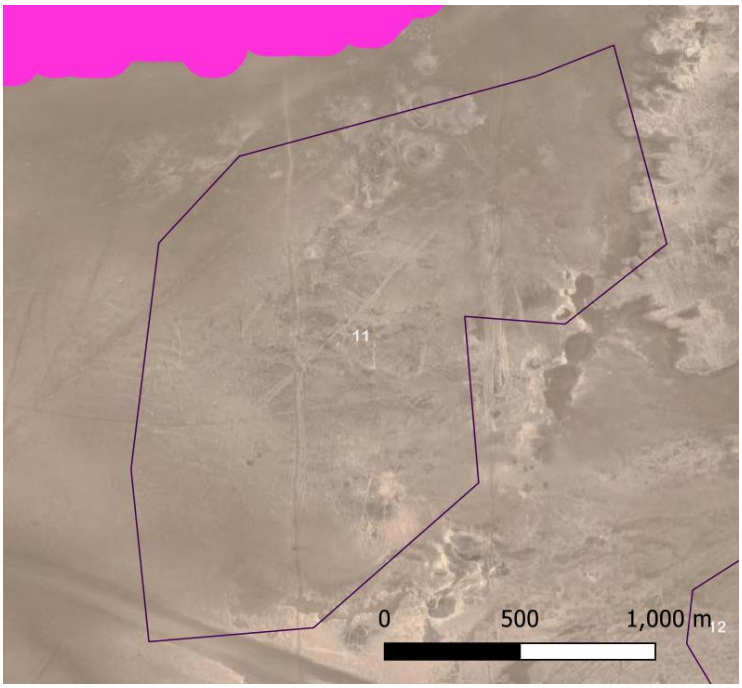
11
0
500
1,000 m
12

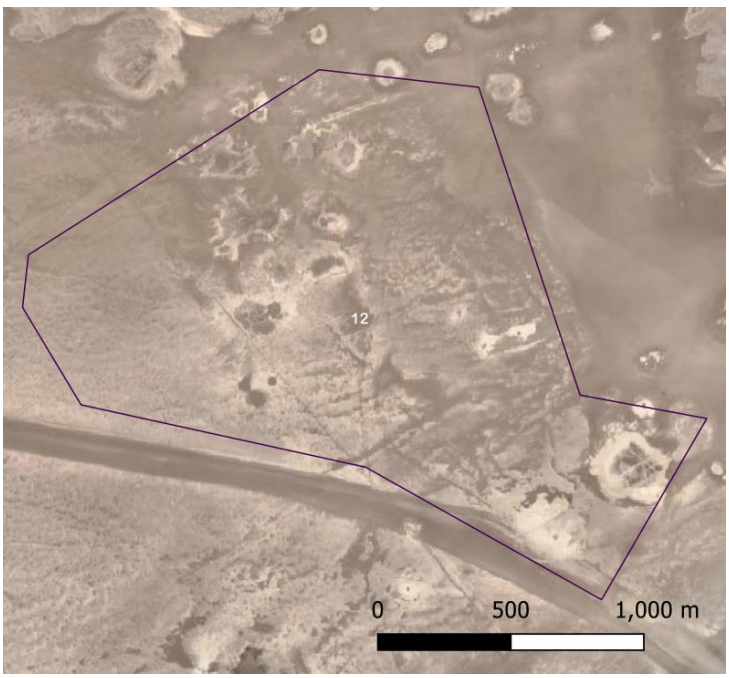
12
0
500
1,000 m

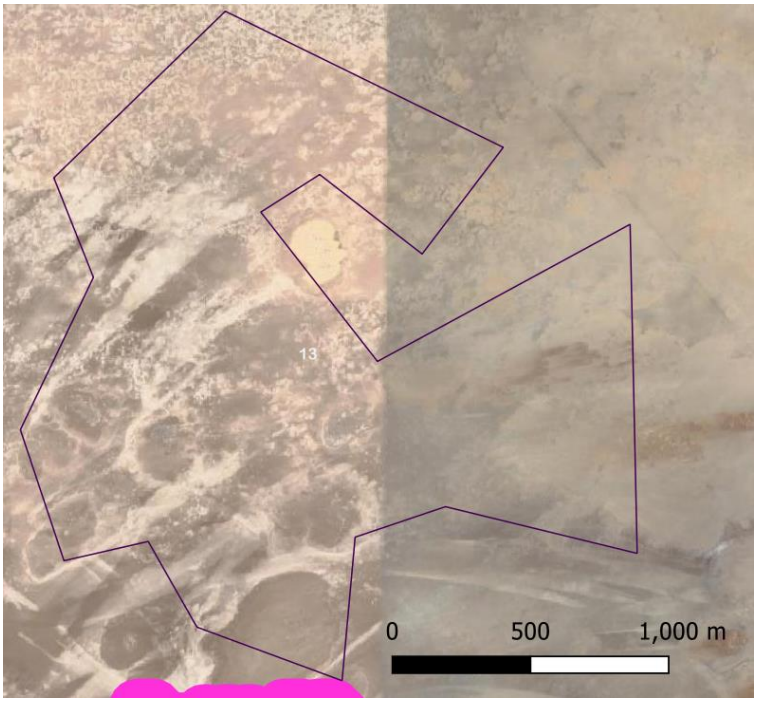
13
0
500
1,000 m

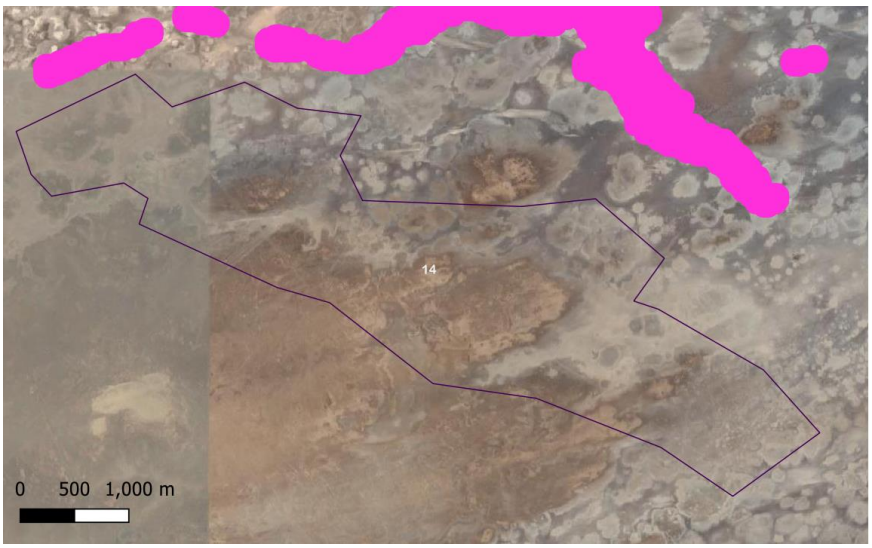
14
0
500
1,000 m

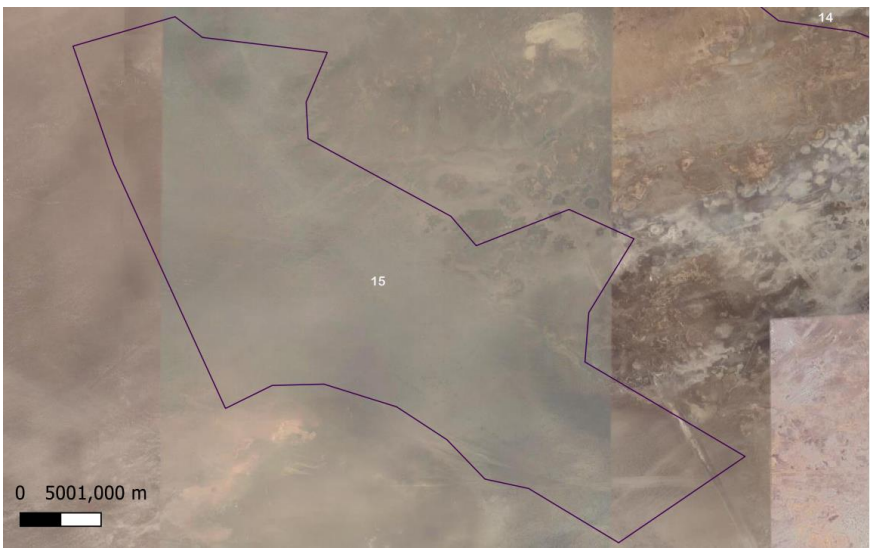
14
15
0
5001,000 m

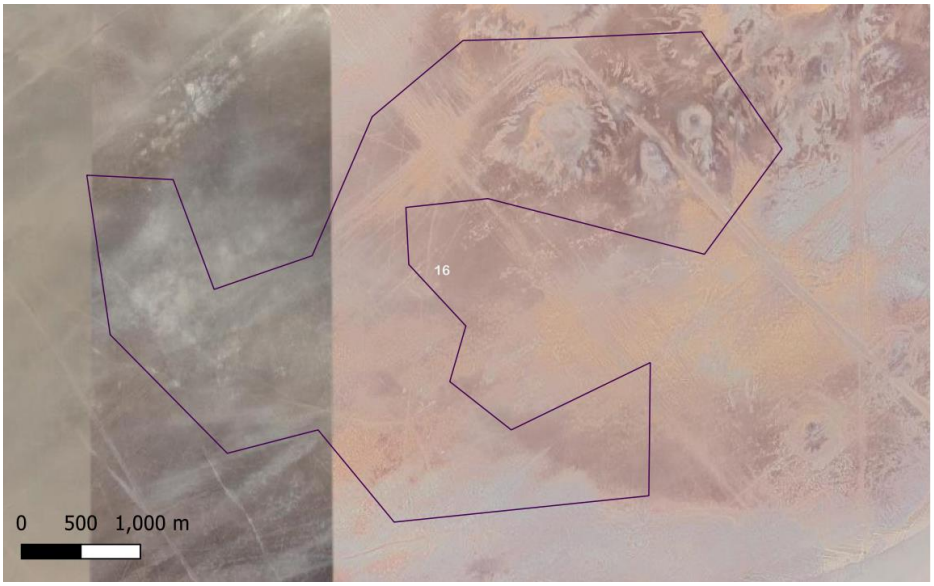
16
0 500 1,000 m

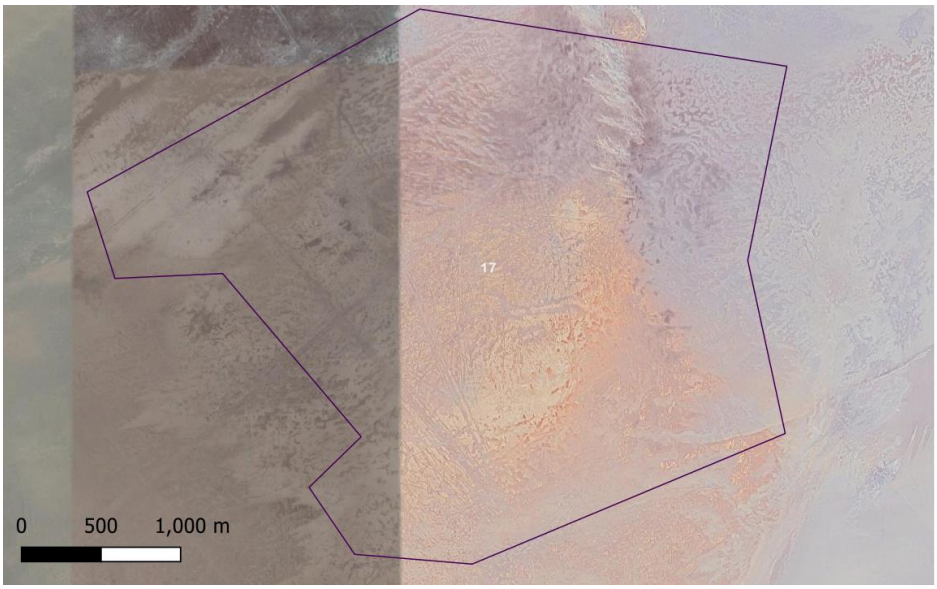
17
0 500 1,000 m


19
18
0 1 2 km

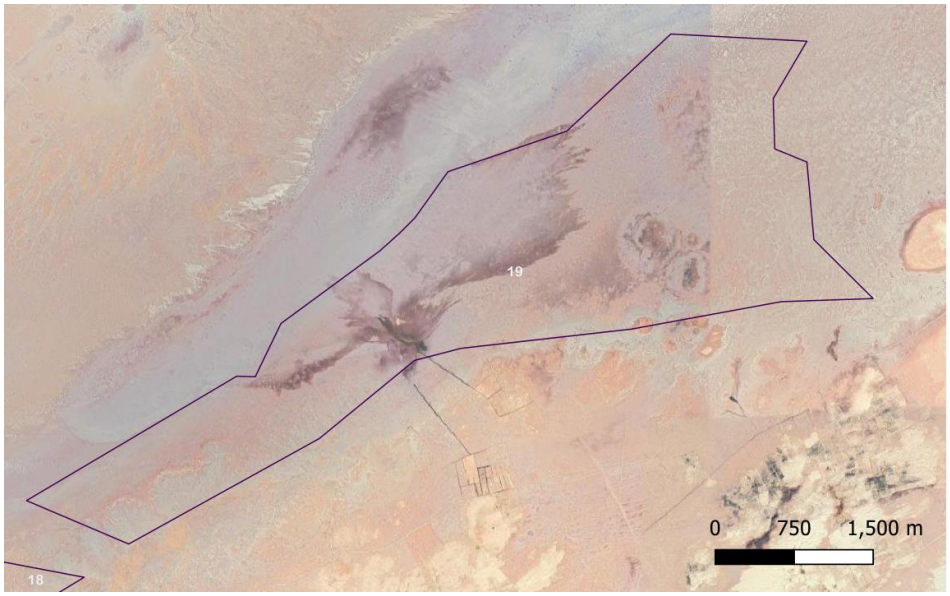
19
18
0
750
1,500 m

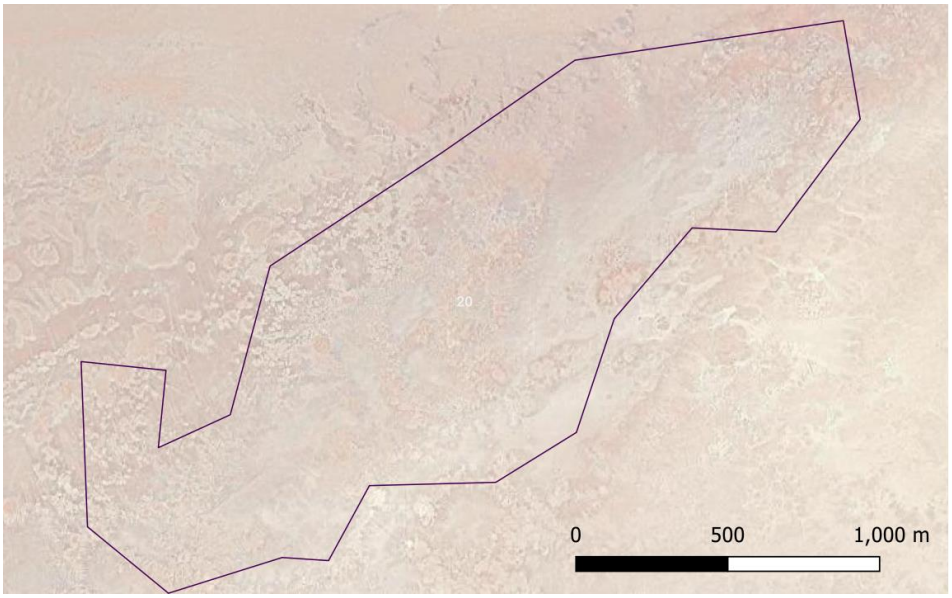
20
0
500
1,000 m

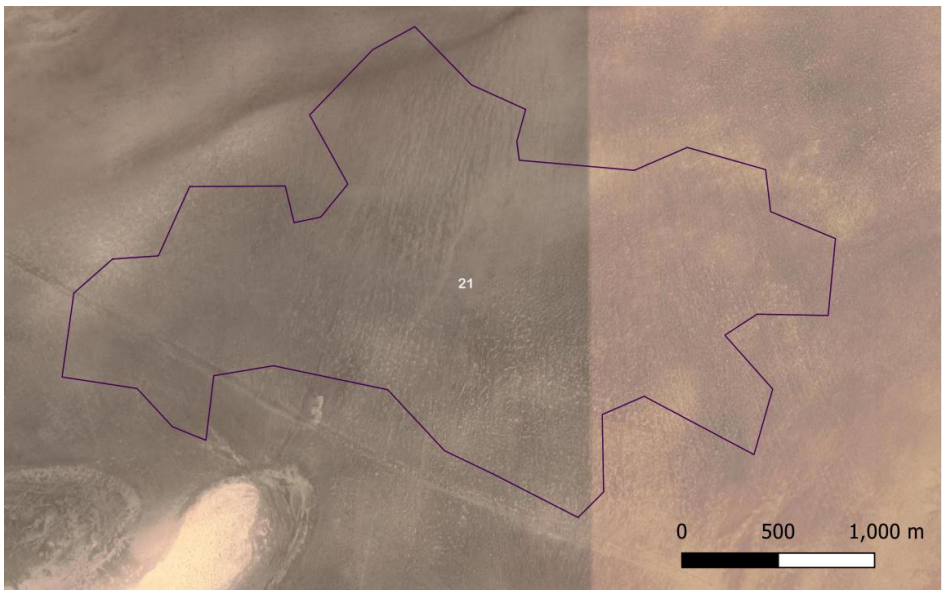
21
0
500
1,000 m